Design, Analysis & Fabrication of Complex Structures using Voxel-based modeling for Additive Manufacturing

Saish Tedia

Thesis submitted to the faculty of the Virginia Polytechnic Institute and State University in partial fulfillment of the requirements for the degree of

Master of Science
In
Mechanical Engineering

Christopher Williams, Committee Chair
Rayne Zheng
Diana Bairaktarova

10/03/2017
Blacksburg, Virginia

Keywords: Additive Manufacturing, Voxel, Manufacturability, Engineering Design Education, CT Scan, Reverse Engineering, Dithering, Functionally graded, Multi-Material

Design, Analysis & Fabrication of Complex Structures using Voxel-based modeling for Additive Manufacturing

Saish Tedia

ABSTRACT

A key advantage of Additive Manufacturing (AM) is the opportunity to design and fabricate complex structures that cannot be made via traditional means. However, this potential is significantly constrained by the use of a facet-based geometry representation (e.g., the STL and the AMF file formats); which do not contain any volumetric information and often, designing/slicing/printing complex geometries exceeds the computational power available to the designer and the AM system itself. To enable efficient design and fabrication of complex/multi-material complex structures, several algorithms are presented that represent and process solid models as a set of voxels (three-dimensional pixels). Through this, one is able to efficiently realize parts featuring complex geometries and functionally graded materials. This thesis specifically aims to explore applications in three distinct fields namely, (i) Design for AM, (ii) Design for Manufacturing (DFM) education, and (iii) Reverse engineering from imaging data wherein voxel-based representations have proven to be superior to the traditional AM digital workflow. The advantages demonstrated in this study cannot be easily achieved using traditional AM workflows, and hence this work emphasizes the need for development of new voxel based frameworks and systems to fully utilize the capabilities of AM.

Design, Analysis & Fabrication of Complex Structures using Voxel-based modeling for Additive Manufacturing

Saish Tedia

GENERAL AUDIENCE ABSTRACT

Additive Manufacturing(AM) (also referred to as 3D Printing) is a process by which 3D objects are constructed by successively forming one-part cross-section at a time. Typically, the input file format for most AM systems is in the form of surface representation format (most commonly. STL file format). A STL file is a triangular representation of a 3-dimensional surface geometry where the part surface is broken down logically into a series of small triangles (facets). A key advantage of Additive Manufacturing is the opportunity to design and fabricate complex structures that cannot be made easily via traditional manufacturing techniques. However, this potential is significantly constrained by the use of a facet-based (triangular) geometry representation (e.g., the STL file format described above); which does not contain any volumetric (for e.g. material, texture, color etc.) information. Also, often, designing/slicing/printing complex geometries using these file formats can be computationally expensive. To enable more efficient design and fabrication of complex/multi-material structures, several algorithms are presented that represent and process solid models as a set of voxels (three-dimensional pixels). A voxel represents the smallest representable element of volume. For binary voxel model, a value of '1' means that voxel is 'on' and value of 0 means voxel is 'off'. Through this, one is able to efficiently realize parts featuring complex geometries with multiple materials. This thesis specifically aims to explore applications in three distinct fields namely, (i) Design for AM, (ii) Design for Manufacturing (DFM) education, and (iii) Fabricating models (Reverse engineering) directly from imaging data. In the first part of the thesis, a software tool is developed for automated manufacturability analysis of a part that is to be produced by AM. Through a series of simple computations, the tool provides feedback on infeasible features, amount of support material, optimum orientation and manufacturing time for fabricating the part. The results from this tool were successfully validated using a simple case study and comparison with an existing pre-processing AM software. Next, the above developed software tool is implemented for teaching instruction in a sophomore undergraduate classroom to improve students' understanding of design constraints in Additive Manufacturing. Assessments are conducted to measure students' understanding of a variety of topics in manufacturability both before and after the study to measure the effectiveness of this approach. The third and final part of this thesis aims to explore fabrication of models directly from medical imaging data (like CT Scan and MRI). A novel framework is proposed which is validated by fabricating three distinct medical models: a mouse skull, a partial human skull and a horse leg directly from corresponding CT Scan data. The advantages demonstrated in this thesis cannot be easily achieved using traditional AM workflows, and hence this work emphasizes the need for development of new voxel based frameworks and systems to fully utilize the capabilities of AM.

Acknowledgements

This material is based upon work supported by the National Science Foundation under Grant No. 1546985 and Stratasys Ltd. through the Voxel Print Research Program. We gratefully acknowledge the financial support from the National Science Foundation. We also wish to thank Stratasys, Ltd., for their invaluable support in materializing the bitmap 3D printing. Any opinions, findings, and conclusions or recommendations expressed in this material are those of the author(s) and do not necessarily reflect the views of either the National Science Foundation or Stratasys.

I owe special thanks to my advisor, Dr. Williams, for his energy, encouragement and guidance. I would also like to thank our colleagues at Georgia Tech, Penn State and Tucker Innovations for help on this project. I would also like to mention Dr. Jason Foerst and Dr. Anish Pithadia at VT Carilion for their support and motivation in the CT project. I also wish to thank Dr. Rayne Zheng and Dr. Diana Bairaktarova, for offering their time and expertise as members of my committee. Finally, I would like to thank each and every member of the DREAMS lab, past and present, for their continuous help and support.

Table of Contents

List of Figures

List of Tables

Chapter 1: Introduction

Additive Manufacturing(AM) (also referred to as 3D Printing) is a process by which 3D objects are constructed by successively forming one-part cross-section at a time. A traditional AM workflow begins with making a solid model in CAD, which is exported in a surface representation file format (typically. STL or STEP file). This file is sent to a program that slices the model into layers and generates toolpath (machine level instructions). The toolpath can be in the form of coordinates or contours or bitmap images, depending upon the process. AM Processes such as Material Extrusion require toolpath in the form of co-ordinates whereas other processes like Material Jetting and Mask Projection Vat Photopolymerisation require toolpath in the form of bitmaps. Some AM systems based on Binder Jetting technology require toolpath in the form of contours. At last, these are sent to the AM system for model fabrication. Fig. 1 shows process flow diagram for a traditional AM system.

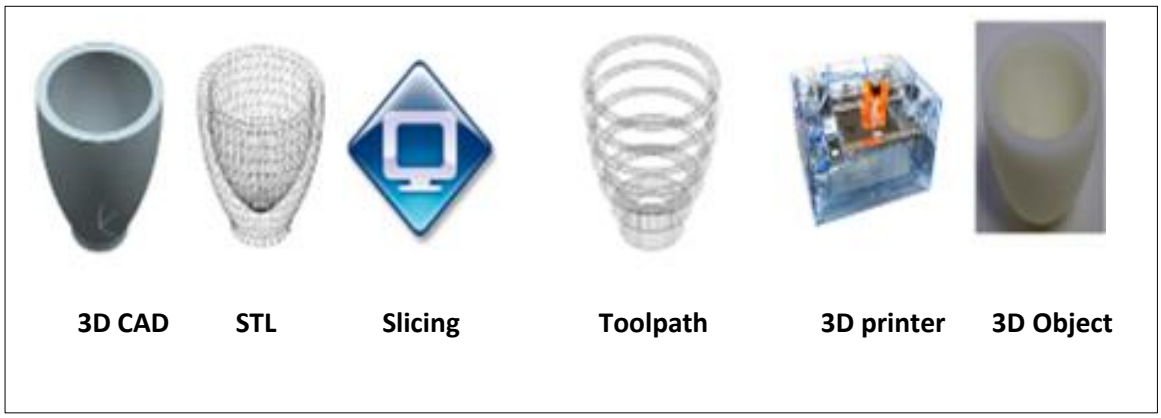

Figure 1: Workflow for an AM system

Typically, the input file format for most AM systems is in the form of surface representation format (most commonly .STL file format) with an individual mesh body for each material. A STL file is a triangular representation of a 3-dimensional surface geometry. The surface is tessellated or broken down logically into a series of small triangles (facets). Each facet is described by a perpendicular direction and three points representing the vertices (corners) of the triangle [1]. Fig. 2 shows an image of a sample STL file where a sample geometry has been tessellated into a series of facets. Despite the superior capabilities of AM, the .STL file format has several drawbacks which limits these capabilities. Firstly, it doesn't have the ability to take full advantage of multi-material capabilities of AM as it contains only surface geometry information, and lacks information about material, physical and other volumetric properties [2]. Secondly, with a surface-based format such as. STL, manipulating complex, multi-scale models can exceed computational capabilities. For instance, manipulating the inside of a surface model requires remeshing the part and often computationally expensive calculations of the intersection of different shells. As the STL file scales in size, retaining resolution means introducing significantly more triangles and hence larger file size which increases computational time significantly.

Also, several translation errors are introduced during the conversion of CAD/ point cloud data to a surface representation model and eventually into a fabricated part. During conversion of CAD to surface representation using tessellation process, there is always some deviation between the true surface and the representative surface [3]. The CAD software prompts the user for acceptable tolerances. The smaller the tolerance, and the more irregular

the surface is, the larger the number of triangles required to represent the surface. Hence, the user has to balance the accuracy issue with the file size issue. The tessellation process may also result in secondary errors such as holes, closures, non-manifold geometry, inverted normals etc [3]. These errors are further cumulated when this representation is converted to layer contours and subsequently toolpath by a process called vectorization [3]. Fig. 3 shows the different type of translation errors discussed.

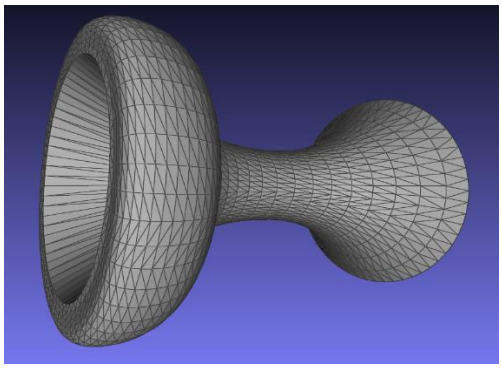

Figure 2: Image of a sample STL file

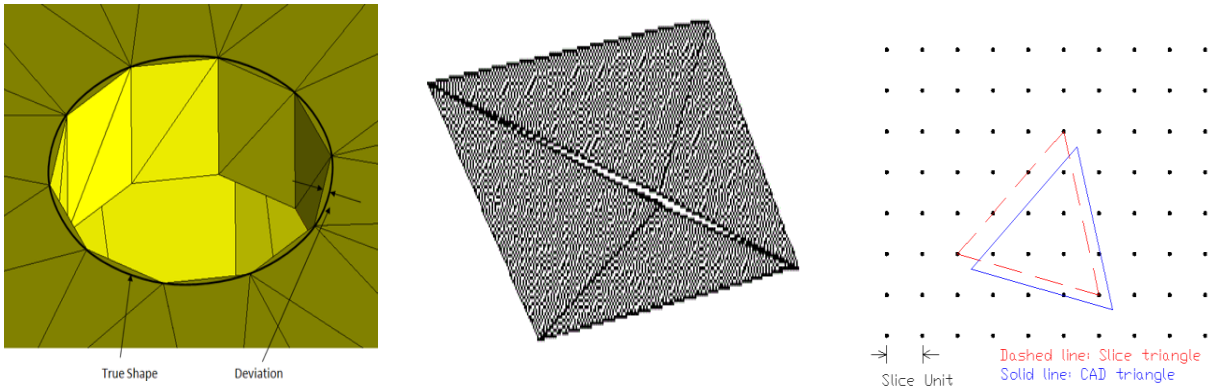

Figure 3: (a) Tessellation generation errors (b) Closure error causing hole in model (c) Error during vectorization

According to NIST standards, to fully leverage the superior capabilities of AM, an ideal geometric representation should have the following characteristics [4]:

- The representation should translate directly to machine control. Hence, secondary representational and translation errors can be avoided and the user can process geometry at the level of machine resolution and toolpath commands
- It should describe an object in a general way such that any machine can build it directly to the best of its ability.
- As the parts to print increase in size and complexity, the file format should scale well. This includes being able to handle large arrays of identical objects, complex repeated internal features (e.g. meshes), and multiple components arranged in the optimal packing for printing (e.g. cellular structures).

- It should be able to represent multiple/graded material information, colors and surface texture values, hierarchical microstructure and mesostructure etc.
- It should be forward and backward compatible with all previous and future versions

An alternative to surface representation which allows for all the above listed advantages is volumetric representation for which voxel is the base feature. Voxels are analogous to pixels in a bitmap. A voxel represents a value on a regular grid in three-dimensional space. A voxel is a cubic unit of volume that is centered at a grid point. A voxel represents the smallest representable element of volume. For binary voxel model, a value of '1' means that voxel is 'on' and value of 0 means voxel is 'off'. In printing, the voxel represents the minimum feature that a machine can fabricate. The layers are represented by a set of bitmaps which are stacked upon each other to form the 3D printed model. This can be visualized in Fig. 4. Also, each voxel can be used to store individual volumetric information about material properties, color, texture etc [5,6]. Voxels also allow for complex volumetric manipulations readily using simple binary operations. For example, to remove material from any portion of this model, the value of corresponding voxels is simply changed to zero. Moreover, for AM processes like Material Jetting and Mask Projection Vat Photopolymerisation, voxel based representation can translate directly into machine control.

This thesis specifically aims to explore the application of voxel based software tools in three distinct fields namely, (i) Design for AM, (ii) Design for Manufacturing (DFM) education, and (iii) Reverse engineering from imaging data. All these applications are described in detail below.

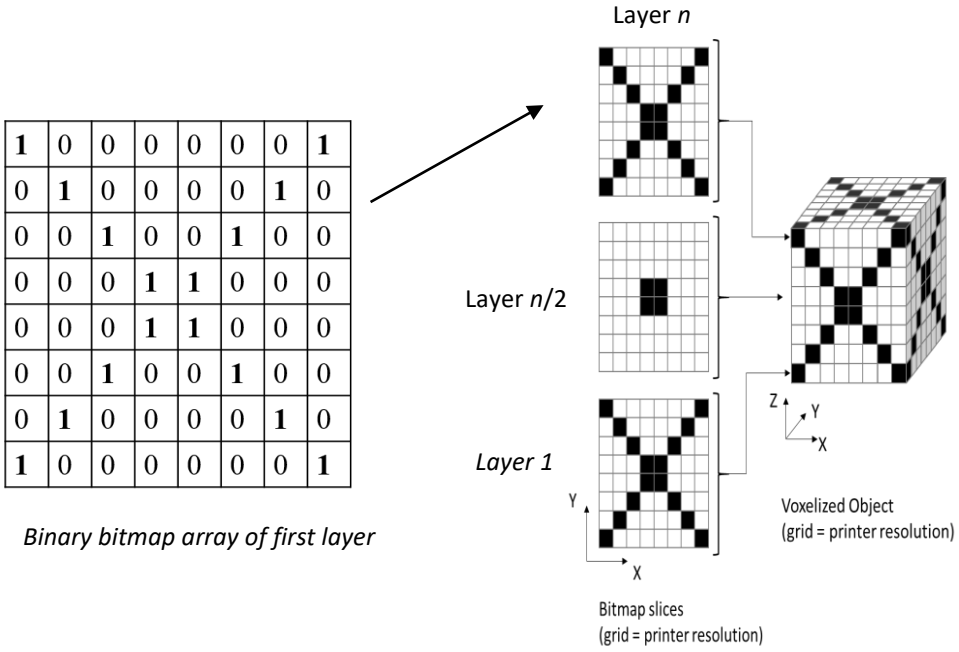

Figure 4: Voxel representation of a sample object

(i) DfAM

One of the key benefits of AM is its ability to fabricate almost any geometry. It is often said that, with AM, "complexity is free" since its layerwise, single-tool fabrication approach negates the need for additional fixturing, jigs, or tooling to create complex topologies. Hence, there is a widespread misconception that any part which can be modeled in a CAD software can be fabricated using AM. In reality, depending upon the AM process and machine,

manufacturability of a given part varies with factors such as minimum feature size, amount of build and support material, build time etc. While process planning tools do exist, they are mostly machine specific and mostly concerned with generating tool path for fabricating the model. They provide users with little help regarding the manufacturability of their parts. To address this gap, Chapter 2 explores the use of voxel representation for manufacturability analysis of parts to be produced using Additive Manufacturing. An automated, process independent software tool is developed in MATLAB which provides the user with feedback regarding the various features governing manufacturability of a given part. Using a voxel representation allows for a unified approach to calculate these factors using computationally simple 2D operations. Moreover, AM processes such as mask projection Vat Photopolymerisation, Material Jetting and Binder Jetting can be used to fabricate a part directly from voxel representation. Hence, the user also has the advantage of using this representation directly for model fabrication after assessing the manufacturability of his/her part.

(ii) DFM education:

The second part of this thesis (Chapter 3) is motivated by the objective of using manufacturability analysis software programs for both Additive and Subtractive Manufacturing (SM) to help engineering students visualize the manufacturability of their designs and select the best process available among AM or SM to fabricate their parts. Engineering students often fail to stop and think about the best way to make a part. They often choose the most easily and readily available manufacturing process without considering the most efficient or cost effective way to fabricate the same part. There are a multitude of design criteria (e.g., materials, quality, cost) that are strongly coupled to each fabrication processes which most students are unaware of. In industrial settings, companies make use of a combination of in-house manufacturing and distributed supply chains to fabricate, source, assemble, and produce their products and drive innovation. In such an environment, process experts make use of general-purpose software systems (i.e., numerical control (NC) programming and verification systems) to validate product manufacturability and generate machine-level instructions. For engineering students, and "makers" at large, access to and familiarity with these manufacturer-centric applications presents a significant barrier toward implementation of complex features in product design. Instead, engineering students use that which is readily available (and known) to them. While students do try to get cost estimates from online sources, these sources of information provide little feedback and further divorce students from understanding the implications of their design decisions on the manufacturability of their parts. In this work, we implement two previously developed voxel based tools, the AM analysis tool developed earlier and Sculptprint, which is SM analysis tool developed by Georgia Tech, in an undergraduate classroom setting to evaluate whether the use of DFM software programs improves the ability of students to select the appropriate manufacturing process and better understand the DFM concepts.

(iii) Reverse Engineering from Imaging data

The third and final part of this thesis (Chapter 4) aims to explore fabrication of models directly from medical imaging data using a voxel based approach. The combination of AM technologies and volume scanning devices (like CT and MRI) is a powerful reverse-engineering platform. A voxel-based modeling package can import the scanned volume data, perform voxel-level, modifications, and then directly fabricate the object, or its tooling, using AM equipment. Current commercially available frameworks for imaging data convert patient specific information to a surface representation format. This conversion introduces inaccuracies in the model which if not repaired/removed may lead to models that may not exactly replicate the exact anatomy. For medical applications, this might lead to inaccurate

treatment or diagnosis etc. which can significantly impact patient care. Also, since imaging data is in a volumetric representation, conversion to a surface representation results in loss of material information. This part of thesis aims to demonstrate that the use of voxel representation to directly fabricate models from imaging data can produce accurate anatomical models and also has the potential to use the underlying material information to fabricate continuous multi-material graded models.

Solid Freeform Fabrication 2016: Proceedings of the 27th Annual International Solid Freeform Fabrication Symposium – An Additive Manufacturing Conference Reviewed Paper

Chapter 2: Manufacturability analysis tool for additive manufacturing using voxel-based geometric modeling

Saish Tedia and Christopher B. Williams
Design, Research and Education for Additive Manufacturing Systems Laboratory
Department of Mechanical Engineering, Virginia Tech, Blacksburg, VA 24061

Abstract

While Additive Manufacturing (AM) processes provide unparalleled design freedom, they still impose some constraints on the geometries that can be successfully fabricated. Thus, there exists a need for predictive analysis of part geometries' manufacturability. Existing algorithms based on surface representations require several computationally intensive manipulations. In this paper, the authors present a framework for performing manufacturability analysis of parts to be manufactured by AM using a voxel-based representations schema. The input triangular mesh is first converted into a voxel representation using Ray Casting. Through a series of simple computations on a binary three-dimensional array, the tool provides feedback on infeasible features, minimum feature size, support material, orientation and manufacturing time for different build orientations. The tool's ability to effectively analyze parts for manufacturability is evaluated against several sample geometries.

2.1. Introduction

2.1.1 Motivation

The advancement of Additive Manufacturing (AM) technologies coupled with the feasibility of producing complex geometries has led to the widespread, but erroneous, belief among users that any model that can be designed in a computer-aided design (CAD) environment can be manufactured using AM. In reality, the manufacturability of a given model is dependent on a combination of printer resolution, layer thickness, print orientation and print process parameters [7]. For example, a limited printer resolution can result in differences between the CAD model and the manufactured part, such as fine features not being manufactured properly or being damaged during post-processing [8]. Currently, there is no provision in CAD software programs to automatically identify manufacturing constraints. Hence, users have to rely upon heuristic design for AM (DfAM) guidelines that are beginning to emerge in literature (e.g., [8-11]). AM service bureaus are required to manually perform digital inspection and evaluation of hundreds of incoming. STL files for their manufacturability. Thus there exists a requirement for automated software applications that can help the users to visualize these factors for a given geometry and give automatic feedback on its manufacturability.

While pre-process planning software exist (e.g., Netfabb, Magics), they are focused in checking the validity of the STL file and performing necessary repairs. Additional functionality has been recently added to these software programs including automated generation of lattice structures, Boolean manipulations of multiple part files, and added process planning functionality such as slicing, orientation, and tool path planning. Most of the

commercially available processes planning software are focused in preparing the part for printing, slicing, support generation and tool path generation. Neither these types of software programs provide manufacturability feedback based on geometric analysis. Moreover, these programs are mostly intended to give results for a specific printer or specific set of print parameters. Some of these programs provide an option to the user to automatically select a build orientation where the software generally provides orientation based on minimum z-height. Subsequently, the models are sliced and sent to a tool path generator that generates instructions to manufacture the part. Build time is estimated only after the tool path has been generated and not upfront in the design stage. These existing solutions are primarily focused on preparing the printing process, instead of evaluating the manufacturability of a part. For better Design for Additive Manufacturing (DfAM), there exists a need for part preprocessing software that also performs manufacturability analysis.

2.1.2. Prior Art

There have been prior attempts in developing manufacturability analysis tools for AM. Specifically, researchers have investigated schema for automating the identification of manufacturing constraints associated with feature size, support material, and manufacturing time. However, each of these tools has been presented independently; there has been no unifying approach that simultaneously computes all of these factors and uses the results to inform processing decisions. These prior research studies are presented below along with the overall goals for a manufacturability analysis tool.

1) Minimum Feature Size: The type of AM process and resolution of the machine being used limits the minimum printable feature size of a part [12]. In addition, high-aspect ratio features (e.g., thin walls) can be so fragile as to not be able to survive post-processing (e.g., [2]); hence a minimum wall thickness has to be maintained to provide sufficient strength to the part. Several automated methods have been proposed in the literature for determining the thickness of 3D features:
   - *Medial Axis Transformation*: The medial axis transform (*MAT*) is a shape model that represents an object by a set of maximal inscribed spheres and the medial axis is the loci of the centers of these spheres, and can be visualized as the skeleton of the object [13]. The thickness can be computed as distance of medial axis from boundary. Medial axis theorem is a well-established concept in Computer Graphics and Computer Vision and considerable work has been done to analyze 3D shapes using this concept [14-16]. MAT also been extended to analyze models for AM. Nelaturi et al. [17] provide a manufacturability feedback model in terms of a printability map based on resolution errors encountered in AM using techniques from mathematical morphology and medial axis theorem. However, MAT is extremely sensitive to small noise and artifacts resulting in many unwanted branches in skeleton which have to be removed. Also special care has to be taken to compute the corners. These result in extra computation and hence thickness maps for intricate shapes are difficult to compute.
   - *Distance Transform*: Distance transform is used to compute Euclidean distance of a point from the nearest point on the surface. Distance transform operation is also a commonly used technique and has been used on voxel models and other volumetric representations to assess shape of 3D objects for various applications [18-20]. This technique has been implemented for AM by Telea et al. [21], where the authors use a voxel based approach that relies on distance transform and morphological operations to perform 3D printability analysis. They classify voxels based on geometry to identify common issues in printing bridges, spikes, and holes. However, not all regions that are detected after distance transform are useful, and extra topological analysis is required to

detect thin features and classify them as critical based on defined metrics, which increases computation. Also, as mentioned by Telea et al., this method is not fully automated. Still, distance transformation appears to be better approach than MAT as it is easier to implement than MAT. However, its implementation in literature till date has been limited to low resolution voxel models.

- *Polygonal offsetting*: An offsetting operation is another way to compute feature size in a given model. Offsetting operations on a solid have been defined in literature [22]. However, algorithms that offset each site of a contour separately generate offset segments that can self-intersect each other. These techniques then rely on Boolean intersections to trim away excess offset geometry. Many cases between points, edges, boundaries, surfaces etc. need to be carefully considered in implementation. It is non-trivial to carry out all the above-mentioned operations using a polygonal model. Such techniques are computationally complex and numerically instable. Chen and co-authors have proposed a new computational method based on point-based offsetting operation of polygonal models for manufacturability analysis based on minimum feature size [23].

2) Support Material: A key feature of process planning software for all non-powder bed AM systems is generating support material for a given polygonal model. Outside conventional approaches, there have been few algorithms in literature to design effective support structures. Das et al. [24] have provided a methodology for calculating support structure volumes with the use of a point Quadtree. Strano et al. [25] developed an optimization algorithm to use pure mathematical 3D implicit functions for the design and generation of cellular support structures. Voxelizer [26], an open source commercial software developed by ZMoprh, uses voxel representation to calculate support structures; however, no literature is available in the area of generating support structures directly using voxels.

3) Build Time Estimate: For better DfAM, users must be aware of the build time estimates required to manufacture their parts in the design stage itself. In most commercial software programs, build time for AM processes is calculated based on toolpath, which is the last pre-processing step. Researchers have adopted different techniques for time estimation in various AM processes. Alexander et. al [27] provided a build time estimate model for FDM which was used to calculate cost estimate for the model. The estimates were based on area of cross-section of each layer calculated from polygonal model and road width of part and support material. Authors have also presented algorithms to develop generalized models for estimating build time based on regression, neural networks etc. [28-30].

2.1.3. Research Goal

The primary goal of this work is to realize a preprocessing software solution that assists designers in product realization by automating the assessment of the manufacturability of their designs. Specifically, the authors aim to use a voxel-based representation schema as a means for automatically identifying (i) minimum feature size, (ii) support material consumption relative to orientation, (iii) build time estimate

Essentially a three-dimensional pixel, a voxel can be used as a base feature for volumetric representation of part models. The voxels are cuboidal in shape and aligned with the Cartesian coordinate system; hence the 3D model is represented as stack of voxel layers and each voxel can be accessed by their x, y, and z indices. As such a voxel representation of a solid body can be represented by a binary three-dimensional array in which a value of 1 means the voxel is ‘on’ and value of 0 means the voxel is ‘off’.

Voxel representation is used in this work as it allows for a unifying approach to easily compute all these factors simultaneously. In addition, voxel representation allows for easy

computations on the part geometry using simple 2D algebraic and Boolean operations, which are usually much less computationally expensive than 3D ones required for polygonal models.

Another motivation for this approach is the voxel representation's compatibility with voxel-based AM processes such as Material Jetting, Binder Jetting and mask-projection Vat Photopolymerization techniques. These AM processes function by converting the input polygonal model to bitmap image files that are used to drive the deposition/imaging tool. Hence, a preprocessing software based on voxel representation can be used to provide manufacturability feedback, as well as serve as direct process control without the addition of any additional steps (and potential information loss) found in model translation. Some work has been done in the area of printing directly from voxels (e.g. Hiller and co. [31, 32], Doubrovski et. al [33], Brunton et. al [34]). Voxel representations can also be used to derive toolpaths for other AM processes for extrusion AM which will be implemented in the future.

In this work, a voxel-based representation is utilized to store geometric information in a discrete and efficient format; simple Boolean and algebraic operations are used to facilitate geometric computations to compute factors central to manufacturability analysis (Sections 2.3 and 2.4). The proposed manufacturability analysis tool could be integrated and automated into a CAD software package to assist a designer in creating a manufacturable product by bringing manufacturability upfront in the design process to guide better Design for Additive Manufacturing (DfAM) practices. **Figure 5** shows a schematic diagram of the various steps integrated in the proposed tool in order to evaluate the manufacturability of a given part and prepare it for printing.

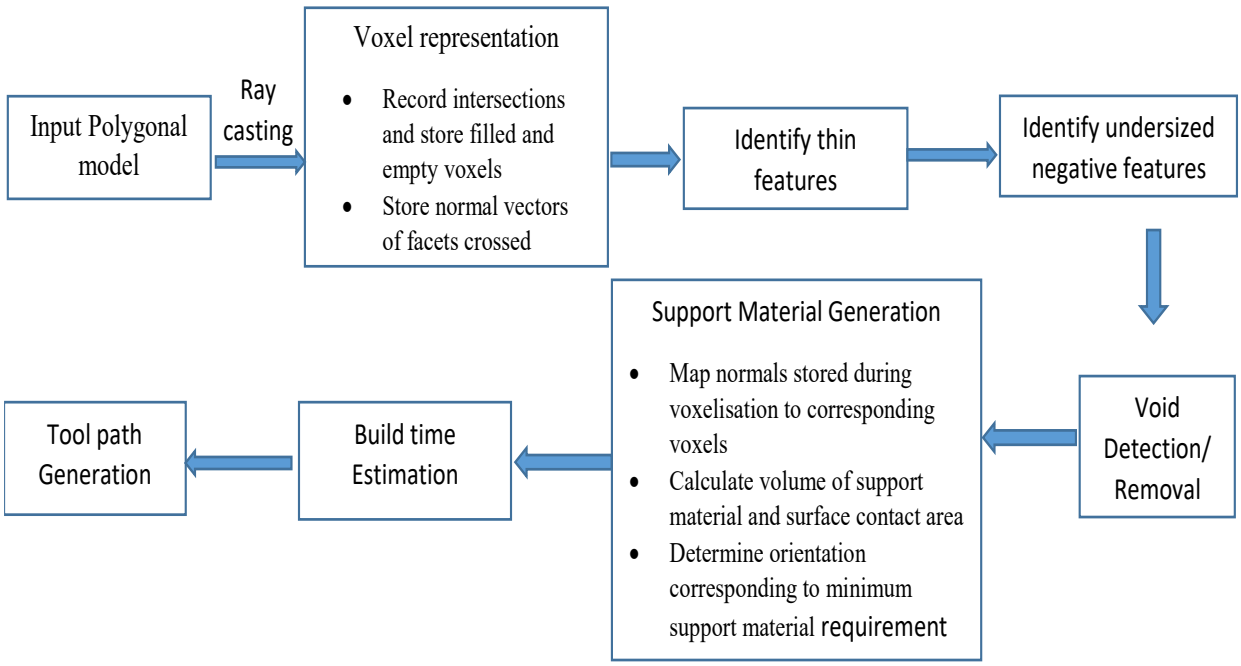

Figure 5: Flow-chart listing the steps integrated in the proposed tool

2.2.Theoretical Framework: Voxelisation and Rendering

The authors present in this paper a new manufacturability analysis approach based on ray-casting and voxel models, both of which are well established concepts in computer graphics. In this section, techniques for voxelization of polygonal models and rending the resulting voxel model for user analysis are presented.

2.2.1. Voxelisation of Polygonal Model

A considerable amount of work has been done in the area of using voxels as base feature for representing geometry of objects in AM (e.g. Chandru et. al [35], Lin et. al [36], Ma et. al [37, 38] etc.). As noted in Section 1.3, voxel representations of solids can be stored as 3D binary arrays. The three-dimensional grid is formed by dividing the bounding box of the input polygonal mesh. The resolution of the grid depends upon the desired voxel size, which in turn depends upon layer thickness and printer resolution. The method implemented in this work for creating a voxel representation from an input polygonal model is based on a ray intersection method similar to that described by Patil and Ravi [39].

In this work, the resulting 3D binary grid array is defined as a MATLAB gpuArray object to transfer some of the further computations on the array to the GPU, which saves computational time for rendering and calculating manufacturability parameters. However, to transfer all computations to the GPU, a custom CUDA kernel script is required, which is beyond the scope of this work. This technique only works for water tight meshes, which means that the input STL file should be free from errors.

2.2.2. Voxel Model Rendering

Rendering of the voxel representation is required so that users can visualize problematic features identified by the tool such as thin sections, overhangs that require support etc. and can modify their design accordingly. The voxel model is displayed as a quadrangular surface mesh. The voxels are classified into boundary voxels (voxels that lie on the surface of the object), exterior voxels (voxels that lie outside the object mesh) and interior voxels (voxels that lie inside the mesh). To increase the speed of rendering, only boundary voxels are used for display. Interior voxels are displayed only while computing manufacturability characteristics, but are reset as empty for rendering. Single stray voxels that occur due to resolution errors which will be absent in normal objects are identified and reset as empty voxels as discussed in [39]. The results of voxelization and rendering are shown in Section 4.

2.3. Manufacturability Analysis Methodology

2.3.1. Minimum Feature Size

In AM, there are three dimensions to consider: the two planar 2D dimensions (X and Y) and the Z dimension. Every AM system has a specific X, Y and Z resolution. Since these resolution values can be different, one needs to evaluate the dimensions of the features in all three directions separately and compare them with the resolution or desired feature size in corresponding direction. We define thickness of a sample section (e.g. section PQ in Figure 6a) of the object along the ray direction as the distance from P to the intersection point of the ray with the opposite surface Q. This is calculated separately each for X, Y and Z directions. Here T_x is the thickness of section RS which would be compared with resolution/desired thickness in X direction. Similarly, T_y is the thickness of section RS which would be compared with resolution/desired thickness in Y direction.

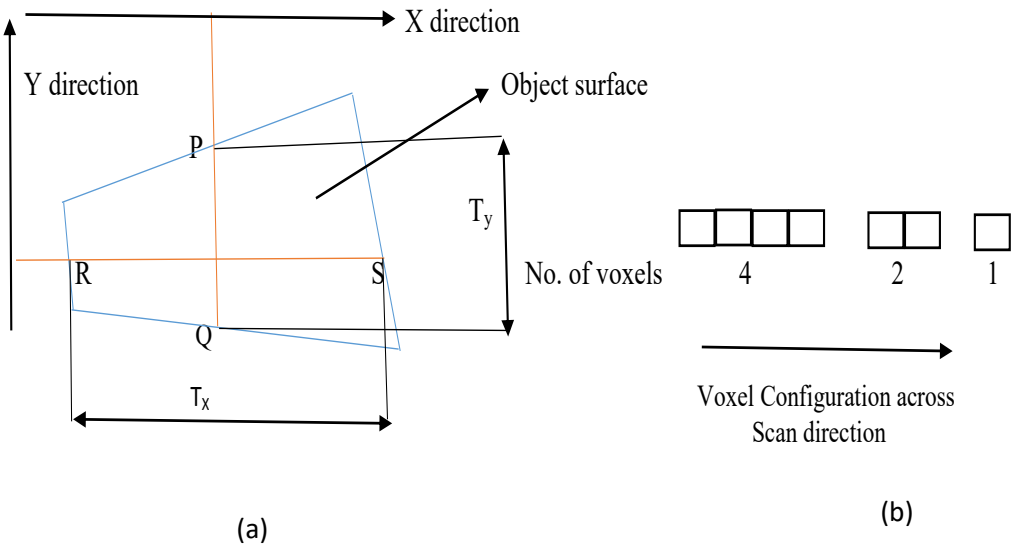

Figure 6: Minimum feature size calculation steps in X and Y direction

The steps involved in minimum feature size calculations include:

- Rays are cast along the Z-direction incrementally to find the locations where they intersect the mesh. The first ray is passed through minimum Z coordinate (Z_{min}) of the model and the process is carried out layer-by-layer from the Z_{min} to the maximum Z coordinate (Z_{max}) of the model.
- The intersections are stored and sorted in ascending order for each ray.
- All the voxels that the ray passes through between two surfaces after crossing one facet before crossing another facet are counted and stored.
- Let n be the number of voxels between two intersections and R_i , R_{i+1} be the points of intersection of the ray at a particular section. The feature size/thickness of any section of the object in Z direction can then be calculated by the following equation:

$$t=\text{dist.}(R_i, R_{i+1}) = n \times d_j \quad (1)$$

where d_j is the voxel dimension in the direction of voxelization

- If this obtained value is less than the resolution or minimum desired feature thickness specified by the user in that direction, than corresponding voxels are highlighted.
- The same procedure is repeated from other two coordinate axis directions and the results are combined together.

Since, in the voxelisation process, we are also passing rays in X, Y and Z direction, this algorithm is implemented as part of voxelisation algorithm to minimize computations.

2.3.2. Identifying Undersized Negative features

Negative features such as holes that are under the machine's resolution might also not be manufactured correctly. In some processes, it is also required to maintain a minimum size of the holes so that support material can be removed during post-processing [8]. The process to identify negative features is similar to that for minimum feature size described in the above section using ray casting. The only difference is that now voxels between each set of even-to-odd intersection (empty voxels between two surface boundaries) are counted and stored. If the product of number of empty voxels and voxel dimension in that direction is less than machine resolution or desired negative feature size specified by the user, those voxels are highlighted.

Another technique is to classify negative features based on area. This may be helpful for circular or regular polygonal holes where a minimum area can be used to control size of the hole. Each xy, yz and zx slice is analyzed where only empty voxels are displayed. The area is measured by calculating the actual number of pixels in each of the empty regions. Hence, user can also specify a minimum area for negative features and if the area of negative feature in any plane is less than the specified value, the voxels are highlighted.

2.3.3. Support Material Generation

After importing the STL file, it is required to set an orientation for the part initially. If V1, V2 and V3 are the row matrices containing X, Y and Z co-ordinates of vertices of all the facets, then the rotation is performed by multiplying the transpose of these matrices by rotation matrices $R_x, R_y \; and \; R_z$ around the X- and Y and Z axes respectively to find new vertices $V1_{new}$, $V2_{new}$ and $V3_{new}$. If the part has to be rotated by θ_x in x direction, θ_y in Y direction and θ_z in Z direction, then the new vertices can be calculated by following equations (2-7):

$$R_x = \begin{bmatrix} 1 & 0 & 0 \\ 0 & \cos(\theta_x) & -\sin(\theta_x) \\ 0 & \sin(\theta_x) & \cos(\theta_x) \end{bmatrix} \quad (2)$$

$$R_y = \begin{bmatrix} cos(\theta_y) & 0 & sin(\theta_y) \\ 0 & 1 & 0 \\ -sin(\theta_y) & 0 & cos(\theta_y) \end{bmatrix} \quad (3)$$

$$R_z = \begin{bmatrix} cos(\theta_z) & -sin(\theta_z) & 0 \\ sin(\theta_z) & \cos(\theta_z) & 0 \\ 0 & 0 & 1 \end{bmatrix} \quad (4)$$

$$V1_{new} = R_z \times R_y \times R_x \times V1 \quad (5)$$

$$V2_{new} = R_z \times R_y \times R_x \times V2 \quad (6)$$

$$V3_{new} = R_z \times R_y \times R_x \times V3 \quad (7)$$

After voxelisation, subsequent rotation is simply done by rotating the 3D grid using the same $R_x, R_y \; and \; R_z$ rotation matrices. Hence, it is not required to voxelise every time the part has to be rotated.

Depending upon the AM process and machine, certain features such as some surfaces, overhangs, negative drafts and undercuts etc. which are at an angle (measured between normal and horizontal) that is less than a critical value require support material to be manufactured. For example, this limiting value is 35^0 for Selective Laser Melting [40]. The steps involved in support material calculations are discussed below:

- During voxelization, while determining the facets that are crossed by rays, the normal vectors of respective facets are also stored. If the normal vector data is not available in the STL file, then normal vectors are computed using simple cross product of the vectors forming the facet.
- For generating support, only Z voxelization data is required since the facets that are not going to be crossed during Z voxelization would essentially be parallel to Z axis (i.e. facets in XZ or YZ planes). These facets will have their normal aligned with the

horizontal and hence the angle that their normals make with the horizontal will always be 0^0 and are not required for support calculation.

- For generating support, all interior voxels are removed from analysis as none of these voxels would require support material.
- Among the remaining voxels, only those voxels are considered for analyses that correspond to facets crossed in Z voxelization. This is done by traversing through each x, y voxel from Zmin to Zmax incrementally and only voxels that are at the start or end of a Z boundary are displayed.
- The corresponding normal data from Z voxelization is then mapped with the respective voxels that represent these facets.
- All remaining voxels which are supported by a voxel below them are identified and removed from analysis.
- For remaining voxels, the angle that normal makes with the horizontal is calculated.
- If this angle is greater than the specified critical angle of the machine, then the empty voxels below them are turned on and marked as support voxels.
- Voxels corresponding to rays that could not be voxelised cannot be mapped with their respective facet normal vector. The normal vectors for these voxels are computed by interpolating from the surrounding voxels.
- Finally, all the support voxels are projected down until any part voxel or base voxel is encountered. The number of support voxels are counted and multiplied by volume of one voxel to find the total volume of support material required.
- In order to compute the support contact area, voxels in contact with support voxels are checked whether they belong to the part volume or not. The surface contact area is simply the area of the faces in contact with support voxels

Subsequently, the tool also identifies optimum orientation with minimum support material. The geometry is incrementally rotated around x- and y-axes, with default resolution of 10°.The algorithm iteration loop is on until the supports for all the orientations are calculated. Once all the possible orientations are investigated, the orientation that requires minimum support volume is identified.

2.3.4. Build Time Estimation

In material extrusion, building a layer of material of a part has several stages. The part's external contours are drawn first and then the interior is filled with a tightly rastered pattern. Support structures are deposited, also in a raster pattern but spaced wider than that used to fill the part interior. To deposit material for the i_{th}layer, time taken can be given by sum of time taken to build external contour, time for infill and time taken to deposit support structures. While calculating time to build an external contour for i_{th}layer, only the boundary voxels are considered for analysis. The time $t_{contour}$ is given by number of voxels in the contour $n_{voxel,}$ the cross-sectional area of a voxel, A_{voxel} , the contour width w and the nozzle velocity for drawing outline, $v_{outline}$, shown in equation (8):

$$t_{contour} = \frac{n_{contour} \times A_{voxel}}{w \times v_{outline}} \tag{8}$$

Next, only the internal voxels are displayed. Each y voxel is traversed from $xmin\ to\ xmax$ and total voxels at each x co-ordinate n_{xi} as well as total no. of roads $n_{roads}$are stored. Here, retraction of nozzle in going from one road to next is also considered. However, retraction of nozzle within one road or between multiple contours is not taken into account. This approach is similar to assuming that the raster angle is 90°. An approximation for the time

taken to generate infill t_{infill}, is determined using the default printing velocity v, nozzle X/Y axis movement speed v_{xy} and infill percentage W_p shown in equation (9):

$$t_{infill} = \sum_{xmin}^{xmax} \left(\frac{n_{xi} \times d_y}{W_p \times v} \right) + \frac{(n_{roads} - 1) \times d_x}{W_p \times v_{xy}} \quad (9)$$

Here d_x and d_y are voxel x and y dimensions respectively.

This method slightly underestimates the true time because the deceleration of the nozzle at corners is also not taken into account. Also the raster pattern could be at an angle which is not taken into account. Next, only the support voxels are displayed. The equation for the time to deposit the support structure for the i_{th} slice is similar to equation (9) except that the support does not fill the entire area. Supports are deposited less densely in widely spaced raster patterns compared to the closely packed raster in the part interior. Hence, support infill percentage, W_s and support infill density $\rho_{support}$ are used to calculate the time taken to deposit support structures, $t_{support}$ for ith layer using equation (10) below:

$$t_{support} = \sum_{xmin}^{xmax} \left(\frac{n_{xisupport} \times d_y}{W_s \times v \times \rho_{support}} \right) + \frac{(n_{roadssupport} - 1) \times d_x}{W_s \times v_{xy} \times \rho_{support}} \quad (10)$$

Finally, approximate time taken to move from one layer to next t_{layer} is added using Z axis movement speed v_z and layer thickness t_z using equation (11) below:

$$t_{layer} = \frac{t_z}{v_z} \quad (11)$$

Total time is given by adding all the time components for each layer as shown in equation (12) below:

$$t_{total} = \sum_{i=1}^{n} (t_{contour} + t_{infill} + t_{support} + t_{layer}) \quad (12)$$

2.3.5. Manufacturability Analysis: Void Detection

Unknown voids in the input model may increase the file size and can significantly decrease the strength of the part [41]. To compare two STL files: one having voids and other without voids, Boolean comparison of one facet of parent model with all the facets of other model is required. Also, removing a void requires remeshing of the model. Hence, void detection and removal using polygonal models are computationally intensive. Voxel based representations on the other hand allows for simple Boolean operations on complex binary 3D arrays in a matter of few seconds as well as void removal by selectively turning on material at detected location. Hence this feature can be used to detect cyber threats or for quality inspection purposes during post processing [41]. Voxel representations can also be used to examine empty spaces for closed voids by checking the surrounding voxels which might trap support material, powder or resin which would be impossible to remove. This feature is in development phase and will be added in the future.

2.4. Manufacturability Analysis Results

Several functions have been written to perform voxelisation, rendering and analysis. All computations are performed in MATLAB R2016 on a Dell PC with 16 GB RAM and Intel i-7 3770K CPU @3.5 GHz.

2.4.1. Voxelisation and Rendering

The time required for voxelisation of some sample models are given in **Table 1**. The Bunny STL model had 10400 facets and the pelvis bone STL file had 41,100 facets (8,978 kB). At the resolution of 1000×1000×1000, the time taken was 50-100 seconds depending on the shape and size. **Figure 7** shows the voxelised Bunny model at two different resolutions.

Table 1: Voxelisation results

Model	No. of facets	Resolution		
		200×200×200	500×500×500	1000×1000×1000
		Time (s)	Time (s)	Time (s)
Bunny	10400	7.142	37.012	97.15
Teapot	57600	4.6	21.459	56.57

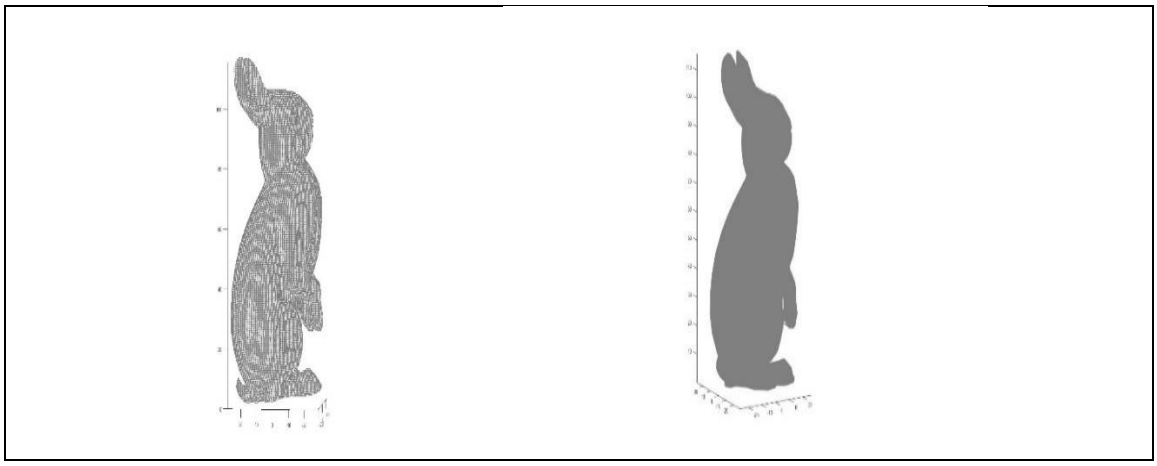

Figure 7: Voxelised model of Bunny at Grid resolution (a) 200 ×200×200 (b) 800 ×800×800

2.4.2. Minimum Feature Size

The results of minimum feature size analysis for few sample models are given in Figure 8. For models (a)-(c), all features which have feature thickness less than 1mm in any direction have been highlighted. The sample widget shown in Fig. 8(a) has rectangular features with wall thickness 0.3 mm, 0.5 mm and 2 mm. If the minimum resolvable size in x-y plane of machine being used to manufacture this part is 1 mm, the highlighted features would not be manufactured correctly. Consider the coupler shown in Fig. 8(b) to be manufactured by Material Jetting. In Material Jetting, the minimum Survivable Feature Size for such circular features has been shown to be 1.13 mm [2]. Hence, these features mostly would not survive post- processing. Similarly, for Snowman model shown in Fig. 8e), the sharp corners at the eyes, nose, buttons and hands have one voxel each with voxel dimension less than 0.2 mm. Hence, these sharp corners would not be manufactured on an AM machine with resolution less than 0.2 mm in all directions.

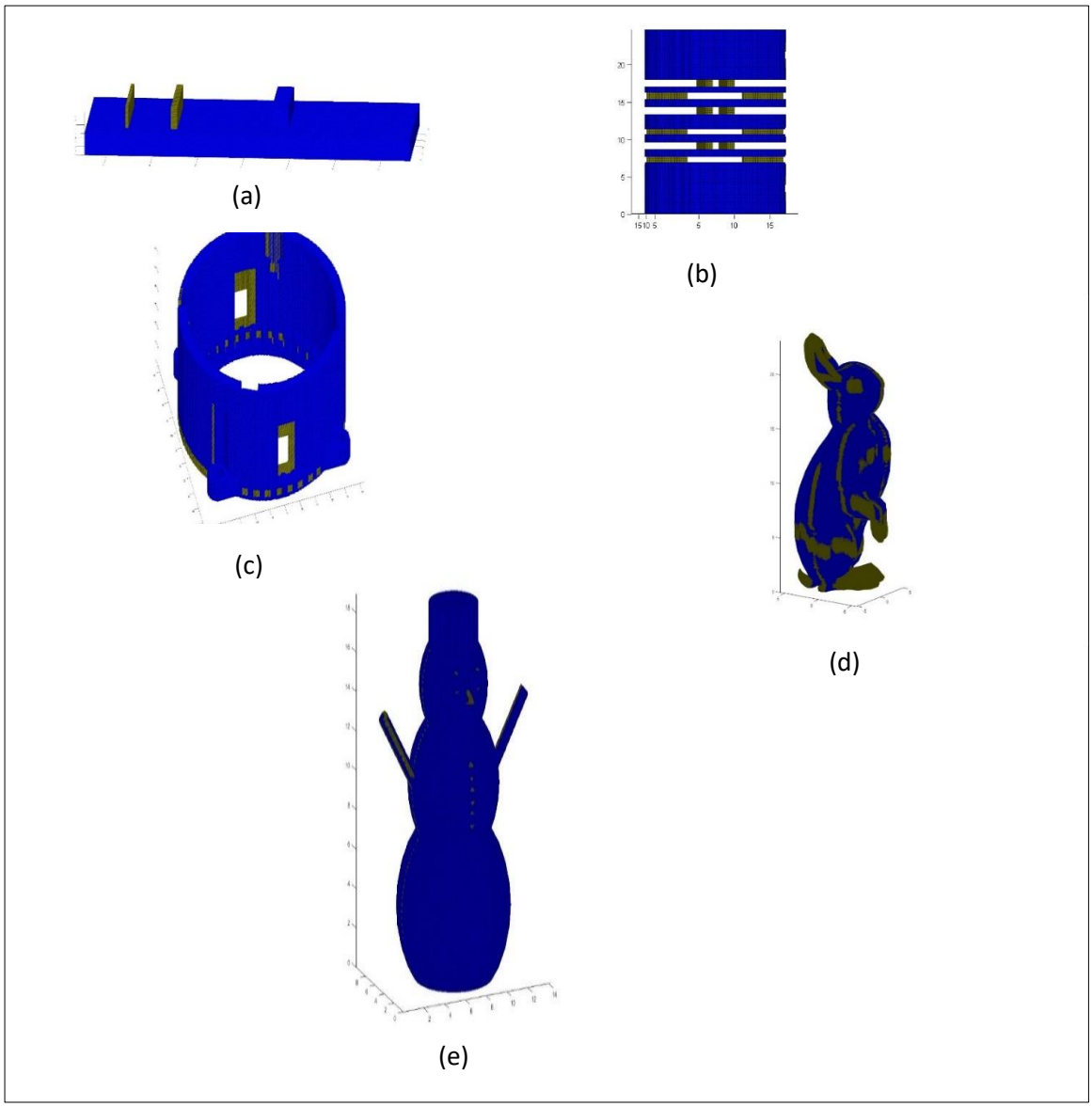

Figure 8: Highlighted Feature sizes, t <=1 mm for a) Sample widget b) Coupler c) Gear Housing, t < 2 mm for d) Bunny and t <0.2 mm for e) Snowman models in any direction

The results of negative feature size analysis for two sample widgets at resolution 500×500×500 are shown in **Figure 9**. The problematic areas which would not be manufactured correctly have been highlighted. Consider a sample widget with a star shaped hole as shown in Fig. 5a. The extreme corners of the star shaped hole have one voxel inside it. The size of this voxel is less than resolution of the AM machine in that plane, and hence the corner would not be manufactured correctly. Here, the machine resolution or minimum desired thickness of negative space has been set to 0.2 mm in all directions. Consider another sample widget with circular holes as shown in Fig. 5b to be manufactured by Material Jetting. In Material Jetting, for efficient removal of support material, circular negative features in Vero WhitePlus specimens must have cross-sectional area less than or equal to $50\ mm^2$ [2]. The highlighted features in Fig. 9b have cross-section area less than $50\ mm^2$ and hence would not survive post-processing. Hence, the area feature can be useful to control the size of regular shaped negative features.

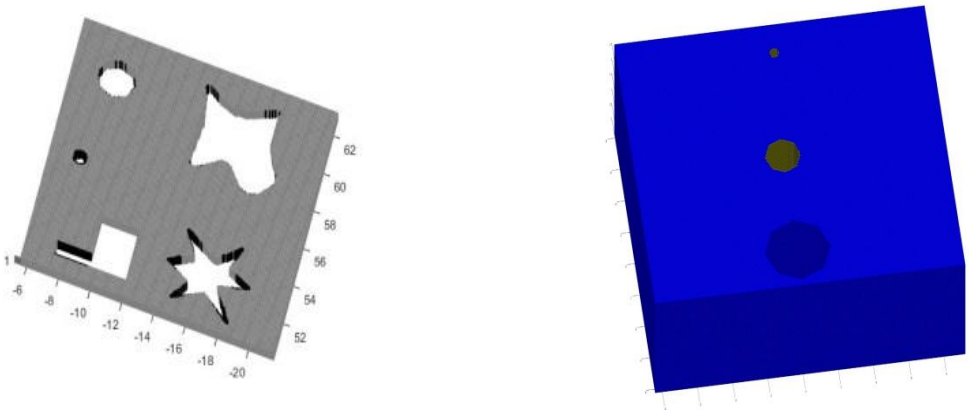

a) b)

Figure 9: Negative feature analysis at resolution 500×500×500 a) Features highlighted with t=0.2 mm between boundary voxels in any direction b) Features highlighted using minimum area criteria, A<50 mm^2

2.4.3. Sample Case Study for Feature Size

Figure 10 shows CAD model of a sample widget to be manufactured using Material Jetting which has three circular holes (1, 2 and 3), one cylindrical feature (4), two overhangs (5 and 6) and a star shaped hole (7). The part is printed in the orientation shown in Fig. 6 using Objet Connex 350 machine.

The results of minimum feature size analysis are shown in **Figure 11**. The voxel size in Objet Connex is 0.09×0.06×0.03 mm. Features with thickness less than the voxel size in respective directions would not be manufactured properly. Moreover, features with thickness less than 1.13 mm in any direction are expected to break away either during printing or post-processing. The results show that features 4 and 5 would either not be manufactured correctly or break during post processing. The results of negative feature size analysis are shown in **Figure 12 (a)** and **(b)**. Circular negative features 1 and 2 are highlighted as they have cross sectional area less than to $50\ mm^2$and hence are expected to have support material trapped inside them. Also, according to the analysis, the corners in feature 7 i.e. star shaped hole will not be manufactured correctly.

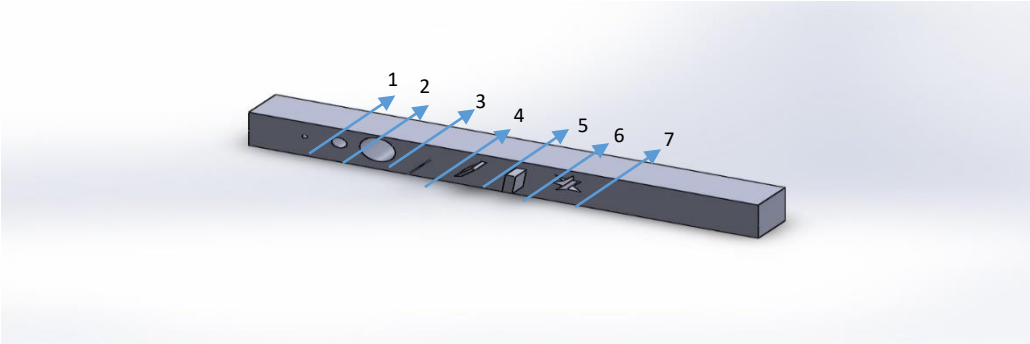

Figure 10: CAD model of sample widget for Case Study

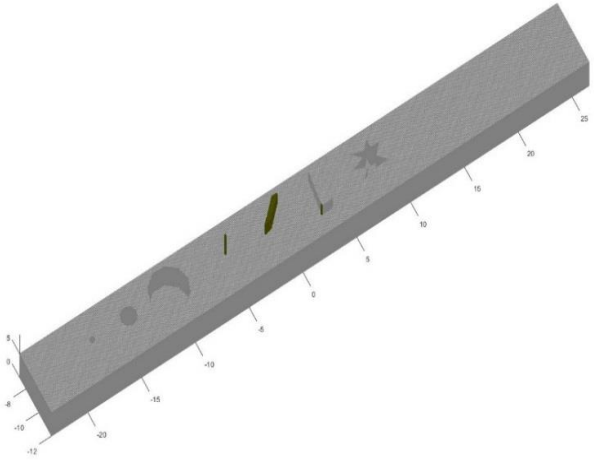

Figure 11: Highlighted Feature sizes, t <=1.13 mm of sample widget for Case Study

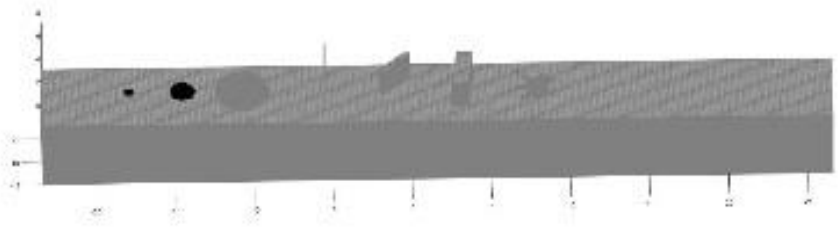

(a)

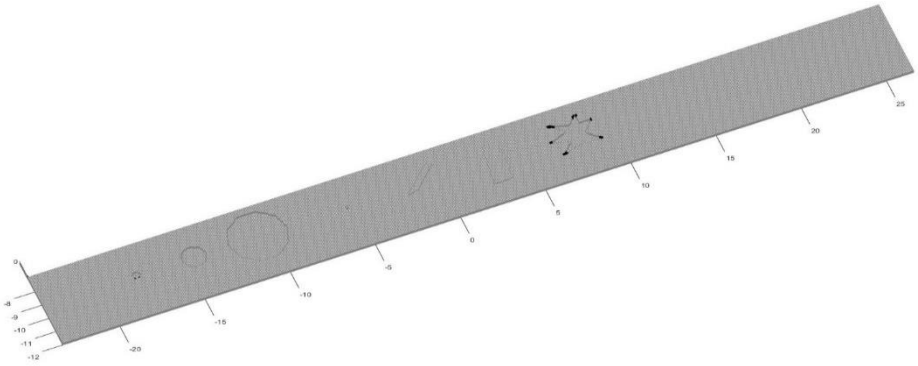

(b)

Figure 12: Negative feature analysis a) Features highlighted using minimum area criteria, A<50 mm^2 b) Features highlighted with t_x =0.09 mm ,t_y =0.06 mm, t_z=0.03 mm between boundary voxels in any direction.

Figure 13(a) shows the image of the printed part after removing support material. It can be seen that features 4 and 5 have not been manufactured. While feature 4 failed to print during the printing process, feature 5 broke while cleaning support material with water jet. **Figure 13 (b)** shows that features 1 and 2 have support material trapped inside them as predicted during feature size analysis. Finally, **Figure 13 (c)** shows that the corners of star-shaped negative feature are nor manufactured correctly and have been approximated. These observations are consistent with the results of analysis.

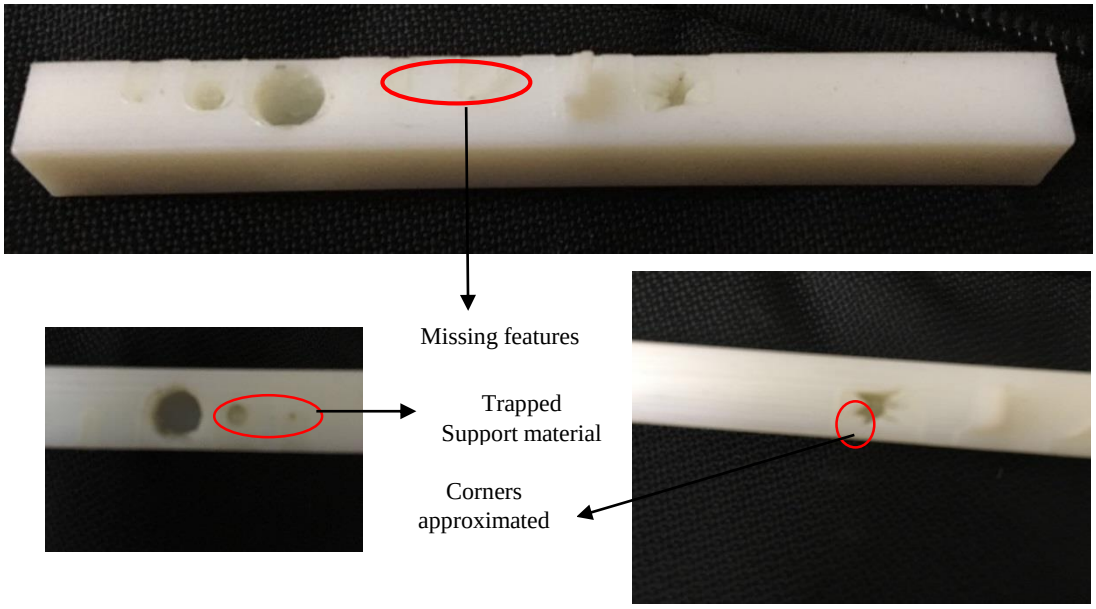

Figure 13: a) Sample widget manufactured using Material Jetting b) enlarged image of printed part showing trapped support c) enlarged image of printed part showing star shaped negative feature

2.4.4. Support Material Generation

Figure 14 shows steps required to generate support material for a sample part with two overhangs at $\theta_1 = 30°\ and\ \theta_2 = 75°$ respectively. Fig. 14(a) shows the voxelised model of the part. At this stage, all normal vectors for surface voxels are calculated. Next, only unsupported boundary voxels at start or end of a Z boundary are considered for further analysis. This is depicted in Fig. 14b). These voxels are mapped with normal vectors of their corresponding facets. Based on these mapped normals, support is generated critical angles 45° and 15° which can be seen in Fig. 14(c) and 14(d) respectively.

The support material feature gives satisfactory results even for models with resolution as low as 200×200×200 and gives accurate estimates of volume of support material required. At low resolutions, the user can get very quick idea of features which would require support material and modify his design accordingly. The accuracy of the estimate increases with increase in resolution. However, if the goal is to prepare the file for printing directly from voxel representation, then the voxelisation should be done at printer resolution. **Figure 15** shows support material generated for a few sample models at resolution 500×500×500 for critical angle $\theta_{cr} = 60°$. The amount of support material required and support surface contact area for these models is given in **Table 2**. The material density value used for support material calculations is 1.25 g/cm^3.

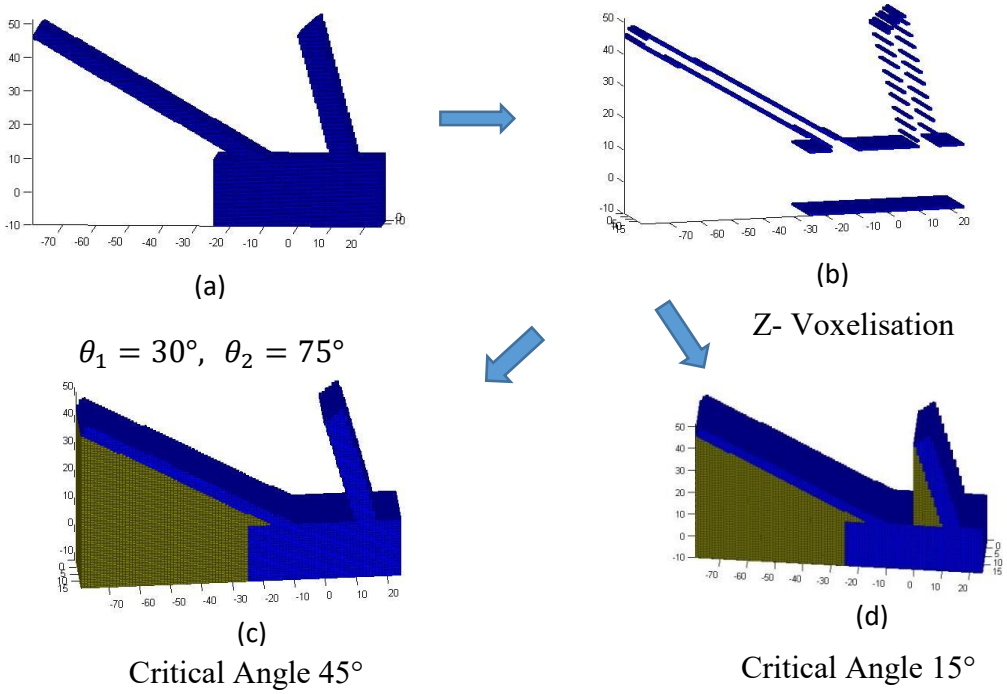

Figure 14: Support structure generation process for a sample part to be manufactured using Extrusion

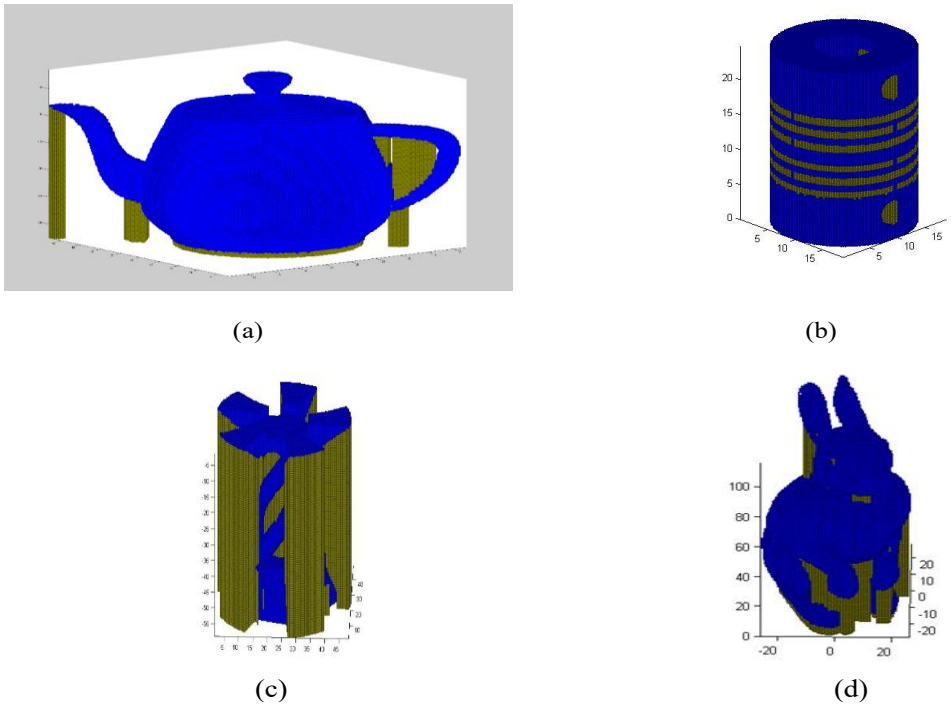

Figure 15: Required support Structures for manufacturing using the extrusion process, θ_{cr}=60° for a) Teapot b) Coupler c) Candle holder d) Bunny models

Table 2:Volume of Support Material and Surface Contact Area for given models

Model	Volume of Support Material (grams)	Support Contact Area (mm^3)
Teapot	0.839	567.3592
Coupler	1.6347	1349.4
Bunny	7.155	1378.7

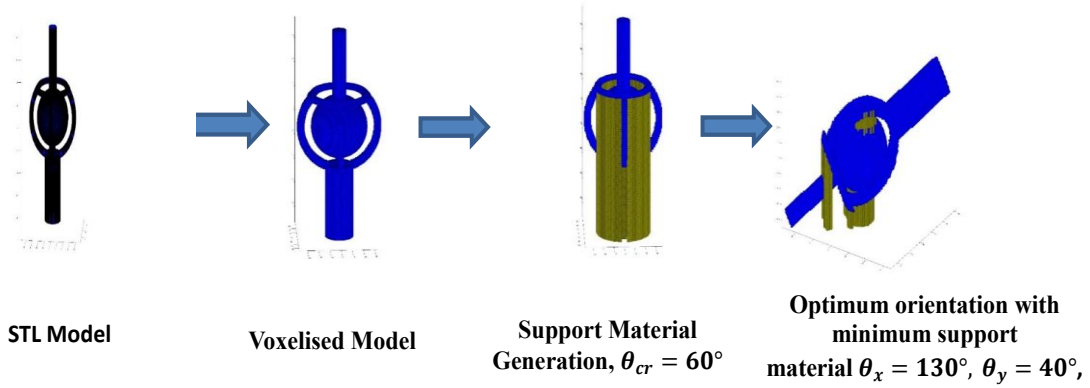

Figure 16: Identification of optimum orientation with minimum support for a sample ball joint

Figure 16 shows identification of optimum orientation with minimum support for a sample ball joint model. Starting from original orientation, the tool computed supports for subsequent orientations at an interval of 10^0 and optimum orientation was identified to be $\theta_x = 130^0 and\ \theta_y = 40^0$. This result was manually verified by generating supports at various orientations using Simplify 3D software.

2.4.5. Build time estimation

After generating support material for above sample parts, build times for these were estimated for manufacturing using Material Extrusion. The build times were estimated using layer thickness 0.2 mm, printing speed 3600 mm/min, outline underspeed 50%, X/Y axis movement speed 9000 mm/min, Z axis movement speed 4800 mm/min, interior and support infill percentage 40% and support density 70%. The estimated build times for some sample models and their actual build times estimated using Simplify 3D software are listed in **Table 3**. The build times are found to very close to the actual build times estimated by Simplify 3D software.

Table 3: Comparison of estimated build time with actual build time using Simplify 3D software

Model	Estimated Build Time	Build time estimated using Simplify 3D software
Teapot	51 mins 32 secs	58 mins
Coupler	31 mins	36 mins
Bunny	144 mins 10 secs	172 mins

2.5. Closure and Future Work

In this paper, a tool has been presented for automated manufacturability analysis of shapes to be manufactured using Additive Manufacturing. The input polygonal model is first converted to a voxel model using Ray Casting Algorithm. Various simple and easy to implement algorithms have been presented to evaluate various factors governing manufacturability. The quick feedback provided by the tool can be easily used as an initial assessment of manufacturability and gives an idea to the user about features that might not be manufactured correctly, estimation of support material, support contact area and build time.

The major problem associated with voxel representation has always been large memory requirement which limits voxelisation resolution [7]. The main focus of this research is manufacturability analysis. However, this problem has been partly taken up in this work. Most of the manufacturability calculations are done during voxelisation process to keep the computations to a minimum. Some of the operations which require large computation time have been shifted to GPU using MATLAB parallel computing. However, rendering of the volume is still slower than polygonal models. This issue can be overcome in the future by using GPU based visualization technique illustrated in [42].

The authors aim to extend the reported work by validating the proposed tool and also providing additional features. For this realization following steps will be undertaken.

- Void detection feature to detect voids which may trap powder, resin or support material will be incorporated in the tool.
- A full case study will be implemented using multiple complex parts to validate the manufacturability analysis results given by the software where the results would be compared with an actual printed part.
- This tool will also be implemented in a classroom setting to evaluate the effectiveness of the tool in making DfAM decisions.
- Efforts will also be made to manufacture sample parts directly from voxel representation using Material Jetting and Material Extrusion. Toolpath generation feature for Material Extrusion will be added.
- Final research investigation will include implementing an Octree based voxelisation technique to optimize memory requirements.

Chapter 3: Implementation of rapid manufacturability analysis tools in Design for Manufacturing Education

Abstract

While modern manufacturing processes provide unparalleled design freedom, they still impose constraints on the geometries that can be successfully fabricated. Engineering students are often unaware of these manufacturing constraints and therefore tend to design parts that are either very difficult or impossible to manufacture. Hence, its necessary to educate students of the intricacies and limitations of the various manufacturing processes available to them. To address this need, this work discusses a vision for implementation of a method for facilitating Design for Manufacturability (DFM) education in Subtractive Manufacturing(SM) and Additive Manufacturing (AM) processes. The goal is to teach students (i) various factors that affect the manufacturability of a given part for both Additive and Subtractive manufacturing and (ii) how to appropriately choose between them. A classroom study was conducted in a sophomore level Mechanical Engineering design course, where students were taught the fundamentals of both technologies and were introduced to manufacturability analysis software programs. Assessments were conducted to measure students' understanding of a variety of topics in manufacturability both before and after the study. The assessment of improvement in students' conceptual manufacturing-related understanding regarding DFM principles and process selection before and after the study along with implementation of the Additive manufacturability analysis tool in the sophomore-level design project is presented.

3.1. Introduction

3.1.1. Background

While designing a component or selecting a manufacturing process for product fabrication, designers need to consider a variety of factors that govern the manufacturability of a part. Different manufacturing processes impose different design considerations and constraints on part geometries. For Subtractive manufacturing processes, manufacturability assessment requires assessing feasibility of equipment and tooling to achieve trajectories required to shape components to final form. To automate this, low-fidelity subtractive manufacturability assessment software programs exist (e.g., Apriori, Plethora [43, 44]), but these applications are severely limited in their ability to analyze and reason with complex part geometry and do not provide the higher fidelity analysis needed to facilitate automated process planning for subtractive manufacturing. In this regard, automated path planning, tool orientation, and geometry selection have been long-standing problems for subtractive manufacturing community [45-47] and still require extensive manual planning and process expertise to enable effective production. As a result, the use of CNC machine tools by students for the manufacture of complex parts is very difficult and not commonly taught in typical engineering programs. While an AM build is relatively easy to begin (e.g., toolpath creation is automated) (e.g., [48-52]), other important aspects of additive processes must be mapped and considered during the design process, including material compatibility, quality limitations (e.g., surface roughness, tolerances), and interactions between build geometry and process parameters (e.g., orientation of layers and thus anisotropy, presence of support structures, and surface area of each layer; if the surface area is too large, it can cause layer warping and delamination). [53]. Because of the ease of use, students tend to seek more user-friendly

additive manufacturing (AM) processes for producing prototype parts, such as Material Extrusion for plastics. However, this might not be the optimum choice always.

Engineering undergraduate students often have little to no practical experience in manufacturing and do not have access to or expertise to make use of manufacturer/ machine centric applications mentioned earlier. Hence, the consideration of factors affecting manufacturability of designed parts is generally difficult for engineering students. Both design and manufacturing are addressed in many undergraduate engineering curricula, but frequently, students struggle to select the best manufacturing process to fabricate their parts. Students tend to use the manufacturing process that is easily and readily available to them instead of analyzing all the factors in play and selecting the best process [54]. This creates a hindrance in effective product design. However, both in educational and industrial settings, designers are expected to be designing parts that can be efficiently fabricated with available manufacturing technologies. Hence, it is required that students gain significant experience to be able to think and visualize effectively about these manufacturing considerations. For students to be effective designers and engineers as they move into the workforce, they must not only be comfortable with both AM and SM processes, but they must also have the ability to fluidly move between the realms of thought needed for AM and SM [54].

3.1.2. Study Motivation and Literature Review

Today, undergraduate engineering curricula include courses in both design and manufacturing. Despite this, many students still struggle with synthesizing knowledge gained from these two separately taught topics to influence their design practice; i.e., design-for-manufacturability (DFM). DFM is the practice of design such that manufacturing considerations are taken into account during the design process. DFM is an essential skill for any designer, as it is essential for the efficient realization of engineered systems. Universities have tried a number of different approaches to get more manufacturing education to their students. However, the ever increasing and dynamic content in the field of manufacturing education has led to universities focusing on teaching basic introductory courses on Manufacturing Technology. Many times, these courses are offered as electives outside the department [55], which not all students prefer to take. Also, sometimes these undergraduate courses teach theoretical concepts supporting analysis of manufacturing processes, but students are frequently not taught to actually implement the processes discussed in the course in a design context. The difficulties in implementation can be attributed partially to the cost required to run the manufacturing lab/ facility [56]. Hence, it is necessary that students visualize the various considerations in these processes using software visualization/analysis/ simulation tools that provide direct feedback to students regarding their designs.

The use of the computer/ software programs for teaching instruction is known as Computer Assisted Instruction (CAI) or Computer Assisted Learning, (CAL) [57]. This work seeks to develop a computer assisted learning (CAL) approach to DFM education that relies on the use of computer visualizations through manufacturability analysis software programs to teach students about design considerations essential for manufacturability of their parts. CAL allows for a large number of students to access a learning resource simultaneously without the help of an instructor, and is useful in visualizing complex concepts [58]. Several studies have shown that groups of students who are using CAL have better results than groups using traditional learning [59-61]. Some studies even demonstrate that students using CAL needed shorter time to reach the learning objectives, achieving better results than students who did not have access to CAL [61, 62]. Another interesting finding is that students with learning difficulties or less previous experience sometimes significantly improve their learning using CAL compared to stronger students [63].

In the field of engineering education, the use of computer-based learning is commonly implemented using computer-aided design (CAD) software in introductory courses. CAD allows students to create digital models of parts and assemblies and visualize them before manufacturing. Additionally, students can use computer-aided engineering (CAE) software to perform simulations of physics in complex systems. Some researchers have applied computer-aided manufacturing (CAM) software in the classroom to help educate students about concepts in manufacturing. CAM has been shown to accelerate the pace of teaching students about subtractive manufacturing concepts [64]. Koh, et al developed interactive simulations to teach students how to operate milling, turning and drilling machines; results from a post-training exercise demonstrated that students exposed to the computer simulations of machine tools had a superior grasp on the operation of those machines than students who were simply lectured on those machine tools [65]. However, the goal of the software was only in training the use of the machines, not in making design decisions on part geometry. In slightly different application, Ebner and Holzinger performed a study with civil engineering students in which a computer game was used to educate students about the theoretical aspects of designing structures with concrete [66]. While the goal of the game was simply to provide an alternative to traditional teaching approaches, the researchers found that students subjected to the experimental protocol scored far higher on user empowerment and fun factor indices than students in the control group. Gillet et. al deployed a web-based flexible learning system to allow students to perform simulated experiments in biomechanics, fluid mechanics and automatic control [67]. The students were also provided with a collaborative workspace in which they could solve problems together; this study showed that engineering students are generally receptive to computer-assisted learning practices.

3.1.3. Research Goal

This research relies on the implementation of two previously developed voxel-based software programs in an undergraduate classroom setting, SculptPrint [68] and Additive Manufacturing Software (described in Chapter 2) [53, 69] to help students visualize the manufacturability of their designs. The aim of this study is to evaluate whether instruction using these software programs improves students' ability to make decisions about process selection between Additive and Subtractive Manufacturing to efficiently design their parts. These software programs use a voxelized representation of the geometry, as opposed to typical surface representations, which enable accurate representation of these processes. Voxels are the three-dimensional equivalent of image pixels, and they can easily be added or subtracted from a part model to simulate material deposition or removal, respectively [53]. In this work, we are looking to answer the following research questions:

- RQ1: What is the prior level of manufacturing experience and understanding of DFM concepts of students at undergraduate level in universities?
- RQ2: How is a student's choice of a manufacturing process influenced by exposure to teaching/instruction using manufacturability analysis software programs?
- RQ3: How does students' prior experience in manufacturing impact the effectiveness of the DFM intervention?
- RQ4: How does the practical implementation of manufacturability analysis software programs affect students' design choices?

3.2. DFM Classroom Intervention

3.2.1. Classroom Context

The students selected to participate in the current study were enrolled in an introductory design course (ME2024) at Virginia Tech (VT). ME2024: Engineering Design and Economics is a sophomore-level mandatory design course at VT. ME2024 is required for all undergraduate students seeking a degree in Mechanical Engineering. The goal of the course is to ensure that students are exposed at an early stage to engineering design methodologies. Students are taught several modules on how to use the problem statement to identify solutions, select criteria and use them to evaluate solutions, determine the design details, prepare graphical representations and explore and discover simple cost effective engineering systems. Students enrolled in this course have some experience in CAD as they have already taken the fundamental Introduction to Engineering freshmen level course. The majority of class time is devoted to in-class activities which students have to complete with their design team. This course serves as students' first formal introduction to the realization of a functional device. ME2024 is a course that also makes use of Project based learning. Students enrolled in the ME2024-Engineering Design and Economics course have to do a mandatory semester long project, which involves applying the concepts taught in class in order to design a product for a business idea. The project is evaluated in three phases with a final presentation and report submission in the end. Some of the essential concepts taught to the students in this class which are also a key part of their final project are summarized below in Table 4:

Table 4: ME2024 Curriculum

Timeline	**Key Topics Covered**
W1	Product development and Process overview
W2	Project Management
W3	Engineering Economics
W4	Design for Manufacturing
W5	Concept Generation
W6	Failure Mode and Effect Analysis
W7	Design for Assembly
W8	Product Architecture
W9	Breakeven and Sensitivity Analysis
W10	DFM- Injection Molding
W11	Design for Environment

The Design for Manufacturing lecture series in week 4 was included in the ME2024 curriculum for the first time because of the DFM intervention and no such module was being taught in any other sophomore level course. However, as we identified a need for implementing rapid manufacturability analysis tools in undergraduate classroom for enhancing DFM education, we decided to carry out a classroom intervention for the same. The intervention was conducted over two classroom sessions of 50 minutes each. The first lecture session was conducted on Subtractive Manufacturing, while the second lecture session focused on Additive Manufacturing. Due to the limited amount of in-person classroom time, a more detailed pre-recording of the lectures and slides were made available to the students before the trial in a "flipped classroom" setup.

3.2.2. Subtractive Manufacturing

The instructional content for in-class lecture was prepared to enhance students' understanding of DFM concepts and make them realize that how product design decisions

affect manufacturing decisions and in turn how manufacturing decisions affect product design. The first lecture was focused on communicating basic DFM concepts for Subtractive Manufacturing, mainly turning and milling. The lecture began with introducing the students with turning and milling, basic terminologies associated, and various types of tools and inserts commonly used along with their applications. Students were then taught about general DFM guidelines about turning and milling. Fig. 17 shows snapshot of one of the lecture slides showing DFM guidelines for Turning.

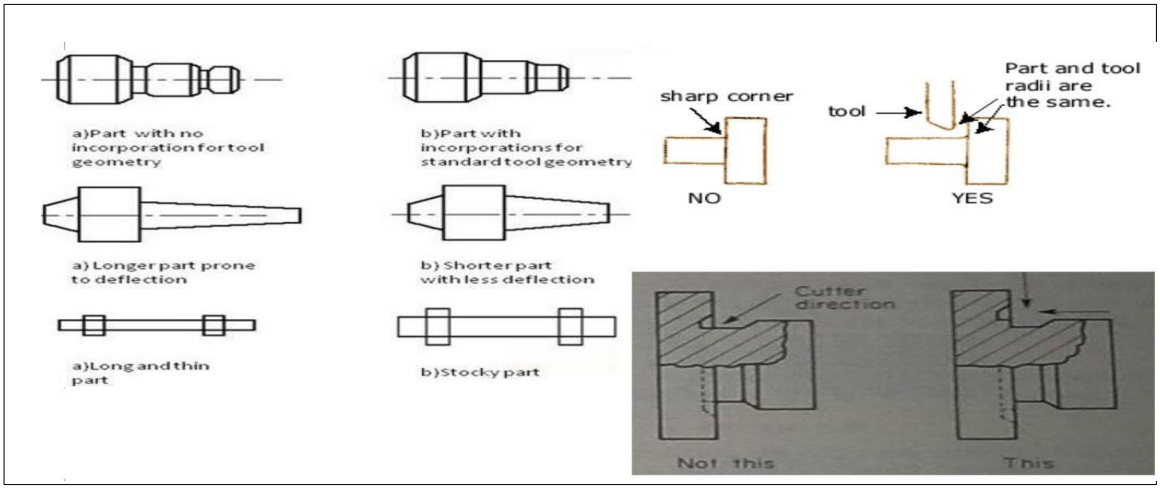

Figure 17: Snapshot of example Lecture slide showing sample DFM guidelines for Turning

This was followed by solving an in-class example. An example question taken up is shown in Fig. 18. The rook sample part shown is to be fabricated by standard 35-degree Right Handed diamond insert tool. This exercise was designed to educate students about the positive and negative relief angles and minimum internal corner radii that can be achieved. As it can be seen, the top of the pawn has a very small radius and both positive and negative relief angles, which cannot be achieved using the standard available tool.

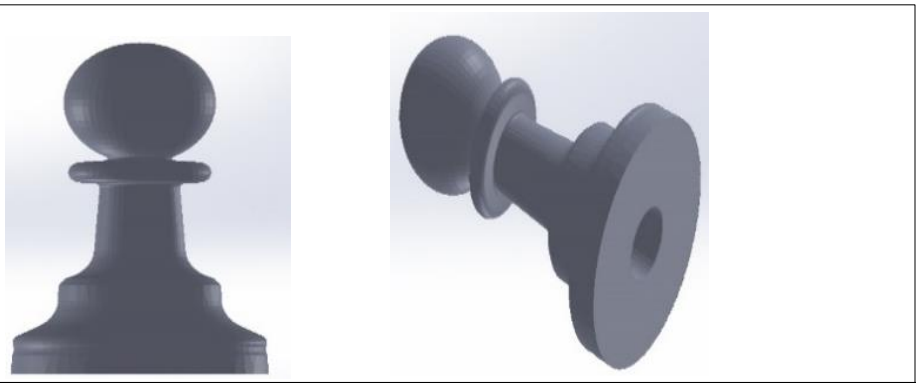

Assume you only have access to a 3-axis CNC machine and a Lathe. Answer the following questions for the above part:
What type of machining process(es) would you choose to make this part (e.g., 2-axis lathe, 3-axis mill, 4-axis mill)? Why?
What features of this part are difficult to machine? Circle these troublesome features and describe why they are difficult.

Figure 18*:* In-Class Example Geometry and Question

To help the students visualize these factors, students were shown a pre-recorded simulation of the Turning process for fabricating the Pawn using the same cutting tool in

Sculptprint software. The output image from SculptPrint simulation of the Pawn is shown in Fig. 19.

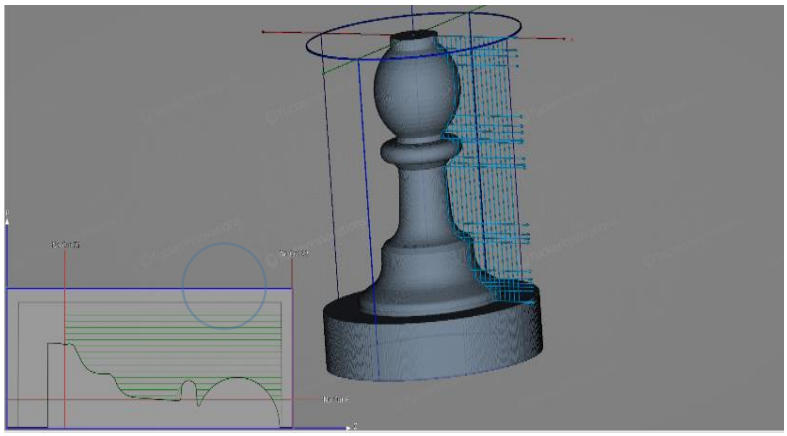

Figure 19: SculptPrint output for Pawn geometry

The lecture was followed by an in-class exercise. A representative sample of these questions is provided in Table 5. The responses were designed to be answered as free (open) responses, with the possibility of visual representation (e.g., sketching) of answers to best capture a range of understanding from the students.

Table 5: Sample Assessment Questions and Type

Type	**Assessment Question**
Machine capability	Which, if any, of the features shown are impossible to create on a 2-axis lathe?
Fixturing	Where would you fixture this part to reach all the features?
Tooling	What is the smallest number of available tools needed to make this part?
Machine Selection	What type of machining process(es) is able to make all features of this part

To complete this exercise, students were allowed to work together in groups of four, which is a general trend in this class. A representative question asked in the in-class exercise is shown in Fig. 20. In this example, the students were asked to use a 35° Right Handed cutting tool to attempt to achieve the target Dumbbell part through Turning. This part contained both positive and negative vertical reliefs that necessitated the use of both right-handed and left-handed tooling. The students were instructed to sketch the final shape of the part after the Turning operation.

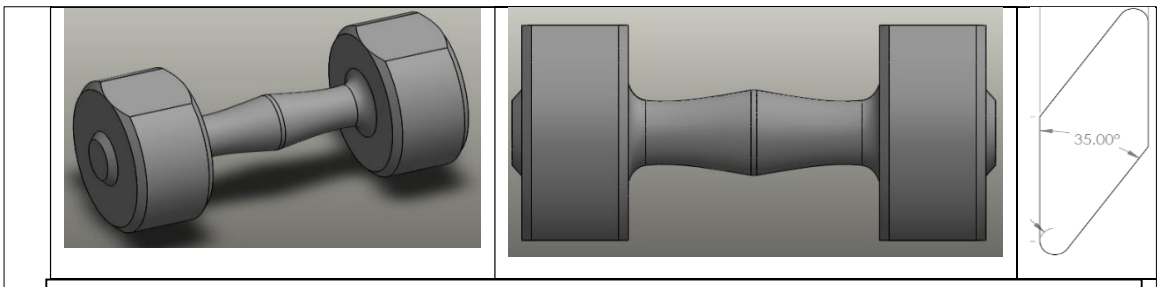

1. Assume you only have access to a 2-axis Lathe and a single, right-handed insert (see figure above). Redraw the side view of this part after the machine has cut all the material it can reach.

2. What type of machining process(es) is able to make all features of this part (e.g., 2-axis lathe, 3-axis mill, 4-axis mill)? Why? Briefly describe the process steps.

Figure 20: Representative in-class exercise question

After the in-class exercise, students were presented with the output images from SculptPrint simulations of all the geometries that appeared in the in-class assessment. The output image from SculptPrint simulation of the Dumbbell question is shown in Fig. 21. The circled blue region shown denotes the region where the desired shape could not be realized by using the 35° RH cutting tool. These output images were intended to help the students visualize the final shape of the part and features that would be impossible to create with the given tooling.

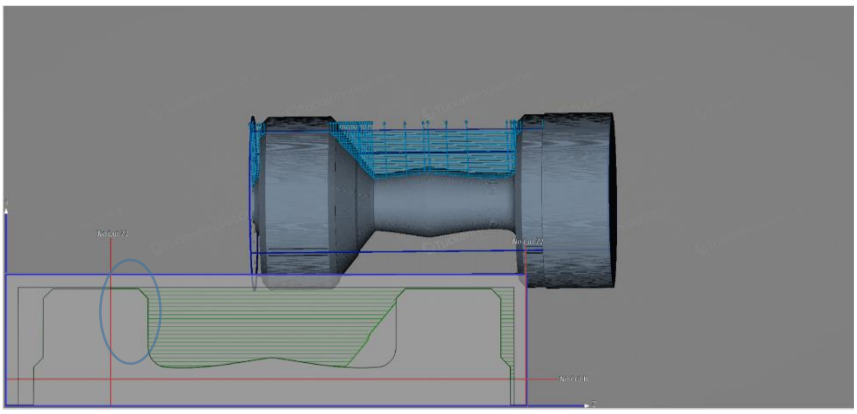

Figure 21: SculptPrint output for Dumbbell geometry

The assessment also contained questions on milling. Fig. 22(a) shows an example of geometry to be fabricated using 3-axis milling. The milling analysis using Sculptprint, which was also shown to the students at the end of the session, demonstrated the machining limitations imposed by a standard 3-axis machining center. The blue points in Figure 22(b) are areas that are inaccessible by the tool when this example part is fixtured to the table of a 3-axis machine.

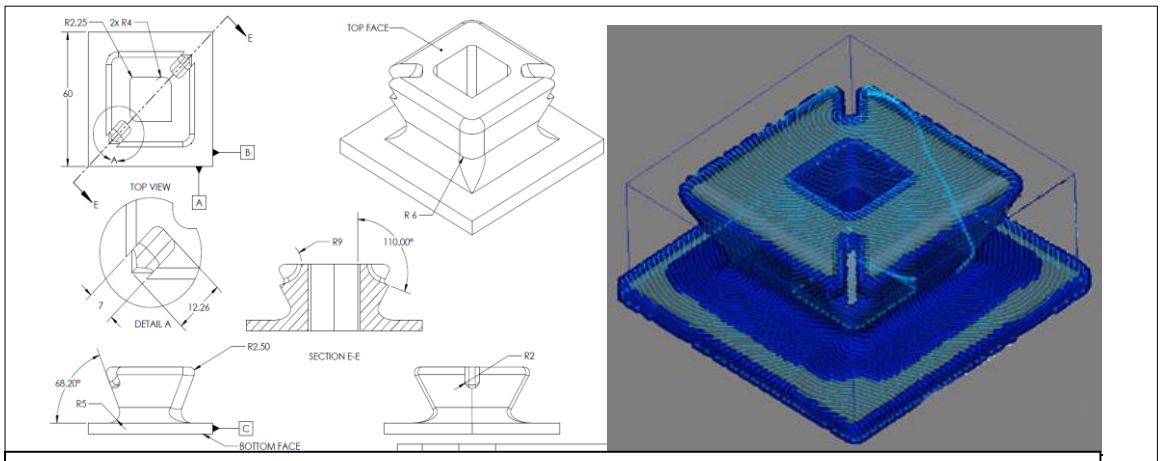

1. Assume that the part is arranged such that datums A, B and C are parallel to the X, Y and Z axes, respectively. The bottom face, shown in the print, is coincident with the table of a milling machine. The machine has three servo axes: X, Y and Z. Redraw section E-E after the machine has cut all the material it can reach.
2. Now assume that the part is arranged such that datum C is parallel to the X axis. The part is fixtured on a vertical machine with four servo axes: X, Y, Z and A, where the A axis rotates around X. With these axes, the tool is able to translate around in XYZ and the part can rotate around X. Redraw section E-E after the tool has removed all the material it can reach.

Figure 22: Sample representative question for milling b) SculptPrint output for widget to be fabricated using 3-axis milling

3.2.3. Additive Manufacturing

The second session began with a lecture on Additive Manufacturing. The lecture content initially focused on the basics of Additive Manufacturing and the different type of Additive Manufacturing technologies. The lecture later focused on factors affecting manufacturability of a part in Additive Manufacturing, namely minimum feature size, amount of support material, orientation of the part, build time and manufacturing cost.

Similar to the previous session, the lecture was followed by solving an in-class example. The example question taken up is shown in Fig. 23. In the example, the ball joint geometry shown was to be manufactured using a desktop Extrusion AM system that can print only one material (ABS) with layer thickness 0.5 mm. The purpose of the question was for students to consider different orientations and choose the one which would save time and material.

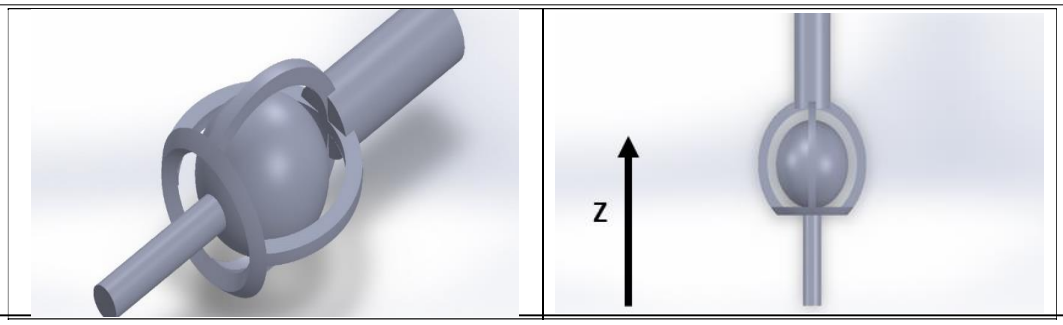

1. Assume you only have access to an Extrusion AM system that can print only one material (ABS). What are the challenges in making this with Additive Manufacturing in the orientation shown on the right?

Figure 23: In-Class Example Geometry-Ball Joint

To help the students visualize these factors, students were shown feedback results for ball joint obtained from Additive Manufacturing software described in Chapter 2. To visualize the best possible orientation for minimizing support material as well as identifying thin features just by looking at the CAD model is sometimes non-trivial. Fig. 24 shows the basic workflow for DFAM analysis of ball joint. The feedback images allowed the students to visualize thin features and support material in different orientations and choose the best possible among them. The software also provided statistics on total material consumption, total support material consumption, build time and cost to manufacture the part which can help understand different build scenarios.

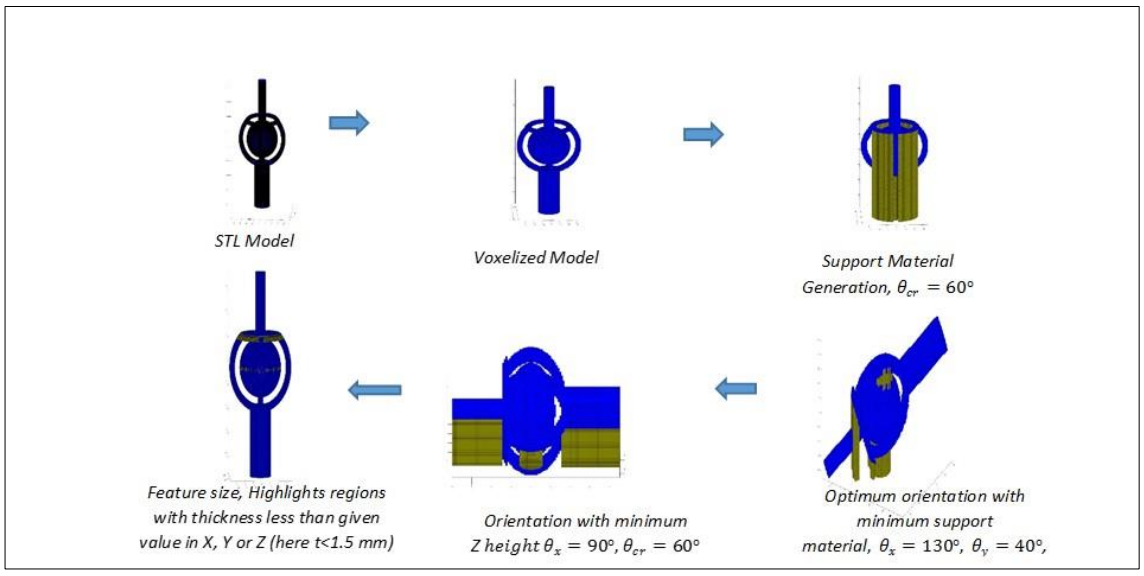

Figure 24: Manufacturability feedback for ball joint geometry using Additive Manufacturing Software

Next, this lecture was followed by an in-class assessment. A representative sample of the questions asked in the assessment is provided in Table 6. The questions were not only based on factors affecting manufacturability in Additive Manufacturing, but also asked the students to choose the best process between Additive and Subtractive Manufacturing. The purpose of this assignment was to make students think about manufacturing decisions simultaneously for using Lathe, Machining and 3D printing for fabricating the same part. Students again worked together in groups of four and were encouraged to give free (open) responses with visual representation (e.g., sketching). Full credit was given even if they did not give the right answer but identified the correct critical design features and gave proper reasoning for their answer.

Table 6: Sample Assessment Questions and Type

Type	**Assessment Question**
Minimum Feature Size	Which of the features are impossible to create on given desktop Extrusion System?
Orientation	Which orientation would you choose to print this part?
Support Material	Identify the features that require support material to be printed?
Process Selection	Would you recommend making this with Additive or Subtractive Manufacturing?

Fig. 25 shows one of the representative questions given in this in-class assessment. The width of the key slots were given to be as S5= 1.2 mm; S6= 1 mm; S7= 0.7 mm; S8= 0.3 mm, and fillet radii were given as: S3= 4 mm; S4= 0.3 mm. The students were asked to identify the features that cannot be manufactured using Additive Manufacturing. The question assumed access only to a desktop Extrusion AM system that can print only one material (ABS) with layer thickness 1 mm. Students were also asked to consider the best process(es) for making the part using Subtractive Manufacturing using minimum number of steps.

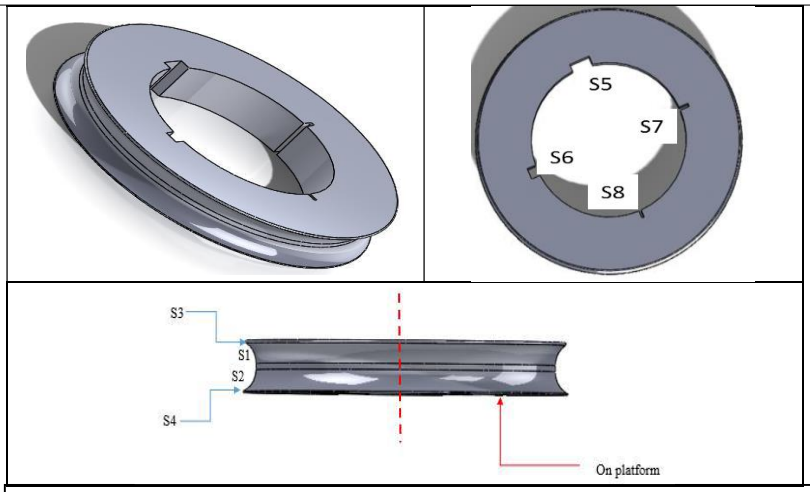

Assume you only have access to an Extrusion AM system that can print only one material (ABS). Width of the key slots: S5= 1.2 mm; S6= 1 mm; S7= 0.7 mm; S8= 0.3 mm, Fillet radius: S3= 4 mm; S4= 0.3 mm

1. Which orientation would you choose to print this part? Justify your answer?
2. For this orientation, identify the features that cannot be manufactured.
3. What process(es) would you use to make this part using Subtractive Manufacturing?

Figure 25: Representative geometry of in-class assessment question

To help students gain practice in appropriately choosing between AM and SM processes, students were also given five questions on process selection. Students were asked to assume that the cost of the technologies for making the same part were to be roughly assumed in increasing order of Lathe, 3-axis machining, 4-axis machining, 3D printing and 5-axis machining. In case of Subtractive Manufacturing, students were encouraged to use minimum number of axes which could make all the features. However, they were also encouraged to think the number of times they had to refixture the part if they choose to opt for a process with lower number of axes and whether it was practical and less cheap than the alternatives.

Fig. 26 shows the geometry for one of the sample process selection questions for the in-class exercise. According to the given dimensions in the CAD geometry, the angle at the neck of the horse is very tight for the standard tool to reach, Also, undercut below the waist cannot be reached and would require refixturing. Theoretically, the part can be made using a 4-axis machine but it would require special tooling and fixturing. On the other hand, AM could easily make both these features. The only consideration in 3D printing that students should keep in mind that the resolution of machine given in the question is high enough to accurately manufacture the gap between the mouth. Students were asked to justify their choices and were given partial credit for correct justification points.

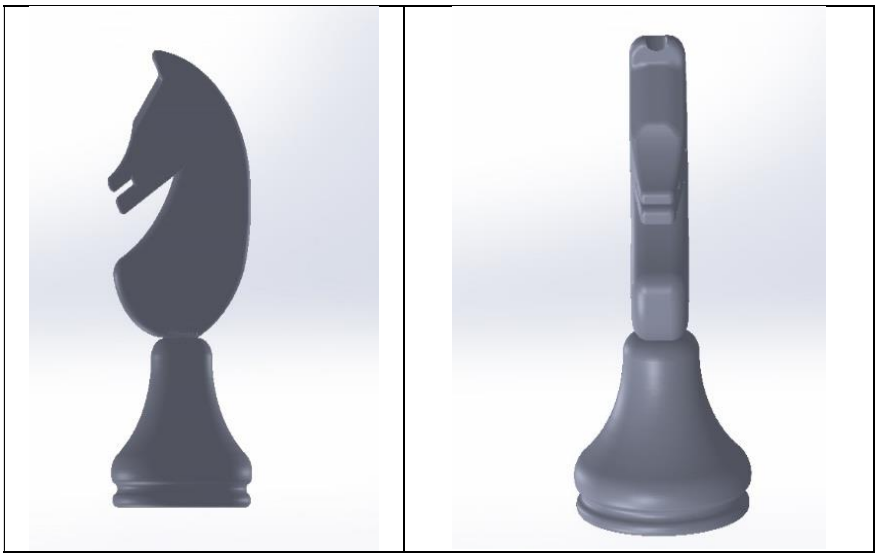

1. How would you recommend making this with Subtractive Manufacturing? (2 axis lathe, 3 axis mill, 4 axis mill, 5 axis mill)
2. What are the challenges in making this with Subtractive Manufacturing? (highlight any difficult to make features)
3. What are the challenges in making this with Additive Manufacturing? (Assume you only have access to an Extrusion AM system that can print only one material (ABS))
4. Would you recommend making this with Additive or Subtractive Manufacturing? Why?

Figure 26: Geometry for sample Process Selection question in the in-class assignment

In order to better visualize the DFM factors and help them understand their choices, students afterwards were shown output feedback images for all the parts shown in the assessment from both Sculptprint and the Additive Manufacturing software. The scope of this exercise was to give them feedback on manufacturability of the parts using both Subtractive

and Additive Manufacturing and help them understand and rethink their choices. The output image from SculptPrint and Additive Manufacturing software for the pulley question is shown in Figs. 27 and 28 respectively.

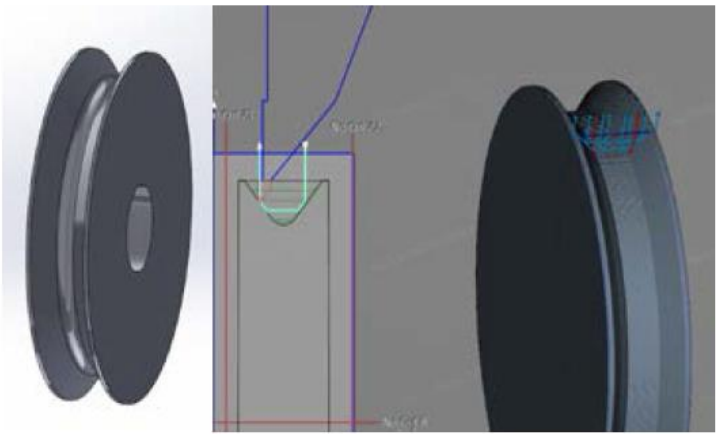

Figure 27: Sculptprint output for pulley geometry

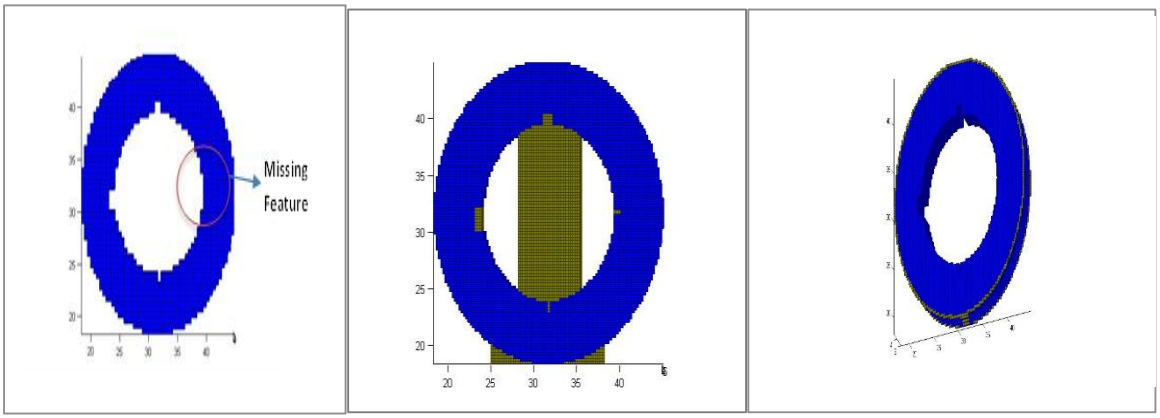

Figure 28: Manufacturability feedback for pulley geometry using Additive Manufacturing Software a) Voxelised Model b) Support Material Generation c) Minimum Feature Size

3.3. Assessment

As stated in Section 3.2, a major goal of the classroom intervention was to educate the future workforce on DFM skills so that they could fluidly choose between AM and SM processes for efficient product design. To assess student gains in these areas, the authors employed a pre/post survey technique. Students were instructed to complete a Pre-Test and Pre-Assessment Survey before coming to the classroom intervention. Both the Pre-assessment and the Pre-Test were given before any lecture material was provided to the students. After the DFM classroom intervention, students were asked to complete a Post-Assessment survey.

The Pre-Assessment questions were focused to gauge any prior manufacturing experience in Lathe, Machining, and 3D printing and their relative level of expertise. The Pre-Test included questions to assess the students' capability to choose between different manufacturing processes in order to fabricate different geometries. The Post-test contained similar category of questions as the Pre-Test. The purpose of post-assessment survey was to evaluate changes in students' understanding of DFM concepts as a result of the DFM exercises. In this study, Sculptprint is used only in a traditional lecture format as described in previous

section, whereas the Additive Manufacturing Software was provided to the class post-trial, which students used in their final semester project to visualize manufacturability feedback and improve their designs. Students reported the results of the software implementation in their final project reports. The schedule of assessment deployment is presented in Table 7.

3.3.1. Pre-Assessment

Before the trial, students were asked to complete both the Pre-assessment survey and the Pre-Test. The purpose of Pre-assessment survey to gather data on their initial understanding of manufacturing processes. The Pre-assessment contained questions to gather data on students' prior experience in manufacturing processes were also asked to rate the level of expertise in Machining and 3D printing experience among four pre-defined categories on a Likert scale based on the Dreyfus model of skill acquisition [70]. The categories along with their definition are listed in Table 8. They were also asked whether they had taken any previous courses on manufacturing processes. The Pre-Assessment was done out of class before the students came for the trial.

Table 7: Assessment Schedule

Session	**Instruction type**	**Lecture/ Instructional Content**	**Assessment**	**Assessment Scope**
Pre- Trial	None	None	Pre-assessment (Online Survey)	Prior Experience
Pre- Trial	None	None	Pre-Test (Online)	Manufacturing process choice
Post-Trial	None	None	Post Test (Online)	Manufacturing process choice, Feedback on improvement
Final Class Project	Video Lecture	Instruction to use DFAM software	Report	Manufacturability feedback for Additive Manufacturing

Table 8: Expertise Assessment Categories in Pre-Assessment Survey

Expertise categories	**Definition**
Novice	(Student has no or very little experience in this area and lacks confidence in ability to complete tasks)
Advanced beginner	(Student has some skills and previous experience in this area, but requires frequent assistance to complete tasks)
Competent	(Student is confident in his ability to complete tasks in this area)
Proficient	(Student has significant prior experience and is confident in his ability to complete tasks in this area and learn new technologies)

The Pre-Test was conducted in class just before the DFM intervention started. The Pre-Test contained questions on Manufacturing Process selection for various geometries. The assessment consisted of a total of 5 such questions. The CAD files for all the geometries were given to the students so that they could visualize and understand the geometry of these parts. This survey was designed to gather data on the prior knowledge/ experience of the students in DFM concepts and evaluate how comfortable they are in evaluating the advantages and disadvantages of each process. It was aimed to quantify the students' ability to choose between fundamental Subtractive Manufacturing processes and 3D printing before the trial. An

example representative question that appeared in the Pre-Test is shown in Fig. 29. The example part shown is axisymmetric and hence can be fabricated easily on a 2-axis lathe. Appendix A lists all the geometries and questions that were given to the students in the Pre-Test.

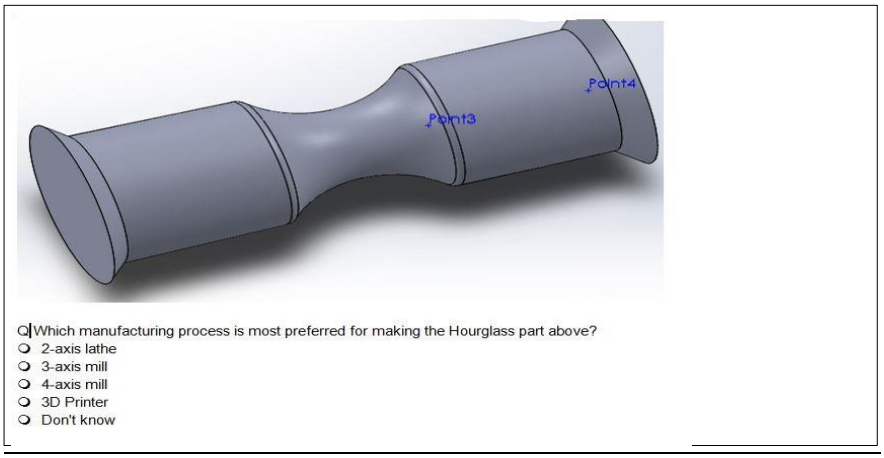

Figure 29: Example assessment question in Pre-Test

3.3.2. Post- Assessment

To gauge the improvement in students' ability to select the most appropriate manufacturing technology among Additive and Subtractive Manufacturing processes for their designs, as compared to before the study, a Post-Assessment survey was conducted out of class after the study. The Post-Assessment survey contained questions similar in format to the pre-test. The assessment consisted of a total of 8 multiple choice single correct answer questions containing different parts. Students had to evaluate the different geometries and select the best manufacturing process to manufacture the part. Similar to the pre-test, the questions were intuitive and had the same assumptions as process selection questions in the in-class assignment.

A representative question that appeared in the Post-Test is shown in Fig. 30. The example teapot geometry shown is clearly a 3D printing part as the tea pot is hollow and material removal from inside the part is not possible. Appendix B lists all the geometries and questions that were given to the students in the Post-Test along with the web links for the geometries.

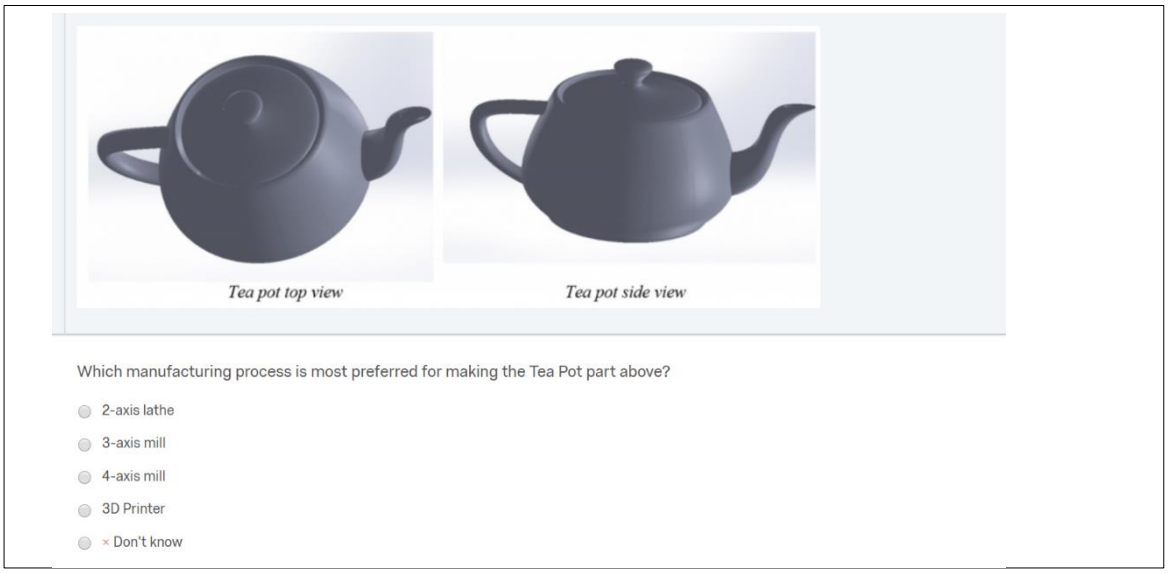

Figure 30: Example assessment question in Post-Test

3.3.3. Final Semester Project

As an additional exercise for their final project, students were instructed to use 3D printing to print one of the components of their design. The parts were to be fabricated using a Material Extrusion machine, namely Fortus 400 mc using Nylon12 material. The problem statement also stated that the designed component should fit in a build envelope of $4 \times 4 \times 4\ in^3$. Students were asked to use the Additive Manufacturing analysis software to perform a DFM analysis and acquire feedback regarding infeasible features, build materials, amount of support material, build time and cost of their design. They were also asked to examine different build orientations to minimize these statistics as much as possible. They were required to submit the STL model for printing with the desired orientation and a report on the implementation of the software. The final report was evaluated only for completion. This exercise was designed to educate students about the importance of considering manufacturing decisions in the design phase itself. The purpose of this assignment was to assess whether the practical implementation of manufacturability analysis software programs helps students to improve their designs choices. The submission was assessed qualitatively on whether students performed multiple design iterations using the feedback received from the software program to improve their designs and were able to successfully fabricate their designed parts in an optimal way (i.e. minimizing material, build time etc., eliminating any infeasible features). Fig. 31 shows final fabricated parts designed by some of the student groups.

Figure 31: Sample Student-Created Parts

3.4. Results

The ME2024 class was divided into two sections in the Spring and consisted a total of 106 mechanical engineering sophomore students. The data for students who failed to fill in their records correctly or answer all the survey questions at the end of intervention was removed. After these unusable student records were removed, data from 33 students remained in Section 1, and 53 students remained in Section 2. The populations of the two sections as well as percentages of the total population of 86 participants are given in Table 9.

Table 9: Groups Used for Classroom Study

Group	**Size (Students)**	**Percentage of Study Population**
Section 1	33	38.4%
Section 2	53	61.6%
Total Population	86	100%

3.4.1. Pre-Assessment Survey

Fig. 32 shows the reported prior experience of all the students combined before any training began. Almost 25% of the students indicated no prior machining or 3D printing experience. The percentage of students that indicated 3D printing experience (~33%) was slightly less than those that indicated prior machining experience (~43%). This indicates that students are still not exposed to 3D printing as much as machining. Although this difference can also be attributed to the fact that some students completed/ were completing a laboratory class in Industrial and Systems Engineering Department on Introduction to Manufacturing processes. So it's likely that they were referring to that one single class exercise as their prior experience.

The results of Expertise Assessment are shown in Fig. 33. The most visible observation is that almost 60% or more students identified themselves in novice category. This means that most of the students, even if they had prior experience in machining or 3D printing, lacked confidence in their ability to complete tasks in their respective fields. This presents a challenge for their future careers: they must be able to carry out tasks confidently with both AM and SM processes in order to succeed in the manufacturing industry. Hence, this survey answers our RQ1 where we have identified that there is a need for introducing formal DFM education in engineering classrooms.

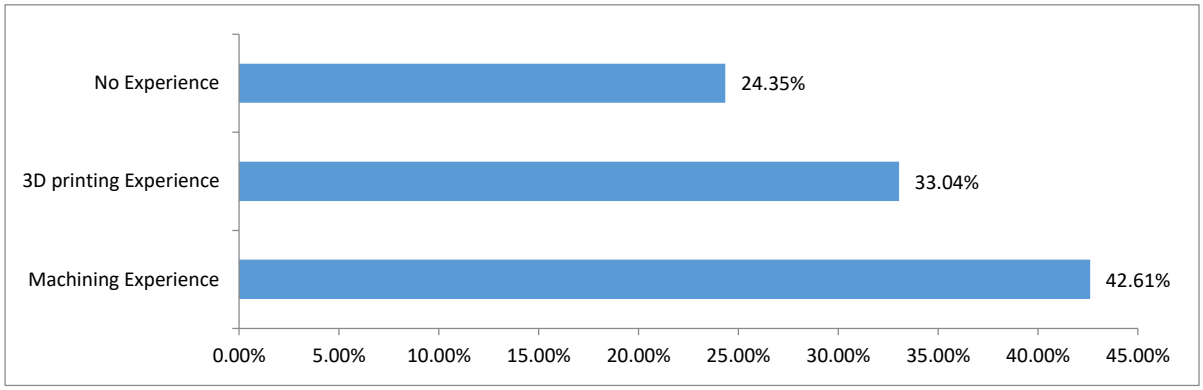

Figure 32: Prior Experience of students before the trial

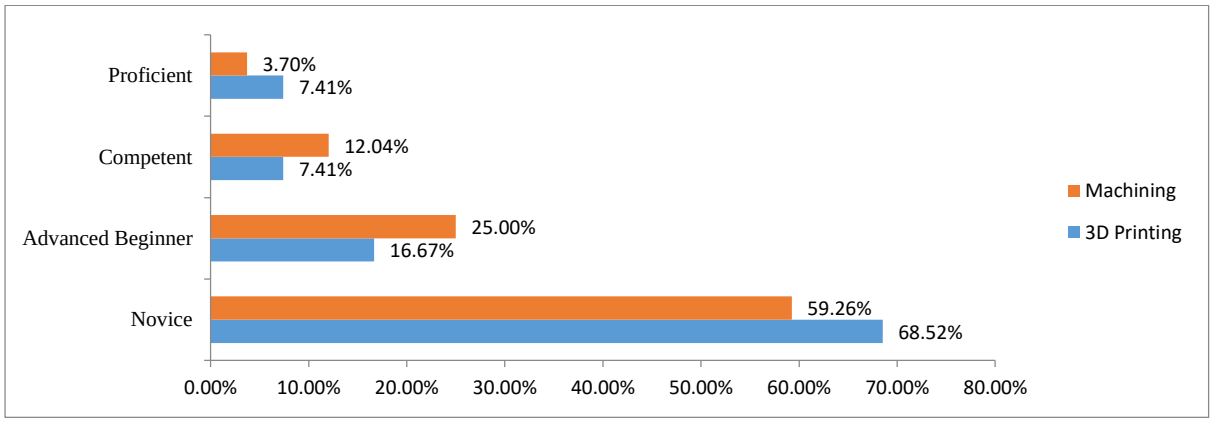

Figure 33: Expertise Assessment of students before the trial

3.4.2. Pre-Test and Post-Test Comparison

The Pre-test was graded out of a total of 5 points, while the Post-Test was graded out of a total of 8 points by a manufacturing expert. For ease of comparison, the scores for both the assessments were normalized. From a statistical analysis of the Pre- and Post-Test results for

both sections (see Table 10 and 11), it is apparent that the students performed far better in the Post-Test than in the Pre-Test. The results from ANOVA single factor analysis demonstrate that the score increase in the Post-test, as compared to the Pre-test, is significant at $\alpha = 0.05$ level (p-value > 1.1E-05). The results indicate that using visual rapid manufacturability assessment tools along with conventional teaching method was effective in teaching students about DFM principles and improved students' performance by 28% in Section 1 and by 34% in Section 2. From the results, it is apparent that some students do not understand when to properly apply additive and subtractive processes, even after subjected to both 3D printing and machining modules. The results also suggest that further treatment of the part characteristics from AM and SM processes is needed.

Table 10: Statistical analysis of the Pre and Post-Test results for Section 1

Groups	*Count*	*Sum*	*Average*	
Section 1 Pre-Test	33	10.4	0.315	
Section 1 Post-Test	33	19.562	0.592	
ANOVA				
Source of Variation	*SS*	*df*	*MS*	*P-value*
Between Groups	1.27199	1	1.271991	1.1E-05

Table 11: Statistical analysis of the Pre and Post-Test results for Section 2

Groups	*Count*	*Sum*	*Average*	
Section 2 Pre	53	9.4	0.178	
Section 2 Post	53	27.4375	0.518	
ANOVA				
Source of Variation	*SS*	*df*	*MS*	*P-value*
Between Groups	3.069353	1	3.069353	1.13E-15

3.4.3. Effect of Prior Experience

To answer RQ3, the effect of prior machining and 3D printing experience on the performance of students was studied The group of students that indicated neither machining nor 3D printing experience actually showed the largest improvement in Post-Test (~36% increase in post test score). The statistical analysis of the Pre and Post-Test results for this group of students indicates that this improvement (about 36% in average score) was significant at $\alpha = 0.05$ level (p-value 6.85E-12). (Refer Table 12)

Table 12: Statistical analysis results of student group with neither machining nor 3D printing experience

Groups	*Count*	*Sum*	*Average*	
No Exp. Pre	28	3.4	0.121	
No Exp. Post	28	13.5	0.482	
ANOVA				
Source of Variation	*SS*	*df*	*MS*	*P-value*
Between Groups	1.821607	1	1.821607	6.85E-12

Also, performing two-way ANOVA with prior machining and 3D printing experience as variables and post-test results as a response factor indicates that prior machining experience has a significant effect on the performance of students at $\alpha = 0.05$ level (p-value 0.04), whereas prior 3D printing experience is not a significant factor (p-value 0.245>>0.05) (see Table 13). This indicates that, although currently students are utilizing 3D printing technology available to them, they do not clearly understand the geometric considerations and manufacturability constraints in 3D printing technology.

Table 13: ANOVA results to study effect of prior manufacturing experience on Post-Test scores

Source	DF	Seq SS	Adj SS	Adj MS	P-value
Machining Exp	1	0.17276	0.10172	0.10172	0.04
AM Exp	1	0.04151	0.04151	0.04151	0.245
Error	83	2.51374	2.51374	0.03029	
Total	85	2.72802			

The effect of prior experience can also be examined by comparing results between students in novice or no experience category with students in advanced beginner, proficient and competent categories combined. It can be seen from Table 14 that the term delta which signifies the difference in mean normalized scores for pre and post-tests is only slightly higher for the Expert category (close to 1%). Hence, prior experience in 3D printing did not influence the improvement shown by students from pre to post test.

Table 14: Statistical results to study effect of prior 3D printing experience categories on Post-Test scores

	Novice 3D Printing Experience				Expert 3D Printing Experience	
	Mean	Sigma			Mean	Sigma
Pre	0.224	0.16505		Pre	0.248	0.24997
Post	0.545	0.2108		Post	0.582	0.260155
Delta	0.321			Delta	0.334	

Fig. 34 shows histogram showing frequency of students in different score ranges for both these 3D printing experience categories. From a visual standpoint also, it can be seen that scores for students among both these categories follow a similar trend where very little number of students scored in the range of 5-8 (out of 8).

On the other hand, in case of machining experience, the difference in mean normalized scores for pre and post-tests is much higher for the Novice category (by about 10%) as seen in Table 15. From visual inspection, it can be seen that scores for students among both these categories are higher than corresponding 3D printing experience categories. This means that students having previous expertise in machining process have a higher mean score on pre- and post-test than group of students having previous expertise in 3D printing process. Fig. 35 shows

histogram showing frequency of students in different score ranges for both these machining experience categories.

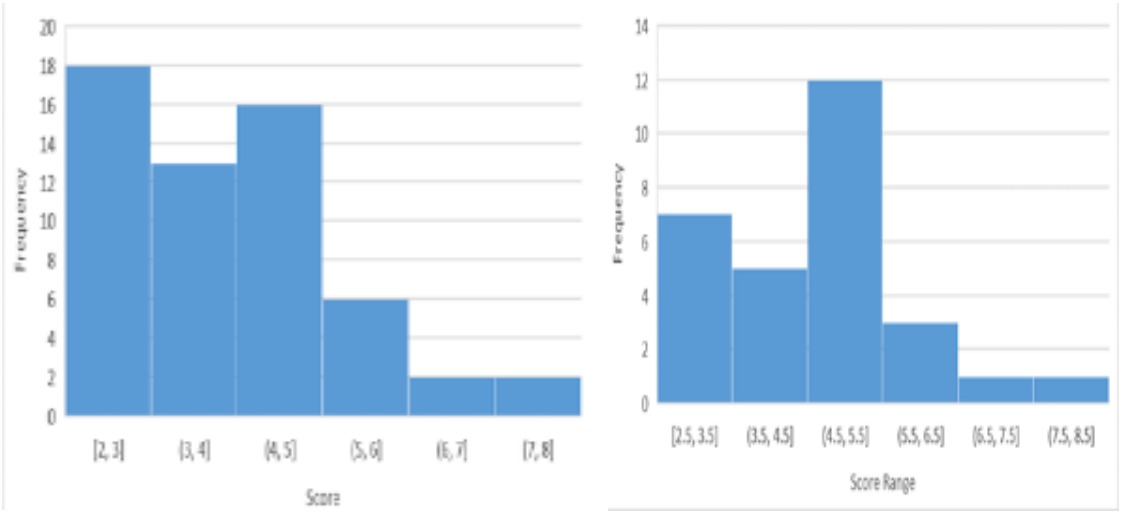

Figure 34: Histogram representing Post-test Scores for 3D Printing a) Novice b) Advanced beginner, Competent and Proficient categories combined

Table 15: Statistical results to study effect of prior Machining experience categories on Post-Test scores

	Novice Machining Experience				Expert Machining Experience		
	Mean	Sigma			Mean	Sigma	
Pre	0.145098	0.186099		Pre	0.354286	0.253369	
Post	0.502451	0.164179		Post	0.610714	0.178089	
Delta	0.357353			Delta	0.256429		

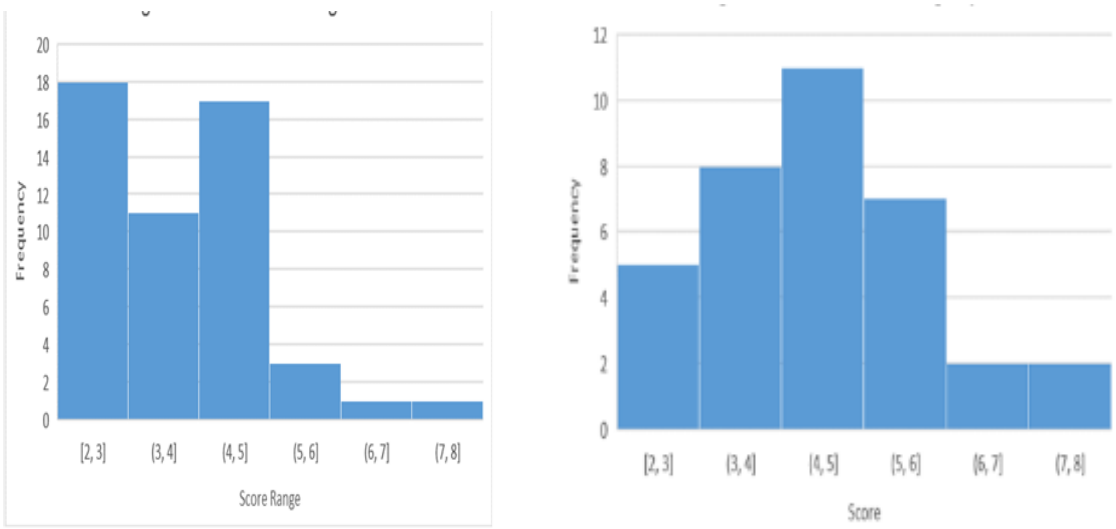

Figure 35: Histogram representing Post-test Scores for Machining a) Novice b) Advanced beginner, Competent and Proficient categories combined

3.4.4. Final Project

For answering the final research question (RQ4), the final project report submissions of student groups were evaluated. According to the submissions received from the student teams, the final project helped them evaluate the manufacturability of their designs using feedback received by the software tool. It also helped them formulate a fabrication strategy by analyzing the material, support, build time and cost statistics. For instance, the submission of one of the teams is summarized in Fig. 36. As it can be seen, the team received feedback from the AM manufacturability software that the top wall as well as the negative feature at the side is too thin (less than the resolution of Fortus 400 mc). This caused them to modify their designs in order to make the part manufacturable. As seen in Fig. 36, they also received feedback regarding support material, build time and cost in three different orientations as shown and made an informed choice to choose the 90° orientation. Without the software feedback, it would have been difficult for them to realize these factors and would have led to a failed/poor quality part.

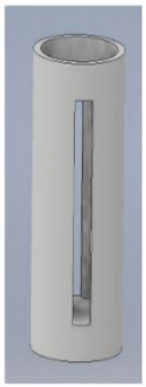

Figure 18. CAD model

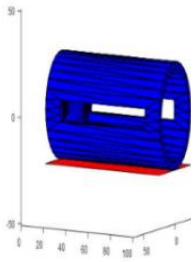

Figure 19. Original orientation

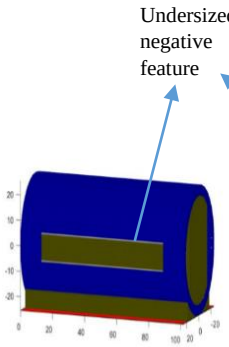

Figure 20. Zero degrees of rotation

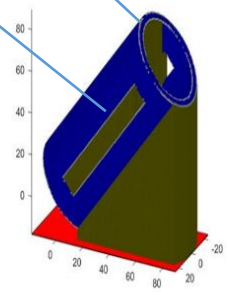

Figure 21. 45 degree rotation

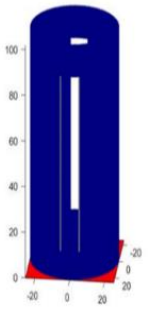

Figure 22. 90 degree rotation

Trials	Cost	Time
Rotation 0 degrees	$69.50	6 hours 6 min.
Rotation 45 degrees around x-axis	$40.54	3 hours 31 min.
Rotation 90 degrees around x-axis	$43.05	3 hours 44 min.

Figure 36: Final project submission of DFM feedback received by a sample team

The feedback received from two other teams along with their fabricated part is shown in Fig. 37 and 38. The first team designed an impeller part. However, the wall thickness of the whole impeller was too thin (less than the resolution of Fortus 400 mc). The second team designed a sample widget. The widget had an undersized negative hole and a thin extension on the top. These would have definitely caused their parts to fail during fabrication. However, due to the received feedback, the teams redesigned the part and fabricated it successfully as shown.

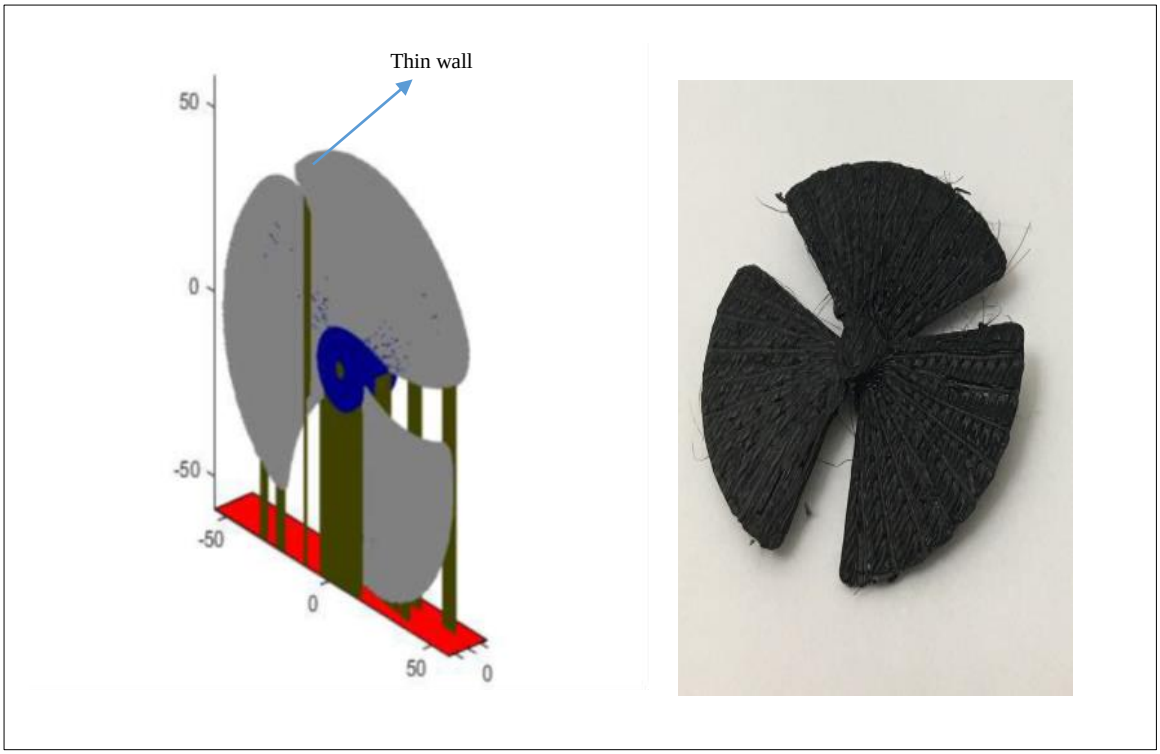

Figure 37: Final project submission of DFM feedback received by another sample team

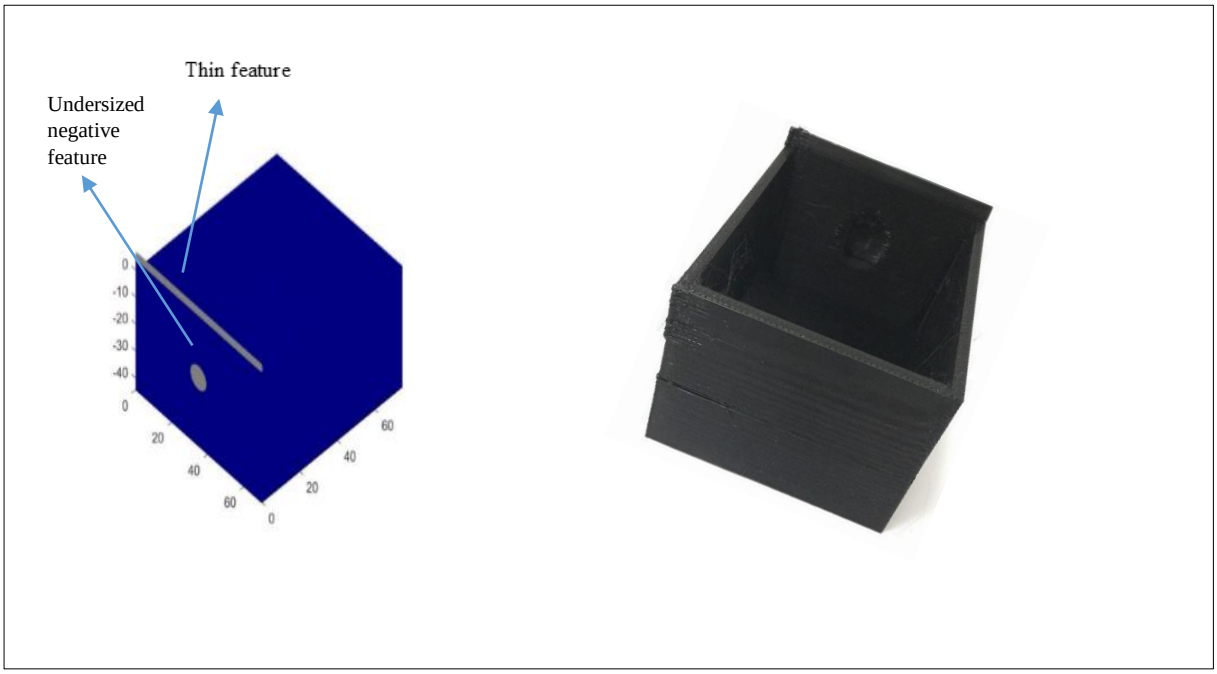

Figure 38: Final project submission of DFM feedback received by another sample team

All teams made use of the analysis provided by the software to get the cost, material consumption and build time of their designs. They were also instructed to review different build orientations and report the most optimum one for fabrication of their parts. This is illustrated in sample submissions by two other teams which are summarized in Figs. 39 and 40. Both these teams performed the manufacturability analysis repeatedly in different orientations to minimize as many criteria as possible. The first team among these two were able to minimize all these

criteria by selecting an orientation angle [90,45,45] as shown. The second team chose to minimize support material and hence selected orientation (a) shown in Fig. 40.

A ramp: 119.95mm x 33.34mm x 50.30mm

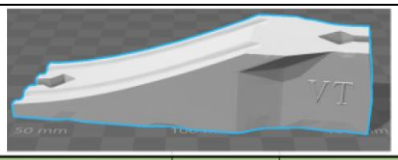

Alternative	X-axis (degree)	Y-axis (degree)	Z-axis (degree)	Model Material(mm^3)	Support Material (mm^3)	Cost	Time Required
1	45	45	0	226042.91	12914.15	$ 20.39	1 hr 43 min
2	45	0	0	226000.69	24966.07	$ 30.97	2 hr 40 min
3	90	45	45	226070.06	15459.16	$ 20.23	1 hr 42 min
4	90	90	0	226071.04	9271.63	$ 21.89	1 hr 52 min
5	45	45	45	226059.88	12898.93	$ 23.60	2 hr 1 min

Figure 39: Final project submission of DFM feedback received by another sample team

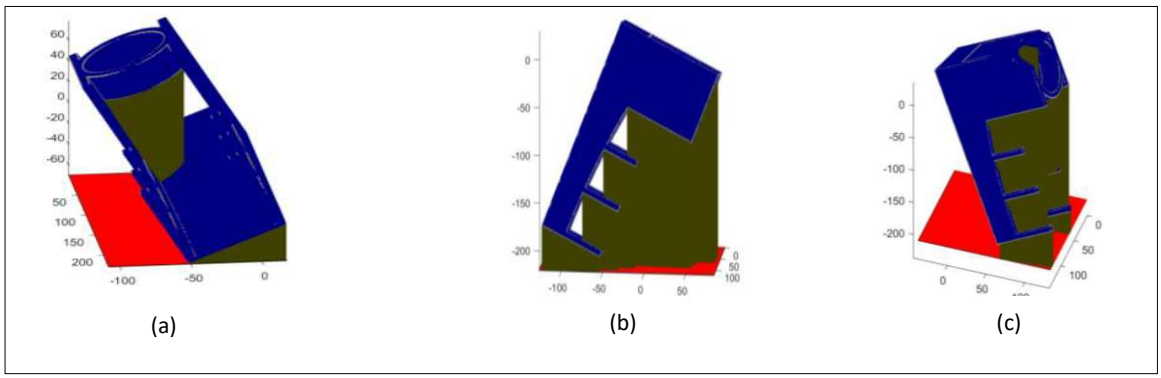

Figure 40: Final project submission of DFM feedback received by another sample team

However, some other teams either designed the parts too simple (for e.g. a spherical ball or a cube) due to the problem statement being vague for which the design and manufacturing considerations were obvious. It was evident that 3D printing was not the most suited process for these parts. Hence, a more specific challenging problem statement with specific scoring guidelines needs to be defined in the future for the final project. Whereas, some other teams were not able to understand the minimum feature size module as sometimes the results can be hard to understand due to highlighted regions showing up because of other reasons such as discrete voxels due to stair- stepping. Hence, for this trial to be a complete success, we also need multiple in-class training sessions for getting the students acquainted with the software. However, in all, the final project was a good first start as students got hands-on experience on the software and learned how different manufacturing constraints govern the manufacturability of their self-designed part. They also learned to minimize the cost/build time/support material etc. by finding an optimum orientation to fabricate their part. According to the feedback received from the class, without the software program, students found it difficult to visualize different orientations and predict the optimum orientation which would reduce build time/ support material etc. even after they had a firm grasp of DFM concepts from the classroom intervention. The teams who were able to understand and successfully use the minimum feature module gave feedback on design iterations and acknowledged that without the software tool, they would not have been able to detect critical design flaws. Since, a majority of students were able to successfully use the software to improve their designs by

removing infeasible features and optimizing other criteria, we can conclude that along with the classroom intervention, undergraduate students need to have access to rapid manufacturability analysis software tools to put their theoretical knowledge of DFM concepts to practical use.

3.5. Conclusion

In this work, we presented the design and implementation of a study to measure the effectiveness of deploying manufacturability analysis tools for both Additive and Subtractive manufacturing in educating students about DFM considerations for process selection. Before the study, students were asked to take a Pre-Assessment Survey and Pre-Test to gauge the prior knowledge and experience of students. Two in-class sessions were conducted where students were given instruction on DFM considerations in Additive and Subtractive manufacturing. After the instruction, students were given in class assessment exercises with different categories of questions intended to help them understand the design considerations involved. Students were also shown the analysis results for these questions obtained from two voxel-based software programs: Sculptprint for Subtractive Manufacturing and an Additive Manufacturing DFM software (Chapter 2), which aimed to help students better visualize the critical design aspects in each part. Students also used the AM manufacturability analysis software in their final project where they used feedback provided by the software to make decisions about the design and fabrication of their part. This work set out to answer four specific research questions. Using the data, analysis and observations presented in this work, those questions are answered below:

RQ1: What is the prior level of manufacturing experience and understanding of DFM concepts of students at undergraduate level in universities?
In the Pre survey, while 75% students indicated some prior experience, 60% self-reported that this experience was limited and categorized themselves in the novice category. Only 33% of students indicated prior experience in 3D printing and 42% of students indicated prior experience in Machining. Of the students who categorized themselves as having prior experience in Machining, a portion of students had just attended a single lab session in ISE Intro to Manufacturing elective course. The average score of students in the Pre-test was only about 33% in Section 1 and 17% in Section 2. Hence, there is a significant need for improvement of students' understanding of various design considerations in both Subtractive and Additive Manufacturing.

RQ2: How is a student's choice of a manufacturing process for a certain part influenced by exposure to teaching/instruction using manufacturability analysis software programs?
The score of the students in both sections increased in the Post-test, as compared to the Pre-test. Using statistical analysis, this increase was found to be significant (p-value>1.1E-05). Although, this result does not necessarily answer the extent of their improvement due to software feedback alone, as further implementation is required where a treatment group needs to be given the software programs in class to work out the problems and another control group where students are given traditional teaching instruction.

RQ3: How does students' prior experience in manufacturing impact the effectiveness of this approach?
This research question was specifically answered as score of students with no prior experience in machining and 3D printing showed the most improvement in the post test as compared to students with prior experience in Machining or 3D printing. Further statistical analysis revealed that Machining experience was a significant factor effecting the performance of students (p-

value 0.04) whereas prior 3D printing experience (p-value 0.245) proved to be insignificant-. Hence, this revealed that students who had prior experience in 3D printing did not clearly understand the DFM considerations involved which are required for successfully fabricating a part using 3D printing. This indicates that, although currently students are utilizing 3D printing technology available to them, they do not clearly understand the geometric considerations and manufacturability constraints in 3D printing technology.

RQ4: How does the practical implementation of manufacturability analysis software programs helps students to improve their design choices?
This research question was partly answered in this work. While we were not able to achieve the practical implementation of Sculptprint software, students did have access to the AM manufacturability analysis software for their final projects. Some teams were successfully able to leverage the use of this software to perform design iterations to successfully fabricate a part which would otherwise result in a failed/defective part. Other teams used the software to get feedback on build time, cost and support material to select best orientation to fabricate the part. In the future, more extensive study will be carried out with specific design problem and scoring parameters to quantify this improvement.

3.6. Limitations and Future Work

While the approach was deemed successful in better equipping students to help select suitable process for their designs, there are limitations to the conclusions that can be drawn. Most importantly, to quantify the improvement in students' choice of a manufacturing process as a result of exposure to software programs alone, a trial with two separate groups: one treatment group which receives instruction through the software programs and another control group which receives traditional classroom instruction is required. Secondly, more factors and their contribution towards students' performance need to be studied in the Pre-Assessment. One such factor is the spatial-visualisation ability of the students coming into the class. Spatial visualization is the ability of an individual to visualize an object mentally and understand its spatial orientation [71]. In order to better understand DFM considerations, students need to mentally rotate the parts and identify the different features that would be difficult to make using AM/SM. This could be significant factor affecting students' performance and learning which needs to be studied. Also, in order to generalize/extend this trial to other populations, we need more information about the students and their demographics. If we need to extend the same trial to the Engineering Graphics or any other class, we need to know what is the difference between the two populations and how does the trial need to be modified as a result. Also as highlighted earlier, multiple in-class training sessions are required for getting the students acquainted with the software programs. The final project needs to be designed such that it can better test the theoretical concepts taught in class and students can gain a more hands-on experience. Also in this study, students could not get hands on experience with Sculptprint software.

To overcome the above limitations, following changes are recommended in the study to increase both the effectiveness and the efficiency of future studies:

- More extensive trials need to be carried out with two different group of students: a treatment group that will be provided access to Sculptprint and the Additive Manufacturing software in class and a control group that will receive manual

instruction. This will define the extent of effect these software programs have on students' choice of manufacturing process.

- More factors and their contribution towards students' performance need to be studied in the Pre-Assessment.
- More information about the participants and their demographics is required so that the trial can be generalised/ applied to other populations.
- The final project needs to be designed in such a way with more challenging design problem such that students learn to implement the theoretical concepts taught in class and gain a more hands on experience in both Additive and Subtractive Manufacturing.

Chapter 4: Framework for Model-Free Additive Manufacturing from Imaging data using Voxel based approach

Abstract

Additive manufacturing (AM) techniques offer the potential to fabricate physical 3D models which can be utilized for development of accurate predictive models to assist in medical applications such as pre-interventional surgical planning, developing custom prosthetics and implants, functional flow models as well as for training/communication tools. Currently available AM pre-processing workflows for imaging data are computationally expensive and based on surface representations. The conversion of imaging data to surface representations and subsequently to layer contour and tool path introduces translation errors at each step. They also do not enable representation of multi-material models, functionally graded materials or control of material properties on a voxel scale. To address these issues, we present a novel voxel-based digital workflow and printing method that can be used to fabricate 3D models by converting patient-specific imaging data directly into machine-specific instructions while retaining information about the anatomical properties. This workflow enables the fabrication of accurate anatomical models directly from imaging data without any translation errors and control of material properties at voxel level. These advantages are demonstrated by fabricating different anatomical models using high resolution multi-material Additive Manufacturing. The ease of model fabrication and level of material control demonstrated in this study cannot be achieved using traditional AM workflows for imaging data, and hence this work emphasizes the need for development of new voxel based frameworks and systems to fully utilize the capabilities of AM.

4.1 Introduction

4.1.1. Motivation

Medical imaging is the technique and process of creating visual representations of the interior of a body in order to diagnose, monitor, or treat medical conditions. [72]. Medical imaging has evolved dramatically in the past few decades and has become less invasive and more informative [73]. Using Additive Manufacturing (also referred to as 3D Printing), physical three-dimensional objects can be fabricated from imaging data [74]. Today, clinical image acquisition can be done at ultra-high spatial resolution (100–600 microns) with good quality contrast. The acquired imaging dataset is exported into a Digital Imaging and Communication in Medicine (DICOM) format [75], which is the standard file format for storing and transmitting medical images. Additive manufacturing from imaging data is a powerful reverse engineering tool and has been widely used in the medical field as a tool for pre-interventional surgical planning [76], developing custom prosthetics and implants [77], functional flow models [78], training/communication tools [79] etc. This work focuses on Computed Tomography (CT) technique, which is widely used in medical radiology with a variety of available systems ranging from single-slice CT to spiral multi-slice CT to dual-energy CT. However, the basic framework that will be proposed here can be extended to integrate with any type of imaging data and file format.

While commercial pre-process planning software exist (e.g., Materialize Mimics [80] etc.), they are based on surface representations and have the following drawbacks:

a) These software programs often use various computationally expensive algorithms to reconstruct triangulated surfaces from volumetric data (e.g. [81].) Due to errors in surface reconstruction, additively manufactured physical medical models fabricated using these software programs can potentially diverge from the exact anatomy of the

patient, and hence distort clinical diagnosis and cause erroneous treatment planning [82].

b) During this conversion process, all the volumetric information is lost and separate surface models are generated for each segmented regions which are fabricated using a single material roughly matching the properties of that region. Hence, fabricating complex multi-material models is challenging.
c) Surface representation models do not allow specification of continuously varying material properties or functionally graded materials. For custom prosthetics and implants, medical models etc. fabricated using imaging data to truly replicate the dynamic and heterogeneous nature of the human body; they should exactly mimic the varying material composition and functional gradients of stiffness inherent in hard and muscle tissues.
d) Another challenge in using these software programs is that a significant level of medical expertise and precision is required to identify and segment each and every abnormal tissue region such as fibrosis, calcifications etc.

In order to address this gap, the authors propose a novel voxel based framework for model fabrication directly from imaging data. A voxel can be thought of a 3-dimensional pixel and can be used as a base feature for volumetric representation of part models. A voxel is a cubic unit of volume that is centered at a grid point. A voxel represents the smallest representable element of volume. For binary voxel model, a value of '1' means that voxel is 'on' and value of 0 means voxel is 'off'. In printing, the voxel represents the minimum feature that a machine can fabricate. The layers of a CT scan set are represented by a set of bitmaps which are segmented and stacked upon each other to form the 3D printed model. This can be visualized in Fig. 41. This new approach will eliminate common issues faced in traditional frameworks, such as the need for surface reconstruction in order to create toolpaths. Hence, this framework would be computationally less expensive and potential inaccuracies which would typically arise due to surface reconstruction algorithms would be automatically eliminated. Moreover, to replicate the dynamic nature and true mechanical properties of an actual human organ that manifests varying tissue properties, imaging data needs to be directly used for fabricating a continuous part with functionally graded materials, without converting the volumetric scan data into a surface representation. Such a framework also wouldn't require segmenting each and every abnormality in the region of interest as the model would be fabricated as a single continuous part.

4.1.2. Research Goal

The primary goal of this work is to propose a new pre-processing framework that assists designers in model realization directly from imaging data using a voxel-based approach. Voxel representation allows for easy computations on the part geometry using simple 2D image processing operations, which are usually much less computationally expensive than 3D ones required for polygonal models (.STL/.OBJ/.PLY). The digital fabrication process in voxel 3D printers involves accurate placement of different materials according to the voxel map (provided as toolpath), which coalesce to form a true solid. These materials can be easily combined in a certain ratio by using Halftoning/Dithering to create a number of hybrid composite materials in a single build setup which could then be used to fabricate the model. Hence, such an approach provides infinite possibilities of creating digital material blends which can replicate the mechanical properties of various tissues to a certain extent. Also, through a voxel-based approach, bulk material properties of the structure can be continuously varied between the properties of each single material to fabricate a continuous functionally graded multi-material part.

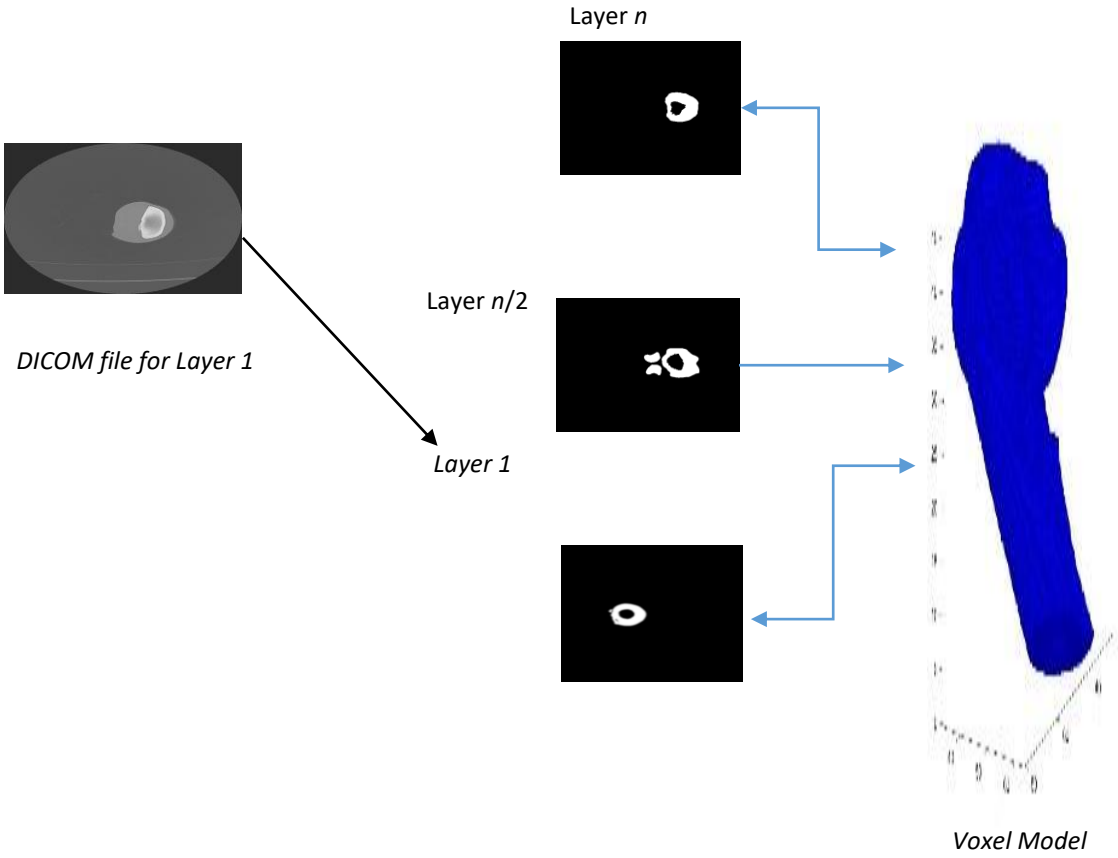

Figure 41: Voxel representation for a sample imaging dataset

In this work, first a set of 2D images are acquired using medical imaging techniques and are rendered for visualization. Dedicated post-processing algorithms for processing the images generated during acquisition are then implemented. This includes segmentation of images to extract the region of interest as well as filtering techniques to remove the noise and smooth the data. Next, each pixel in the final processed image is mapped with a material value using corresponding pixel value in the original images. Using a 2D dithering technique, the resulting images are converted into bitmap files on a local, voxel-scale level which serve as toolpath to the printer for model fabrication. Figure 42 shows a schematic diagram of the various steps integrated in the proposed framework. Each of these steps is discussed in detail in the following section.

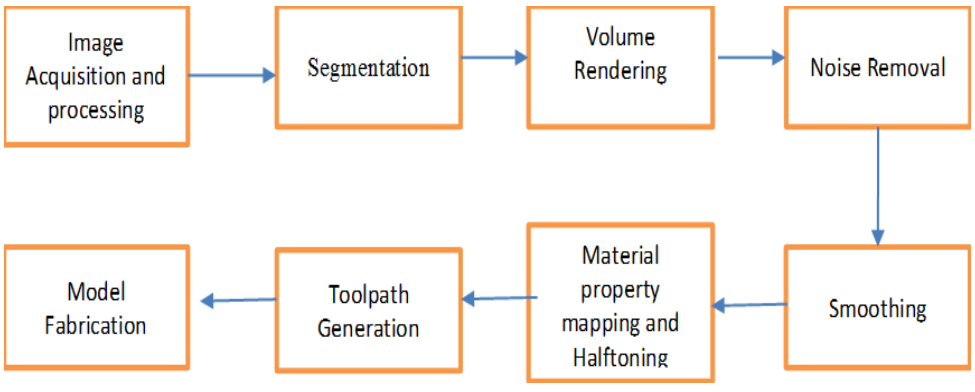

Figure 42: Flow-chart listing the steps integrated in the proposed framework

4.2. Prior Art: Literature and Challenges

4.2.1. Additive Manufacturing from imaging data

AM using imaging data has found a lot of applications in the medical field which can be summarized into the following main categories:

a) Surgical tool: Additive manufacturing has been widely used as a tool for pre-interventional surgical planning. AM has been use to assist in pelvic surgery [83, 84], neurosurgery [85, 86], spine surgery [85], cardiovascular surgery [86,87], craniofacial and maxillofacial surgery [90,91] and many other surgical procedures as it has helped in surgical planning and better understanding and visualization of complex underlying anomaly. However, AM has mostly been used as more of a visualization tool rather than a predictive tool to determine and simulate the feasibility and success of novel surgical therapies.
b) Design of prosthetics: Customized prostheses have been successfully fabricated in the past from imaging data such as mandible [92, 93] and dental restoration [94], Hip [95], femoral [96], and hemi-knee joint reconstruction [97, 98] etc. However, one of the drawbacks is still the lack of appropriate replication of material properties to correspond with the patient's biological tissue.
c) Functional flow models: AM from patient specific data has been used for functional flow modeling mainly in cardiac interventions. Additively Manufactured cardiac models have been used by researches in cases of modeling in-vitro conditions for studying aortic valve stenosis [99], coronary artery bed [100] and aortic valve in diastole [101]. However, complex flow evaluation would require that cardiac tissue and vessels be fabricated with a more compliant 3D printing material than the ones currently commercially available [99].

4.2.2. Representation of heterogeneous objects

The .STL file format has been the standard file format for Additive Manufacturing since the beginning when it was developed by 3D Systems. Since then, the field of Additive Manufacturing has seen a lot of development and the current capabilities of AM processes are far superior to back in the day. Despite this, the .STL file format doesn't have the ability to take full advantage of multi-material capabilities of AM. The .STL file contains only surface geometry information, and lacks information about material and physical properties among other drawbacks [4]. To address these issues, the ASTM committee in 2009 announced a new file format. AMF [4] for Additive Manufacturing. AMF is an XML-based open format that provides complete information through five main elements: object, material, texture, constellation, and metadata and hence provides a better representation of physical and material properties [4]. Similarly, Microsoft in its latest OS - Windows 10 has integrated a new file format 3MF [102] for Additive and Subtractive Manufacturing which has similar capabilities. However, the physical properties described in both AMF and 3MF formats are still only the properties of corresponding facets and not of the volume element. The AMF format uses curved triangles as base feature which are used to describe their parent volume feature. Although, this provides a better representation of geometry than STL, it still doesn't provide the user pixel-level control over material properties. Despite developments and research in the area of new file formats, the current pre-processing software programs convert imaging data directly to STL file format as it is the de-facto standard and most of the AM systems still use .STL/.OBJ etc. as input file format.

Since, imaging data is already in a volumetric representation, a better solution would be to use a voxel-based representation of the geometry directly for AM. A voxel-based representation allows the selective specification of material at any location and can take full advantage of multi-material capabilities of AM. The use of voxels as base feature for representing geometry for Additive Manufacturing has been proposed in several literatures (e.g. Chandru et. al [35], Lin et. al [36], Ma et. al a, b [37, 38]). Some work has also been done in the area of printing directly from voxels (e.g. Hiller and co. [31, 32], Doubrovski et. al [33], and Brunton et. al [34]). AM processes such as Material Jetting, Binder Jetting and mask-projection Vat Photo polymerization have the capability to fabricate parts directly from voxels. However, this capability has not been utilized for creating parts directly from imaging data.

4.2.3. Surface Reconstruction

Various algorithms have been presented in literature for conversion of a series of 2D imaging data to create 3D surface representations. These can be generally classified in following four categories:

i. *Marching Cubes*: The most common method for surface reconstruction is using marching cube/marching squares [81] to extract a polygonal mesh of an isosurface from a three-dimensional voxel field. However, this approach suffers from a number of drawbacks. Firstly, during the surface combination of every two adjacent neighbor cubes, this method may produce an incorrect surface for the cubes due to multiple surface configuration choices. Secondly, during the assembly of the facets some holes, aliases, and overlapping might be generated in the mesh [37, 103]. These disadvantages restrict the application of the marching cubes method as the resulting mesh has to be repaired to get rid of these errors which requires manual intervention. Researchers have continuously tried to modify these algorithms in order to reduce these errors (e.g. [104, 105]).
ii. *Interpolation*: Another method of surface reconstruction is by first reconstructing a NURBS, Bezier or a B-spline surface from control points in each layer which is then used to reconstruct a surface model using interpolation techniques [106, 107] This technique cannot be applied without constructing the curve model, since the NURBS/spline etc. must first be constructed before modeling can take place and hence it is extremely complicated [108, 109].
iii. *Contour Extraction*: In this method, contours are detected for each layer and used to construct the triangular STL model for fabrication by connecting the vertices of two parallel polygons [110–112]. This method suffers from drawbacks in the contour detection for each CT layer and file errors in the construction and use of STL meshes [113–115].
iv. *Miscellaneous techniques*: Recently, new techniques such as Heterogeneous implicit solid based approach [116] and Gray prediction algorithms [117] were introduced to fabricate surface models directly from voxel data. These techniques were used to fabricate accurate models in some cases; however, in other cases dimensional inaccuracies were observed [118].

Using a framework that converts imaging data directly to fabricate patient specific models would entirely eliminate the step of surface reconstruction. Hence, this framework would be computationally less expensive and potential inaccuracies which would typically arise due to surface reconstruction algorithms would be automatically eliminated.

4.2.4. Halftoning

Common multi-material AM machines usually can print two or three materials at a time. A technique called Halftoning can be applied in order to print various digital materials

having properties intermediate between these materials and produce gradients that appear continuous while still using limited set of inks. In a Halftone image, printed dots are varied either in size or spacing and thereby produce the illusion of a smooth gradient. Several researchers have investigated advantages of halftoning in AM. Using a case study, Hiller et. al. demonstrated that by using by using material Halftoning algorithms, continuous control over density, elastic modulus and coefficient of thermal expansion of tunable digital materials for voxel printers can be achieved [119]. Lou and Stucki discussed the challenges presented by Halftoning algorithms in Stereolithography (SLA) [120]. Cho et al. use Binder Jetting as a prototypical multi-material AM technology while presenting new workflows for the design, processing, and fabrication of heterogeneous objects [121]. The authors present a process that is based on traditional 2D digital Halftoning and is optimized for the AM machine, taking into account uncertainties in droplet placement. Aremu et. al used a 2D dithering technique to fabricate graded multi-material lattice structures [122]. In more recent and related work, Doubrovski et. al. have proposed a voxel-based design framework through material property mapping and used 2D dithering to fabricate multi-material prosthetic using bitmap printing [33]. We hypothesize that Halftoning/dithering algorithms can be applied on greyscale images obtained through imaging data after pre-processing and used to fabricate complex functionally graded models directly from this represenation.

4.3. Methodology

4.3.1. Image Acquisition and processing

The creation of a patient-specific 3D model begins with clinical imaging. The radiographic density (i.e., the X-ray attenuation) represented by each voxel in a CT dataset (DICOM images) is expressed by the CT number. The denser the tissue, the more X-rays are attenuated and higher is the corresponding CT number [123]. For example, X-rays are attenuated more by bone (hard tissue) as compared to soft tissue. The scale of CT numbers is specific for each type of equipment and varies with technique factors. For systems of recent design, the available range of CT numbers is usually between 2^{12} (4048) and 2^{16} (65,536) for 12-bit and 16-bit acquisition, respectively [124]. The Hounsfield unit (HU) scale that is used in CT is calculated from the linear attenuation coefficient (μ) value of each tissue and takes into account the linear attenuation coefficient of water. Hence, both the CT no. and corresponding HU unit is directly related to the density of the corresponding imaged pixel. For HU calculation, the radiodensity of distilled water (at standard pressure and temperature) is defined as zero HU, while the radiodensity of air (at standard pressure and temperature) is defined 1000 HU. For a material *X*, with linear attenuation coefficient is given by μ_x, the HU value is given by [125]:

$$HU = \frac{\mu_x - \mu_{water}}{\mu_{water} - \mu_{air}} \times 1000 \tag{13}$$

In this work, the imaging data was imported into MATLAB and converted into a 3D voxel representation. The DICOM header consists of various attributes [75] that are read and used to convert the patient specific imaging data into a real world volumetric image. Some of the important attributes required are listed below:

- Pixel Spacing (Tag 0028, 0030): Physical distance in the patient between the center of each pixel, specified by a numeric pair - adjacent row spacing (delimiter) adjacent column spacing in mm.

- Image Orientation (Patient) (Tag 0020, 0037): The direction cosines of the first row and the first column with respect to the patient.
- Image Position (Patient) (Tag 0020,0032): The x, y, and z coordinates of the upper left hand corner (center of the first voxel transmitted) of the image, in mm
- Slice Thickness (Tag 0018, 0050): Nominal slice thickness, in mm.
- Slice location (Tag 0020, 1041): Relative position of the image plane expressed in mm.

After the images are read and converted to a voxel model with associated HU and intensity data, it is sent to the segmentation module to extract the desired features.

4.3.2. Segmentation

Image segmentation is a process that is used to partition the spatial domain of an image into mutually exclusive regions. Each of these regions is uniform and homogeneous with respect to some property such as intensity, texture etc., which is different from the property value of each neighboring region [126]. The purpose of segmentation is to separate the desired tissue regions to be fabricated from the rest of the scan. Several classical approaches of image segmentation and analysis have been reported in the literature (e.g. [127-130]). The selection of an appropriate segmentation technique depends upon the type of imaging data and the intended goal. In this work, we have implemented two commonly used segmentation techniques in MATLAB, which are discussed below.

4.3.2.1. Intensity-based Segmentation

The most common method for segmentation is Intensity-based segmentation. In this method, a suitable intensity threshold is identified. All pixels with a value higher than the threshold value are classified as image pixels and are assigned a value of 1. All pixels with a lower value are classified as background pixels. Hence, a new binary image is created according to the following relation:

$$I_T = \begin{cases} 1 & for\ I_{xy} \geq T \\ 0 & for\ I_{xy} < T \end{cases} \tag{14}$$

where I_{xy} refers to the original image pixels and I_T is the thresholded image. If the image consists of multiple distinct regions, two or more threshold values can be defined. Using two thresholds, T1 < T2, the new images $I_{T1}\ and\ I_{T2}$ are formed according to the following relation:

$$I_{T1} = \begin{cases} 1 & for\ T2 > I_{xy} \geq T1 \\ 0 & for\ I_{xy} < T1 \end{cases} \qquad I_{T2} = \begin{cases} 1 & for\ I_{xy} \geq T2 \\ 0 & for\ I_{xy} < T2 \end{cases} \tag{15}$$

A number of algorithms exist to find this threshold level automatically. In this work, we use the Otsu's method [131], which chooses the threshold value such as to minimize the infraclass variance of the black and white pixels. Fig. 43 shows segmented bone (hard tissue) images from corresponding head CT scan images using this technique.

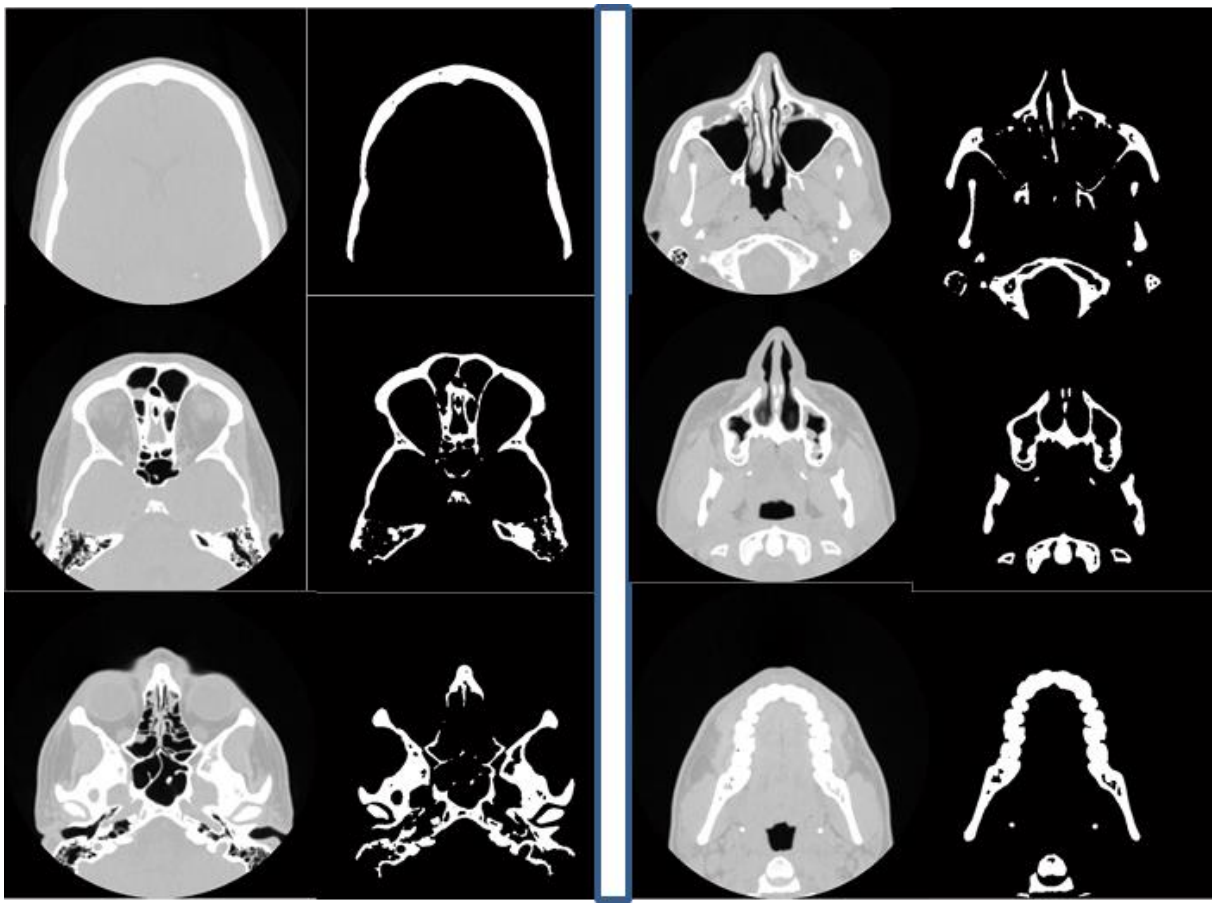

Figure 43: CT and corresponding Segmented Images using Intensity based Segmentation technique

4.3.2.2. Dynamic Region Growing

In certain images, multiple regions may have similar HU values and hence similar intensity values. In such cases, intensity-based segmentation method is not sufficient to extract the required region of interest unless the connectivity of the regions is also taken into account. Two adjacent feature pixels are considered connected and therefore considered belonging to the same region. Two possible definitions of connectedness exist: 4 or 8 connectedness for 2D images, and 6 or 26 connectedness for 3D. In this method, one or more seed points inside the region of interest and also a criterion to separate two similar connected regions are required. Seed points may be provided interactively or may be predefined special points determined by a criteria or geometry. Next, neighboring pixels of initial "seed points" are examined to determine whether the pixel neighbors should be added to the region. The N (where N=8 for 2D and 26 for 3D) neighbor pixels of each seed point are examined, and each neighbor pixel that meets the threshold criterion is added to the feature set and in turn becomes a seed point. The threshold criteria can be based on any characteristic of the regions in the image such as average intensity, variance, range of HU values etc.

For large 3D stacks it is necessary to scan the entire volume iteratively and add neighbor pixels to the feature set until no more pixels are added between iterations. A demonstration of the effect of region growing with different seed points for a sample DICOM image obtained from chest CT is given in Figure 44. This example assumes 8-connectivity and implements a simple threshold condition where all pixel candidates for region growing need to be within a ± 100 HU value limit. This threshold condition can easily be extended to include multiple threshold regions.

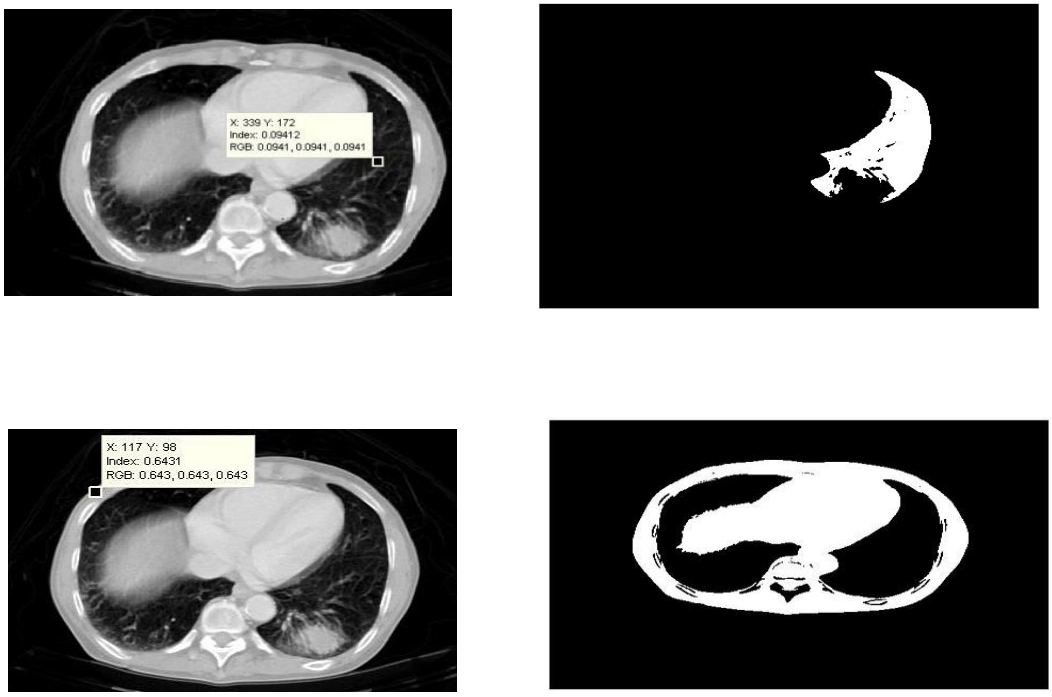

Figure 44: CT of a chest CT scan and corresponding Segmented Images using Dynamic region growing with different seed points

4.3.3. Rendering

After segmentation, the 3D voxel model is rendered so that users can visualize the segmented volume and make sure that they have extracted the correct desired volume. The 3D voxel model is displayed as a quadrangular surface mesh. The voxels are classified into boundary voxels (voxels that lie on the surface of the object), exterior voxels (voxels that lie outside the object mesh) and interior voxels (voxels that lie inside the mesh). To increase the speed of rendering, only boundary voxels are used for display. Interior voxels are considered for computations, but are reset as empty for rendering. A sample rendered model of heart from corresponding CT scan images is shown in Fig. 45.

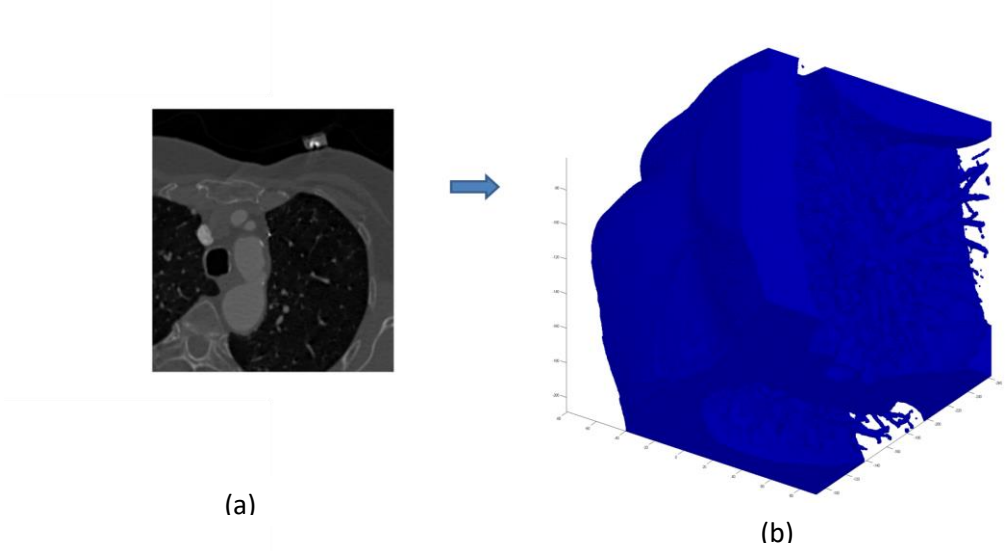

Figure 45: (a) Sample DICOM image from a Heart CT Scan (b) Rendered Segmented volume of the heart

4.3.4. Noise Removal and Smoothing

In Computed Tomography (CT), exposure of high amounts of radiation could result in problems. In order to reduce the dose, a common approach is to decrease the intensity of X-Ray source, which leads to high noise level in the raw data collected by detectors. On the other hand, the detectors used in industrial CT systems usually suffers from an upper limit of counts with 12 bit or 14 bit. Therefore, in order to get the correct projection data, the dose is limited to ensure that the raw data scanned without the object will be less than 2^{12} (or 2^{14}) [132]. In this case, while scanning large or high density object, the counts of the raw data would be low. Also in some cases, some background noise/foreign objects may also appear on the scans. Hence, to overcome these issues and produce good quality images, some denoising procedure needs to be employed.

An optimal noise filter must smooth dissimilarities of pixels in homogeneous regions, preserve edge information and not alter natural information. In this work, a number of commonly used filters, to enhance and process images such as deconvolution, edge detection, filters, smoothing algorithms, and frequency transformations are implemented in MATLAB. For most typical applications, image noise can be modeled with either a Gaussian, uniform, or impulsive distribution. Gaussian noise can be analytically described and has a characteristic bell shape. With uniform distribution, the gray level values of the noise are evenly distributed across a specific range. Impulsive noise generates pixels with gray level values not consistent with their local neighborhood.

In the presence of impulsive noise, linear filters, which consist of convoluting the image with a constant matrix to obtain a linear combination of neighborhood values, can produce blur, poor feature localization the appearance of secondary lobes in the frequency domain and incomplete noise suppression [133]. To overcome these shortcomings, nonlinear filters have been widely proposed. The most popular nonlinear filter is the median filter [134]. When considering a small neighborhood, it is highly efficient and has proved to be very effective in removing noise of an impulsive nature despite its simple definition. Fig. 46 shows final image after applying median filter on a sample micro-CT image of a tissue scaffold after segmentation. However, sometimes the median filter often fails to provide sufficient smoothing of non-impulsive noise and its results is sometimes unpredictable [135]. Examples of those techniques to solve the problem based on the average performance of the median filter are the weighted median filter [136], the adaptive trimmed mean filter [137], the center weighted median filter [138], the switching-based median filter [139], the mask median filter [140], and the minimum–maximum method [141].

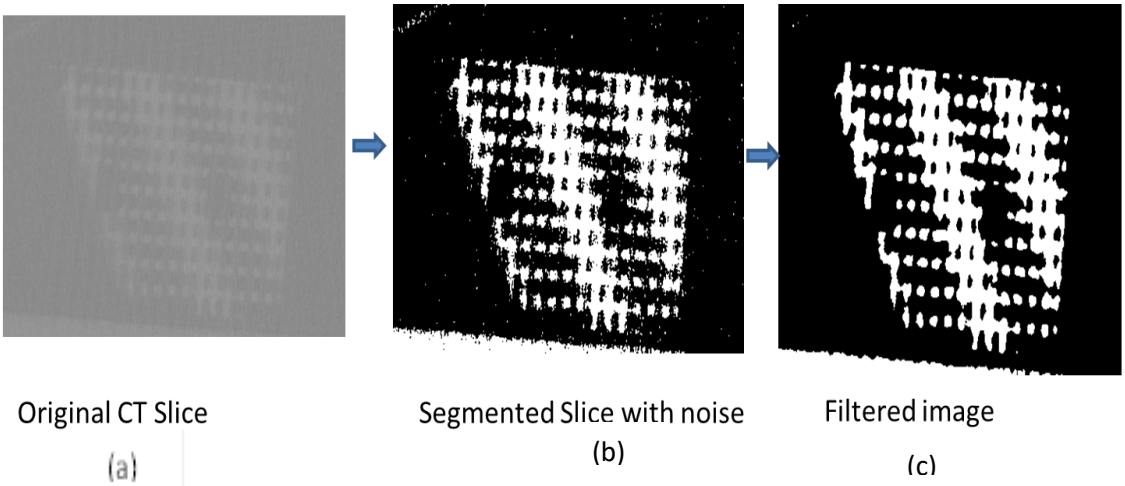

Figure 46: Noise removal using median filter

Gaussian smoothing algorithm [142] which is widely used in image processing is used to smooth the images. The Gaussian smoothing operator is a 2-D convolution operator that is used to `blur' images and remove detail and noise. The program loads the volumetric image, applies the smoothing algorithm in each direction, and then creates a new stack with the smooth images. Figure 47 shows one of the sample images where Gaussian smoothing algorithm is applied to 3D domain of segmented horse leg CT scan data.

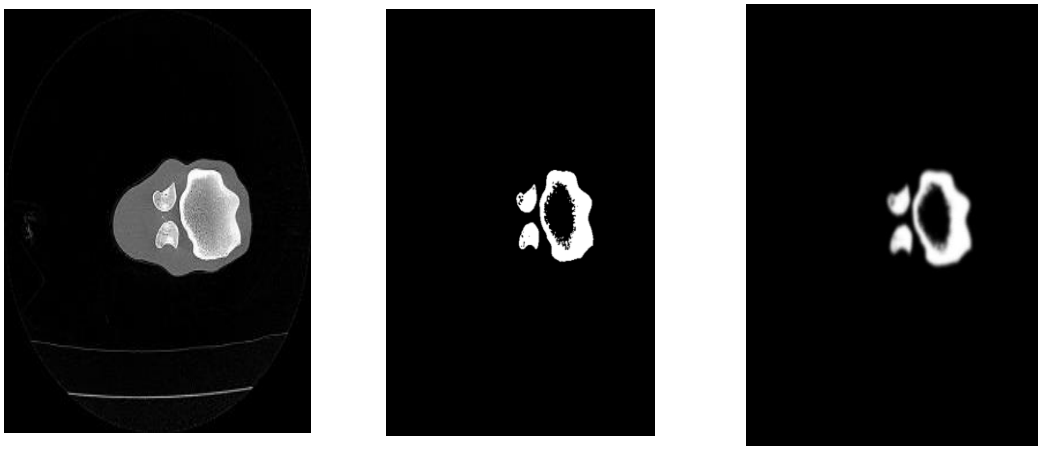

(a) (b) (c)

Figure 47: Gaussian Smoothing (a) Sample DICOM image from a horse leg CT scan (b) Corresponding Segmented Image of bone tissue c) Segmented Image after Gaussian Smoothing, σ=3

4.3.5. Material Property Mapping and Halftoning

After segmentation and image processing, the intensity and HU information is lost. Hence, the obtained binary images are compared pixel by pixel with the original image stack obtained by reading in DICOM images to map the intensity and HU information. One of such mapped slices obtained from segmenting hard tissue from a head CT is illustrated in Fig. 48. The required shades and gradients shown can only be achieved by patterning one or more materials through Halftoning/dithering principles. The percentage of each material patterned at this scale determines the overall hardness/stiffness of each region.

(a) (b)

Figure 48: One of the DICOM images for Head CT (b) Corresponding mapped segmented image

In this work, a 2D dithering algorithm using error diffusion proposed by Floyd et. al [143] is implemented in MATLAB. The algorithm is based on the principle that the average intensity over regions in the output bitmap is approximately the same as the average over the same region in the original greyscale image. The error made in replacing each original pixel by a single bit is added to the intensity value of neighboring pixels in such a way that the average value remains the same. The resulting algorithm generates a binary image for each slice where each greyscale area is approximated by combination of black and white pixels. The black pixels are assigned to a material with lower stiffness value and white pixels are assigned to material with higher stiffness value. Hence, as the intensity/ HU values are directly related to radiodensity, a continuous functionally graded model can be fabricated which roughly replicates true nature of different tissues. This step can be skipped when fabricated models using a single material.

Ideally, to truly replicate the properties of the imaged part, the black pixels need to be assigned a digital material that approximately matches the mechanical properties of region with lowest HU value (i.e., material 1) and white pixels need to be assigned a digital material that approximately matches the mechanical properties of region with highest HU value (i.e., material 2). Fig. 49 shows a mapped segmented image for head CT consisting both hard/bone and soft tissue and corresponding binary images obtained after dithering. A relationship that best maps each gray-scale index in a given CT scan to a specific digital material needs to be established similarly demonstrated in a previous work specific to Stratasys materials VeroWhitePlus and TangoBlack [144]. As a result, this framework has the capability to print multi-material CT models that reasonably match the range of stiffness of tissues and calcifications at high resolution.

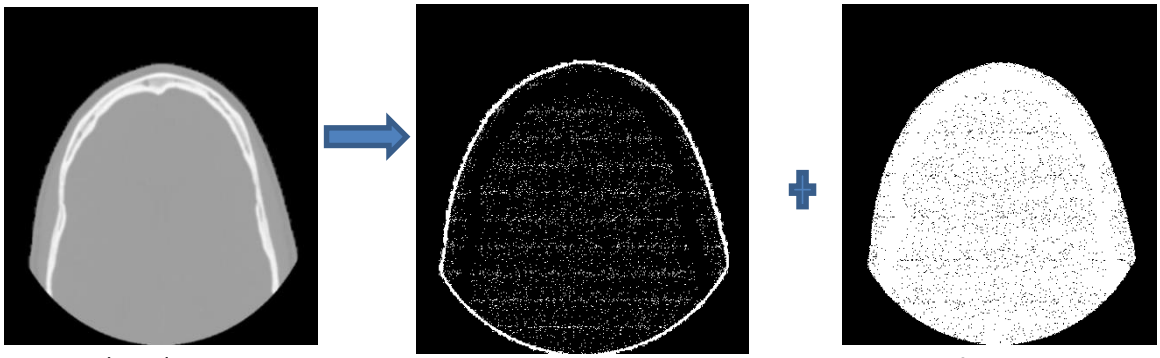

Figure 49: (a) One of the segmented images from a Head CT Scan and Corresponding dithered image for (b) Material 1(c) Material 2

Another approach can be to overlay a greyscale image on to the domain corresponding to a digital material that approximately matches the mechanical properties of the whole domain. The resulting image is then dithered into a binary image and mapped with materials corresponding to black and white pixels as described above. A simple example would be to overlay a greyscale gradient, as demonstrated in Fig. 50. After dithering, the resulting binary images are sent for toolpath generation.

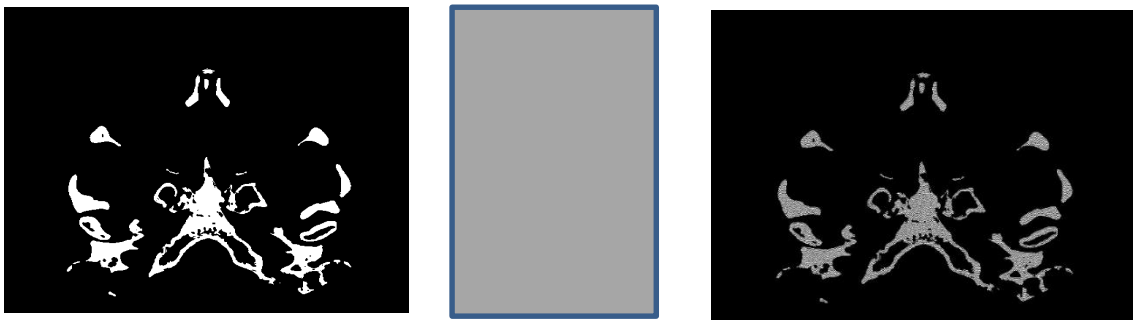

(a) (b) (c)

Figure 50: a) One of the segmented images from a Head CT Scan (b) Gradient bitmap overlayed (c) Corresponding dithered image

4.3.6. Bitmap file generation

Following the mapping of materials, toolpath files are generated for model fabrication. Typically, the input file format for Objet software is .STL/.OBJ file for each individual material body. Since we require pixel level material control and a model with continuous material grading or with smooth material transition at boundaries, we use a method called bitmap printing, where we directly use these bitmaps as input for model fabrication instead of converting them into a surface representation. If the resolution of the original imaging data does not match the resolution of the printer, the data set needs to be resized to match the resolution of the printer. The bitmaps obtained after dithering are scaled to the printer resolution using Bicubic interpolation where the output pixel value is a weighted average of pixels in the nearest 4-by-4 neighborhood. For each Z layer, two bitmap files, one for each material say 1 and 2, are written at the printer scale and format on a local voxel level. If the model is to be fabricated using a single material, a set of blank bitmaps of same resolution are given as input for material 2. The printer software puts support material at empty unsupported voxels. Fig. 51 shows input bitmap slices for a sample layer for fabricating a horse leg model from corresponding CT scans.

(a) (b)

Figure 51: One of the Toolpath image set for fabrication of a continuous functionally graded part for fabricating cross-section model of horse leg a) Toolpath for material 1 b) Toolpath for material 2

4.4. Results

Among the available 3D printing methods, Material Jetting is most suitable for fabricating patient-specific models, as it allows for selective deposition of materials at each voxel. In this work, we have used Objet Connex 350 from the Stratasys PolyJet™ series which can simultaneously print multiple materials at a resolution of 85×43×30 μm3. The models are fabricated using Stratasys Tango™ and Vero™ families of materials [145]. All computations are performed in MATLAB R2016 on a Dell PC with 16 GB RAM and Intel i7 3770K CPU @3.5 GHz and all models are fabricated on Objet Connex 350.

In order to show multiple applications of the framework, three case studies were carried out which are described in detail below:

4.4.1. Case Study 1: Micro-CT of Mouse Skull

Goal: To demonstrate ease of model fabrication from ultra-high resolution micro-CT scans

Method: For the first case, the data was obtained from a micro-CT scan of a mouse skull from Mouse Imaging Centre (MICe), Canada [146]. The scans were taken at a very high resolution with voxel size 50×50×30 μm^3 and contained almost no noise after segmentation. The Z resolution of the scan was 30 μm, which is exactly the same as that of Objet Connex 350, and hence no Z interpolation was required in this case. The skull tissue was segmented from the images using Intensity based segmentation technique described earlier. The images were resized in X and Y to match the printer resolution and directly sent for fabrication to the printer using voxel printing technique described earlier. The mouse skull fabricated using VeroWhitePlus (Shore hardness 85) is shown in Fig. 52b. This case emphasizes the ease of model fabrication where high resolution accurate CT images can be segmented and directly fabricated using a single material without any intermediate steps.

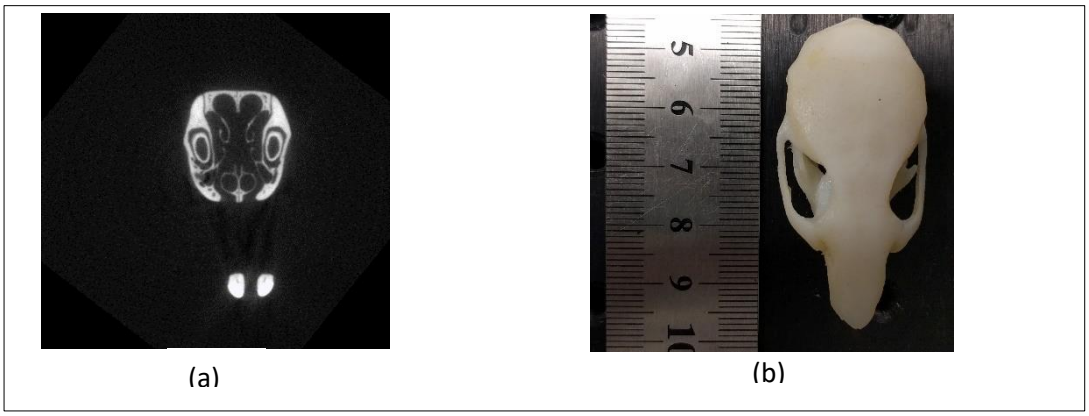

Figure 52: Sample micro-CT image of mouse skull (b) Fabricated model of mouse skull

4.4.2. Case Study 2: Head CT

Goal: To fabricate accurate anatomical model containing single tissue region using single and functionally graded materials

Method: Next, another case study was carried out using partial head CT scan data consisting of 188 DICOM images with voxel size 0.3613×0.3613×0.6250 mm^3 obtained through Carilion Clinic at Virginia Tech. This case study was carried out in two steps. First, a model of only the hard/bone tissue in head CT using a single material was fabricated. Using intensity based segmentation method described in Section 4.2.2.1, the hard/ bone tissue was segmented from corresponding CT images. After post-processing, the resulting binary images were sent directly for toolpath generation for bitmap printing. The resulting voxel stack was scaled (interpolated)

to printer resolution (voxel sixe 85×43×30 μm^3) and fabricated using VeroWhitePlus material. The resulting full scale fabricated model and framework is shown in Fig. 53. Hence, models to be fabricated using single material can be directly fabricated with this framework after simple image processing operations. This example again emphasizes the ease of model fabrication using this framework.

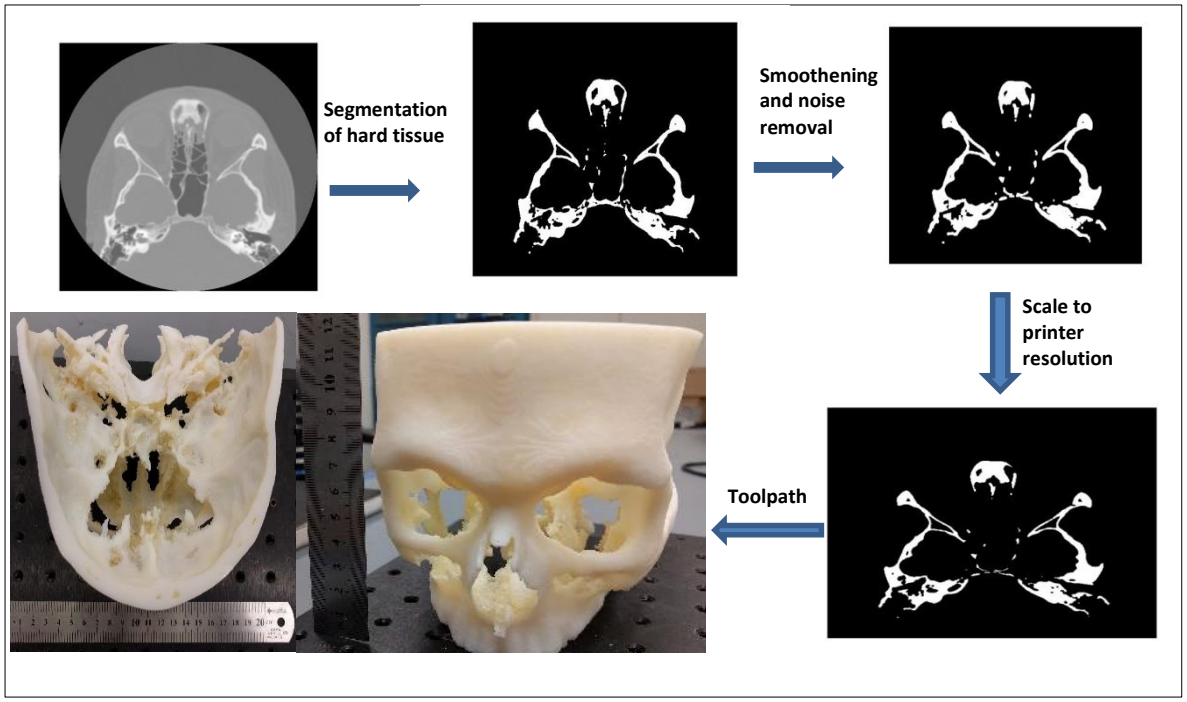

***Figure 53**:* Flow chart for fabrication of model of bone tissue from a head CT scan using a single material (Vero WhitePlus)

However, while segmenting hard bone tissue, it can be seen that not all corresponding pixels have same HU value. This is because not all bones have same density. Moreover, theoretically if any bone is fractured or cancellous it will have a much lower density. Hence for the second step of this case study, the same head CT model is fabricated as a continuous functionally graded part. In this step, again first the hard/bone tissue is segmented using Intensity based segmentation. Noise removal and Gaussian smoothing filters are applied and resulting images are sent for material mapping to map intensity and HU values from corresponding DICOM images. 2D dithering algorithm described in section 4.2.5 was used to covert the greyscale images into binary. The white image pixels were mapped with VeroWhitePlus (Shore hardness 85) whereas the black image pixels were mapped with Tango BlackPlus material (Shore Hardness 26-28). The resulting bitmaps were sent for toolpath generation. The fabricated model along with framework is shown in Fig. 54.

4.4.3. Case Study 3: Horse Leg CT

Goal: To fabricate accurate anatomical model containing multiple tissue regions using functionally graded materials

Method: This framework can also be used to fabricate a continuous functionally graded model of more than one type of connected tissue regions. For demonstrating this, we carried out a third case study to fabricate a continuous multi-material graded structure containing both hard bone tissue and soft tissue from a CT scan of a horse leg. The CT stack consisted of 1100 slices with a voxel size of 0.4830×0.4830×0.5 mm^3.

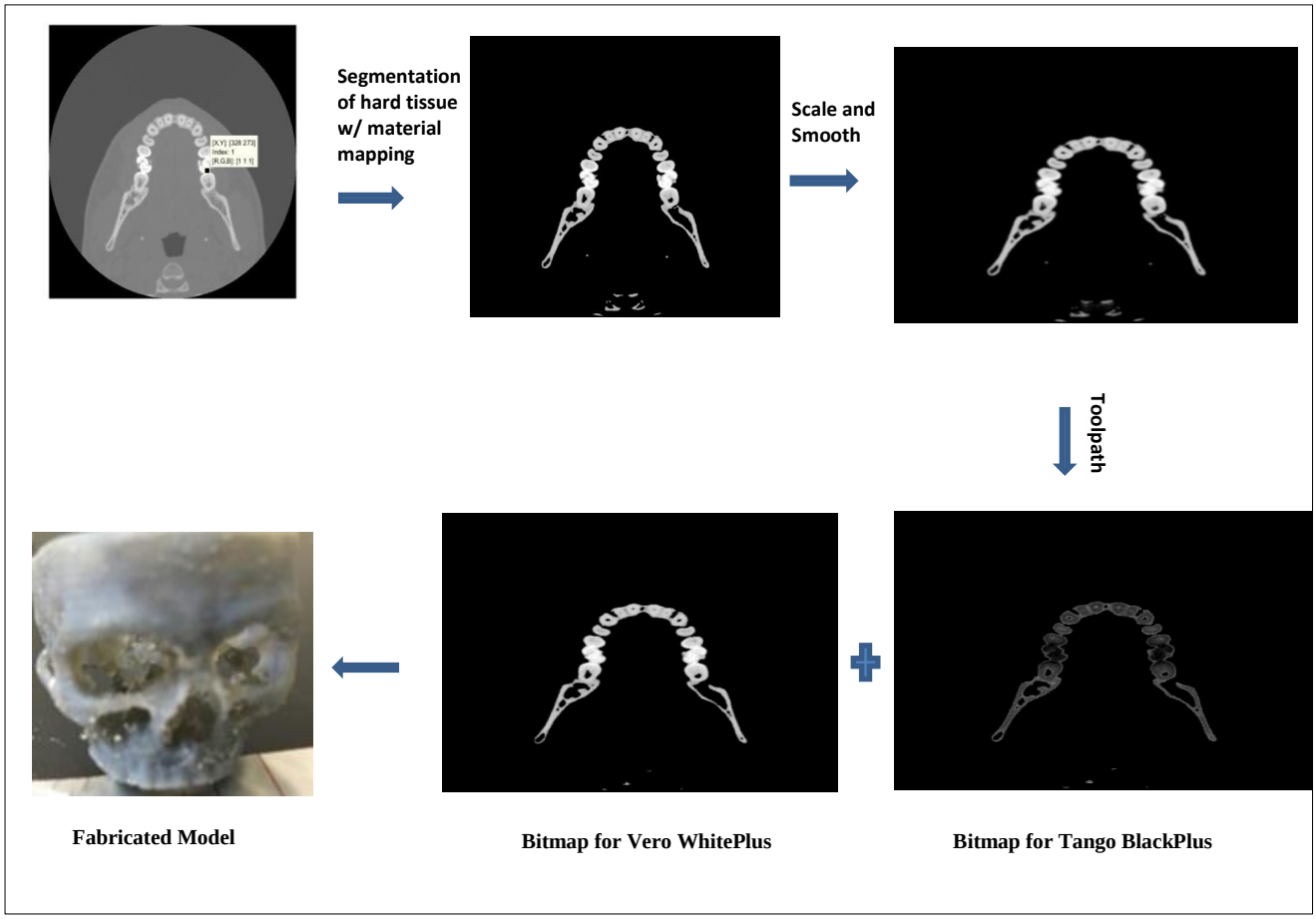

Figure 54: Flow chart for fabrication of continuous functionally graded model of skull model from a head CT scan

In this case study, using region growing method described above in Section 4.2.2.2, both hard and soft tissue region is segmented simultaneously from DICOM as a single image. After post processing, the segmented images are sent for material mapping to map intensity and HU values from corresponding DICOM images. The resulting greyscale images are then converted into binary images using dithering. Here, the white image pixels were mapped with Vero WhitePlus (Shore hardness 85; a stiffer material), whereas the black image pixels were mapped with TangoPlus material (Shore Hardness 27; a softer transparent material). Hence, all the intermediate different greyscale values correspond to a different material blend of Vero WhitePlus and TangoPlus according to the dithering pattern.

Since different blends of Vero WhitePlus and TangoPlus are not transparent, the bitmaps were cut in half along the length so that different tissue regions could be identified on the interface. Also since the entire horse leg model model was too big to fit inside the build volume of the Objet Connex, the resulting bitmaps were scaled down by a factor of three as compared to the printer resolution to 900×1800×2550 dpi and sent for toolpath generation.

The fabricated multi-material model along with framework is shown in Fig. 55. As it can be seen that, due to lack of availability of completely transparent material blends for Material Jetting, the interior structure of the model is only partially visible. The different bone and soft tissue regions can be clearly distinguished at the half cross-section of the model which can be clearly seen in Fig. 55(b).

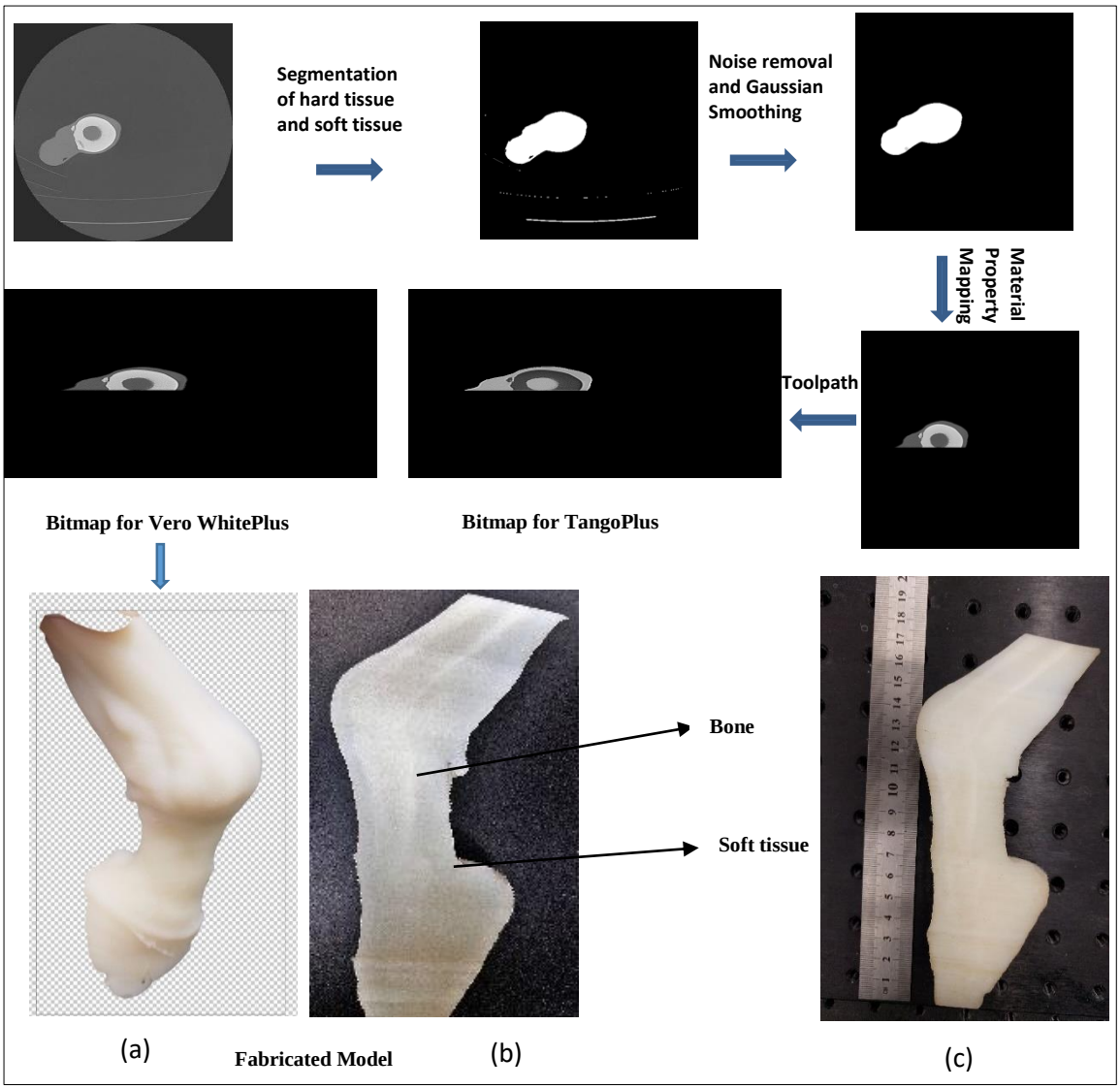

Figure 55: Flow chart and Fabricated multi-material graded model of down scaled horse leg model (a) Front View (b) XZ cross-section zoomed (c) XZ cross-section with dimension

The last two examples show that the framework has the capability of fabricating continuous functionally graded patient specific models comprising of one or more tissue regions.

4.4.4. Verification

In order to verify the dimensional accuracy of the framework, the skull model from Case Study in Section 4.3.2 was reconstructed using Materialize Mimics [80] software and the resulting surface model was imported in Netfabb software [147]. Materialize Mimics has been widely used by researchers for various applications involving imaging data including accuracy measurement of three dimensional measurements using CT [148, 149], accurate surgical planning [150], finite element analysis [151,152] and computational modeling from imaging data [153]. The following three dimensions in the reconstructed skull model were measured in Netfabb:

a) Wall thickness at the top center (will be referred to as dimension label A1) (Fig. 56)
b) Distance from top center to the center of the beginning of nose feature (will be referred to as dimension label A2) (Fig. 57)

c) Thickness at the top of the nose feature (will be referred to as dimension label A3) (Fig. 58)

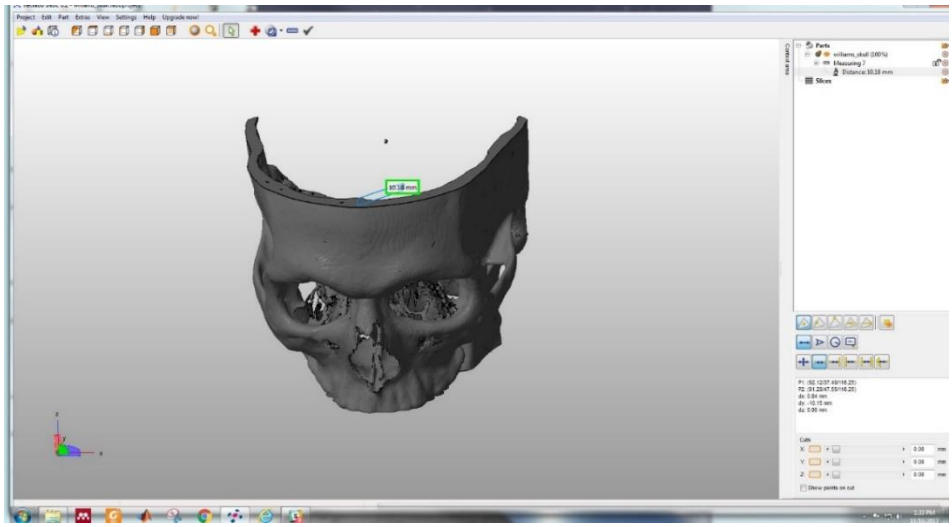

Figure 56: Wall thickness at top center of skull model measured in Netfabb

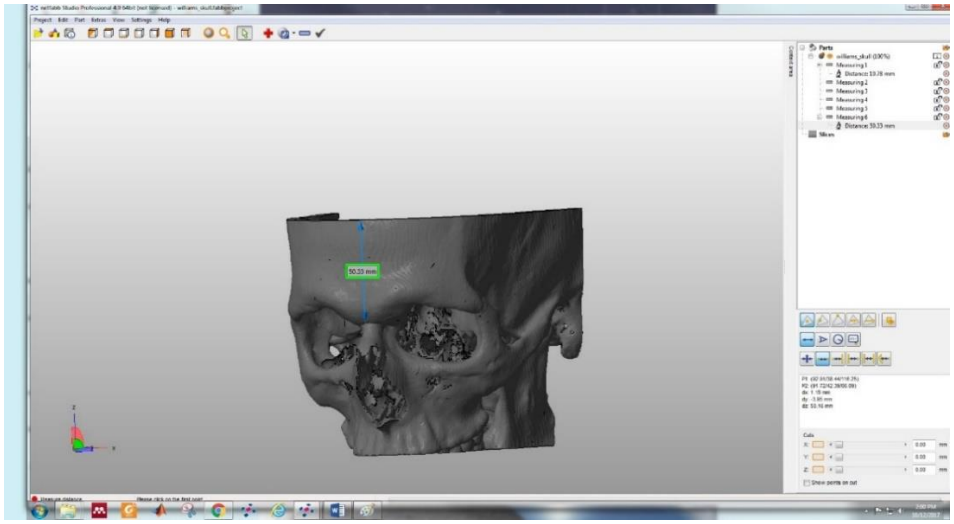

Figure 57: Distance from top center to the center of the beginning of nose feature measured in Netfabb

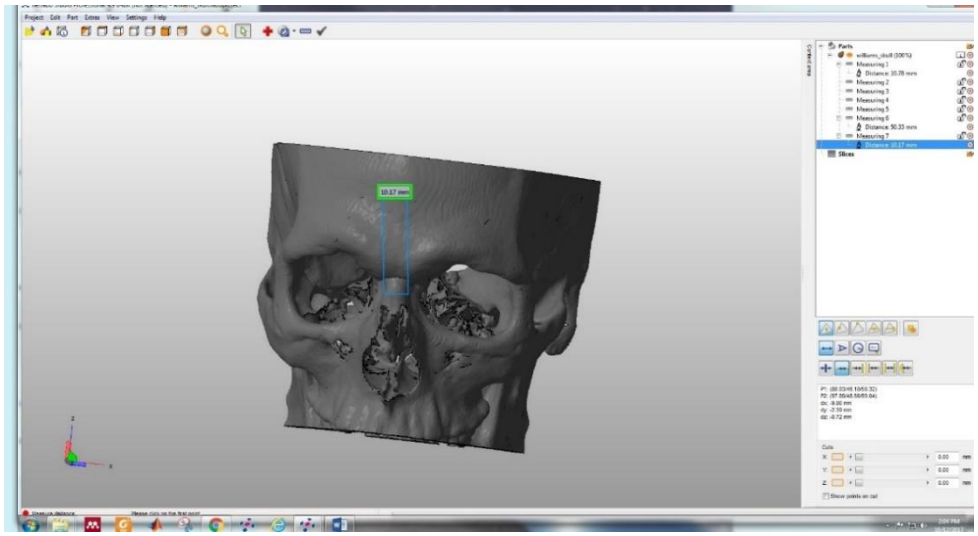

Figure 58: Thickness at the top of the nose feature measured in Netfabb

The measurements corresponding to the above dimensions in the skull model fabricated in the case study in Section 4.3.2 were taken using a Vernier Caliper. These can be seen in Fig. 59 and the comparison between theoretical values obtained from Netfabb and corresponding measured values is summarized in Table 16.

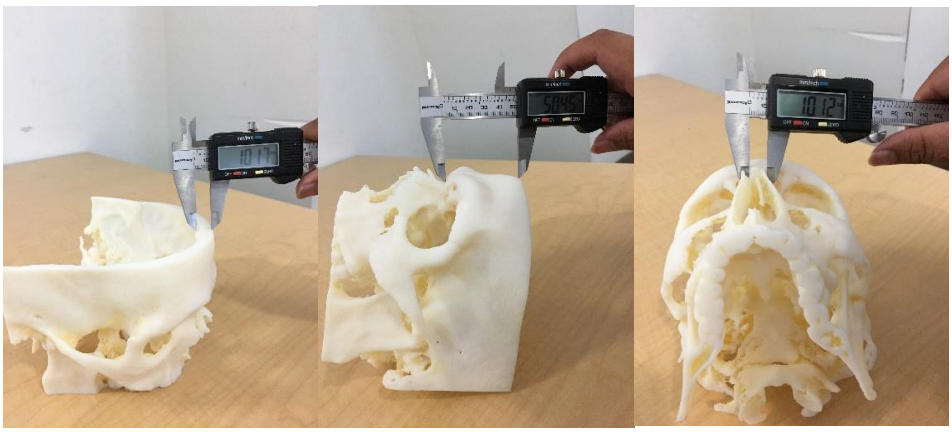

Figure 59: Corresponding dimensions in fabricated skull model measured using Vernier Caliper

Table 16: Comparison between theoretical values obtained from Netfabb and corresponding measured values

Dimension Label	Theoretical value from Netfabb (mm)	Measured value (mm)	% Difference
A1	10.18	10.17	0.09
A2	50.33	50.45	0.24
A3	10.17	10.12	0.49

From the above table, it can be concluded that the fabricated skull model is fairly accurate and closely matches with the reconstructed model in Netfabb. The maximum percentage error observed among the three dimensions is found to be 0.49%.

The same procedure was carried out for fabricated horse leg model in Section 4.3.3. The horse leg model was reconstructed in Materialize Mimics, rescaled to the resolution of our printed model and exported to Netfabb. The following three dimensions in the reconstructed horse leg model were measured in Netfabb:

a) Length at center of top cross-section (will be referred to as dimension label B1) (Fig. 60)
b) Width at center of top cross-section (will be referred to as dimension label B2) (Fig. 60)
c) Overall Z-height of the model (will be referred to as dimension label B3) (Fig. 61)

Similar to the previous skull model study, the measurements corresponding to the above dimensions in the horse leg model fabricated in the case study in Section 4.3.3 were taken using a Vernier Caliper. These can be seen in Fig. 62 and the comparison between theoretical values obtained from Netfabb and measured values is summarized in Table 17.

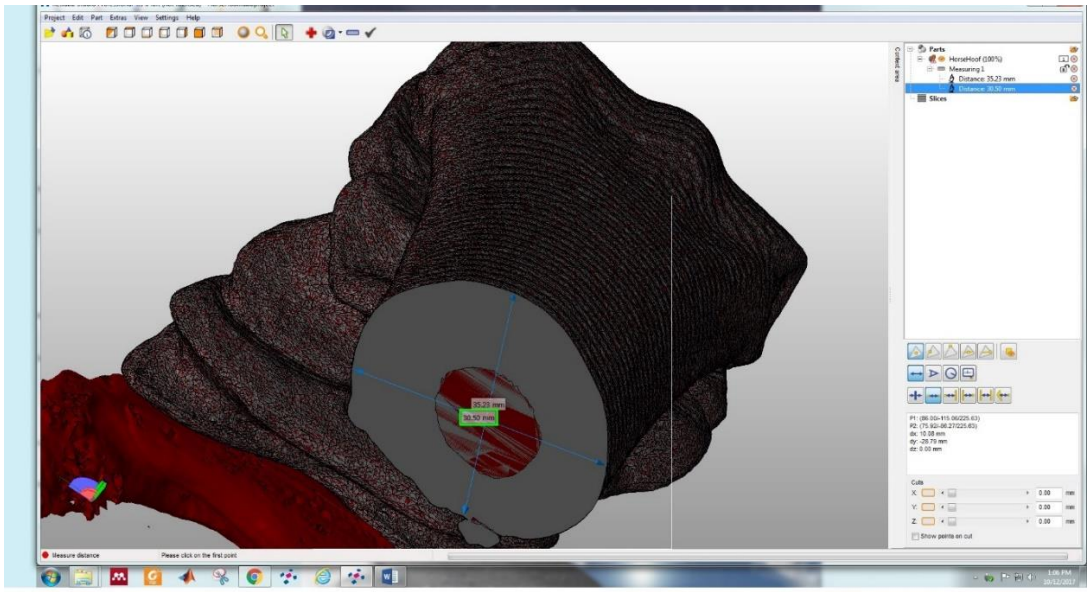

Figure 60: Length and width at center of horse leg top cross-section measured in Netfabb

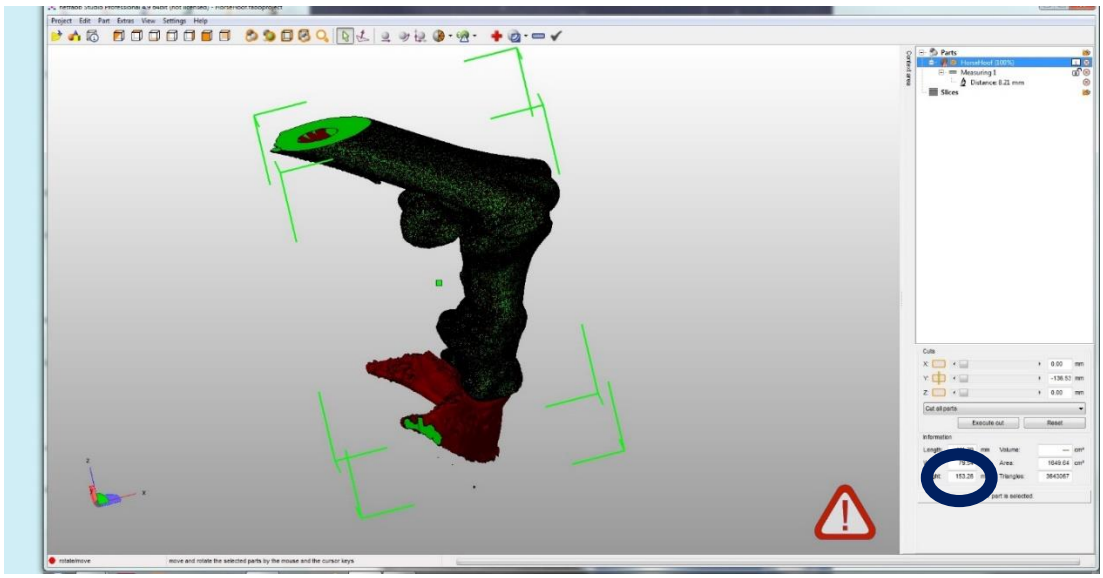

Figure 61: Overall Z-height of the horse leg model measured in Netfabb (Circled)

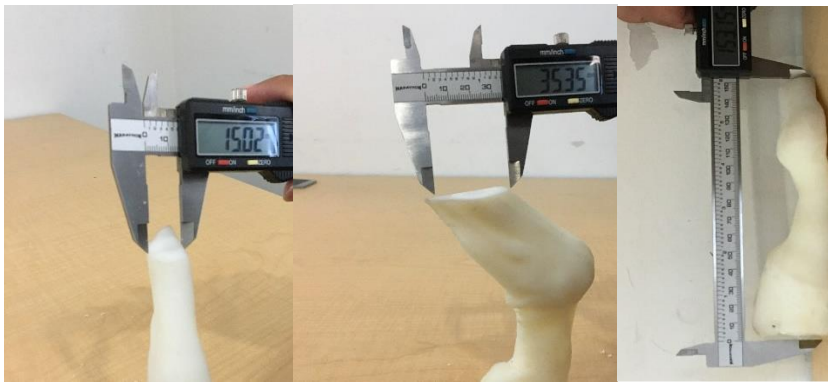

Figure 62: Corresponding dimensions in fabricated horse leg model measured using Vernier Caliper

Table 17: Comparison between theoretical values obtained from Netfabb and corresponding measured values

Dimension Label	Theoretical value from Netfabb (mm)	Measured value (mm)	% Difference
B1	15.25 (half cross-section length)	15.02	1.5
B2	35.23	35.35	0.34
B3	153.26	153.15	0.07

Again from the above table, we can conclude that the fabricated horse leg model closely matches the reconstructed model obtained from Mimics. In this case, the maximum percentage error among the three measured dimensions is 1.5%. Some of the error can be attributed to discrepancies in hand measurements. In the future, more sophisticated reverse engineering techniques will be implemented for accuracy measurements. Also, in this study, we could not separately study the error contribution due to segmentation, noise removal and segmentation techniques and the error contribution due to the fabrication process separately. Efforts will be carried out in the future to quantify these separately. The successful duplication of these parts implies a great potential for Model free additive manufacturing. Also however, more process and material limitations still need to be studied.

4.5. Conclusion and Discussion

4.5.1. Conclusion

In this work, we have presented and validated a new voxel-based framework for fabricating models directly from CT scan data with multi-material property allocation.

The paper also introduces the concept of voxel printing to fabricate patient specific models directly from imaging data using simple 2D image processing and signal processing operations. This is in contrast to the commercial pre-processing frameworks for imaging data which convert the imaging data into a surface representation using various computationally expensive reconstruction and smoothing algorithms. Hence, the ease of model fabrication and accuracy can be greatly improved by this framework.

This paper also integrates the concept of dithering which enable the functionality to map different materials at pixel level and generate a continuous functionally graded approach. To illustrate the approach, using this framework we fabricated models directly from imaging data using single and multi-material additive manufacturing. First, a model of mouse skull was fabricated from corresponding high resolution micro-CT scans to demonstrate the ease of model fabrication in such cases using this framework. A set of partial human head CT scan and horse leg CT scan images were used for case study. The bone tissue (skull) was segmented and resulting model was fabricated first directly using a single material, and then as a continuous functionally graded part. Finally, a multi-material functionally graded model of a horse leg CT Scan was fabricated depicting both hard and soft tissue to illustrate the advantage that this framework provides for fabricating more than one different connected tissue regions as a single functionally graded model.

4.5.2. Discussion

As shown previously, by generating the bitmaps for the Objet Connex 3D printer, we can directly control the material composition of models on the voxel level, which is considered a significant component of the printing strategy. This strategy can be useful not only in the future for reverse engineering using imaging data but also in digital design and fabrication

using voxels which is currently beyond the capability of traditional CAD and AM workflows. Hence, this work emphasizes the need for development of more AM workflows which allow the designer to work at a voxel level.

This framework also emphasizes the need for development for more compliant materials which can mimic the heterogeneous nature of human body and utilize the full potential of such a voxel based framework described above. The currently available materials for Material Jetting such as Tango BlackPlus and TangoPlus etc. are not flexible enough to mimic the range of soft tissues in the human body. Also as seen above while fabricating the horse leg model, the current commercially available materials cannot fully make use of the dithering/halftoning feature even if one of the parent materials is transparent as the resulting different material blends are not fully transparent. Hence, we as a community need to push the limits of 3D printing with development of algorithms/materials to achieve transparency/ translucency in material blends for representing multiple distinct surfaces in a model.

We envision that 3D printed medical models with graded material properties using voxel-based algorithms are only the first component of a major shift in how medical intervention is achieved. This framework in the future could support fundamental research in variety of other areas such as continuum mechanics, computational fluid dynamics, experimental dynamic flow modeling and structure/process/property relationships of novel 3D printed elastomeric materials. This could provide a considerable boost in the development of novel medical therapies and in the process, save thousands of lives.

4.6. Future Work

In order to further validate the proposed methodology, the authors aim to extend the reported work by providing additional features and further validation of the framework. For this realization following steps will be undertaken.

- More advanced segmentation techniques will be implemented for better and more efficient segmentation
- More non-linear filters and smoothing algorithms from literature will be incorporated
- More advanced 3D Halftoning and dithering techniques will be incorporated and compared to better replicate heterogeneous object
- More accuracy validation techniques will be implemented both for measuring error during segmentation process and during the fabrication process
- A real-life case study with VT Carilion to accurately simulate complex structural cardiac interventions in the operating room will be performed
- Final effort will include research on new polymers to fabricate more multi-material functionally graded models which replicate the human anatomy more closely

Chapter 5: Summary

5.1. Conclusions

In this thesis, various advantages of using a volumetric representation instead of a surface representation were demonstrated using software tools for applications in Design and Manufacturing, Engineering Design Education, and Reverse engineering using imaging data for medical applications.

In Chapter 2, a tool was presented for automated manufacturability analysis of shapes to be manufactured using Additive Manufacturing. The input polygonal model is first converted to a voxel model using Ray Casting Algorithm. Various simple and easy to implement algorithms have been presented to evaluate various factors governing manufacturability viz. minimum feature size, support material, build orientation and build time. The results from this tool were successfully validated using a simple case study and comparison with an existing pre-processing software Simplify 3D. One of the problems associated with voxel representation has always been large memory requirement. To address this issue, efforts would be carried out in the future to convert surface representation into volumetric representation and store it in a data structure format like Octree.

In Chapter 3, the above developed software tool along with Sculptprint was implemented in an undergraduate sophomore classroom study for teaching instruction regarding DFM considerations in AM and SM. Before the study, students were asked to take a Pre-Assessment Survey and Pre-Test to gauge the prior knowledge and experience of students. Almost 25% of the students indicated no prior machining or 3D printing experience and almost 60% of the students identified themselves in the novice category. After the study, a post test was conducted where students were asked questions on process selection similar to the Pre-Test. Comparing the pre-test and post-test results using statistical analysis, we observed that using visual rapid manufacturability assessment tools along with conventional teaching method was effective in teaching students about DFM principles and improved students' performance by around 30%. We also observed that the group of students that indicated neither machining nor 3D printing experience actually showed the largest improvement in Post-Test. Further analysis showed that prior 3D printing experience was not a significant factor in students' performance in the Post-Test. The AM manufacturability analysis tool was also given to students to help them visualize design considerations for their final project. A portion of students used the software to perform design iterations based on the software feedback to improve their designs and fabricate them successfully. Almost all students used the software to receive feedback regarding amount of material, build time and cost required to manufacture their parts and select the most optimum orientation. Sources of error were discussed, limitations of the study were given, and ideas for improvement of future implementations based on the outcomes of this study were presented.

In Chapter 4, a new voxel based framework was presented for model fabrication using CT scan data with material property allocation. We have also introduced the concept of voxel printing to fabricate patient specific models directly from imaging data using simple 2D image processing and signal processing operations. This is in contrast to the commercial pre-processing frameworks for imaging data which convert the imaging data into a surface

representation using various computationally expensive reconstruction and smoothing algorithms. Three separate case studies were performed to validate the framework to fabricate single and multi-material anatomical model containing one or more tissue regions. In the future, more advanced segmentation techniques will be implemented for better and more efficient segmentation. Also, more non-linear filters and smoothing algorithms and more advanced 3D Halftoning and dithering techniques from literature will be incorporated. A real-life case study with VT Carilion to accurately simulate complex structural cardiac interventions in the operating room will be performed. Final effort will include research on new polymers to fabricate more multi-material functionally graded models which replicate the human anatomy more closely

Hence, this work emphasizes the need for development of further voxel based frameworks and algorithms to explore further advantages over surface representations and fully unlock the superior capabilities of AM. Finally, several conference papers were published by the author throughout the timeframe of this dissertation study which are summarized below:

1) S. Tedia and C. B. Williams (2016). "Manufacturability analysis tool for Additive manufacturing using voxel-based geometric modelling", 27th Annual International Solid Freeform Fabrication (SFF) Symposium, 2016
2) S.Dinda, S.Tedia, "Expediting Build Time, Material, And Cost Estimation For Material Extrusion Processes To Enable Mobile Applications", IDETC 2017, In Press
3) Lynn, R., Saldana, C., Kurfess, T., Reddy, N., Simpson, T., Jablokow, K., Tucker, T., Tedia, S. and Williams, C., 2016. Toward Rapid Manufacturability Analysis Tools for Engineering Design Education. Procedia Manufacturing, 5, pp.1183-1196.

5.2. Scientific Contribution

The following scientific contributions have been made through the successful completion of this dissertation study:

1) Proposed a framework for manufacturability analysis of AM parts using voxel based modeling (Chapter 2)
2) Developed a new DFM module for undergraduate classroom instruction (Chapter 3)
3) Understanding whether instruction using rapid manufacturability analysis software programs improves students' ability to make decisions about process selection between Additive and Subtractive Manufacturing to efficiently design their parts (Chapter 3)
4) Proposed a framework for model free AM directly from imaging data using voxel based modeling (Chapter 4)

5.3. Broader Impact

The presented work in the development of voxel based algorithms supports the following broader impacts (i.e. outside of improving the scientific knowledge base of the research community):

1) The manufacturability analysis framework can be integrated with open source maker spaces at Universities and cloud based mobile and desktop applications and made readily available to students to quickly gauge the feasibility of 3D printing their parts, manage their budgets, and save time.

2) The framework proposed for fabricating parts directly from imaging data in the future could support medical intervention and fundamental research in variety of other areas such as continuum mechanics, computational fluid dynamics, experimental dynamic flow modeling etc. in the process impacting thousands of lives.
3) This thesis as a whole emphasizes the need for development of more AM and CAD workflows which allow the designer to work at a voxel level.

Bibliography

[1] Roscoe, L.E., 1988. Stereolithography interface specification. America-3D Systems Inc, p.27.

[2] Hiller, J.D. and Lipson, H., 2009, August. STL 2.0: a proposal for a universal multi-material Additive Manufacturing File format. In *Proceedings of the Solid Freeform Fabrication Symposium* (No. 1, pp. 266-278).

[3] Georges M. Fadel, Chuck Kirschman, (1996) "Accuracy issues in CAD to RP translations", Rapid Prototyping Journal, Vol. 2 Issue: 2, pp.4-17

[4] http://www.nist.gov/el/msid/infotest/upload/Lipson-Cornell-NIST-AMF.pdf

[5] A. Kaufman, "Volume Graphics GmbH …," *IEEE Comput.*, vol. 26, no. 7, pp. 51–64, 1993.

[6] U. Tiede, T. Schiemann, and K. H. Hohne, "High quality rendering of attributed volume data," *Proc. Vis. '98 (Cat. No.98CB36276)*, vol. D, 1998.

[7] W. Gao, Y. Zhang, D. Ramanujan, K. Ramani, Y. Chen, C. B. Williams, C. C. L. Wang, Y. C. Shin, S. Zhang, and P. D. Zavattieri, "The status, challenges, and future of additive manufacturing in engineering," Comput. Des., vol. 69, pp. 65–89, 2015.

[8] N. Meisel and C. B Williams, "An Investigation of Key Design for Additive Manufacturing Constraints in Multimaterial Three-Dimensional Printing," J. Mech. Des, 137(11), 111406, 2015.

[9] "Designing mechanical parts for 3D printing." [Online]. Available: http://www.shapeways.com/tutorials/designing_mechanical_parts_for_3d_printing/.

[10] C. C. Seepersad, T. Govett, K. Kim, M. Lundin, and D. Pinero, "A Designer's Guide for Dimensioning and Tolerancing SLS parts," 23rd Annu. Int. Solid Free. Fabr. Symp., pp. 921–931, 2012.

[11] Fernandez-Vicente, M., Canyada, M. and Conejero, A., "Identifying limitations for design for manufacturing with desktop FFF 3D printers" International Journal of Rapid Manufacturing, 5(1), pp.116-128, 2015.

[12] S. Moylan, J. Slotwinski, A. Cooke, K. Jurrens, M. Alkan Donmez, "Proposal for a Standardized Test Artifact for Additive Manufacturing Machines and Processes," International Solid Freeform Fabrication Symposium, Austin, Tx, 2013.

[13] R. Tam and W. Heidrich, "Shape Simplification Based on the Medial Axis Transform," Proc. IEEE Vis. Conf., pp. 481–488, 2003.

[14] C. W. Niblack, D. W. Capson, and P. B. Gibbons, "Generating skeletons and centerlines from the medial axis transform," [1990] Proceedings. 10th Int. Conf. Pattern Recognit., pp. 881–885, 1990.

[15] J. Damon, "Determining the geometry of boundaries of objects from medial data," Int. J. Comput. Vis., vol. 63, no. 1, pp. 45–64, 2005.

[16] N. Iyer, Y. Kalyanaraman, K. Lou, S. Jayanti, and K. Ramani, "A Reconfigurable 3D Engineering Shape Search System Part I: Shape Representation," Proc. DETC' 03, pp. 1–10, 2003.

[17] S. Nelaturi, W. Kim, and T. Kurtoglu, "Manufacturability feedback and model correction for additive manufacturing," J. Manuf. Sci. Eng., vol. 137, no. 2, p. 21015, 2015.

[18] Lu, S.C., Rebello, A.B., Miller, R.A., Kinzel, G.L. and Yagel, R., "A simple visualization tool to support concurrent engineering design," Computer-Aided Design, vol. 29, no. 10, pp. 727–735, 1997.

[19] Jones, M.W. and Satherley, R.A., "Shape Representation using Space Filled Sub-Voxel Distance Fields," International Conference on Shape Modeling and Applications, 316-325, 2001.

[20] F. S. Nooruddin and G. Turk, "Simplification and repair of polygonal models using volumetric techniques," IEEE Trans. Vis. Comput. Graph., vol. 9, no. 2, pp. 191–205, 2003.

[21] Telea, A. and Jalba, A., "Voxel-based assessment of printability of 3D shapes", International Symposium on Mathematical Morphology and Its Applications to Signal and Image Processing, Springer Berlin Heidelberg, pp. 393-404, 2011.

[22] J. R. Rossignac and A. A. G. Requicha, "Offsetting operations in solid modelling," Comput. Aided Geom. Des., vol. 3, no. 2, pp. 129–148, 1986.

[23] Y. Chen and X. Xu, “Manufactruability analysis of infeasible features in polygonal models for web-based rapid prototyping,” Proc. - 2010 Int. Conf. Manuf. Autom. ICMA 2010, pp. 120–127, 2010.
[24] P. Das, R. Chandran, R. Samant, and S. Anand, “Optimum Part Build Orientation in Additive Manufacturing for Minimizing Part Errors and Support Structures,” Procedia Manuf., vol. 1, pp. 343–354, 2015.
[25] G. Strano, L. Hao, R. M. Everson, and K. E. Evans, “A new approach to the design and optimisation of support structures in additive manufacturing,” Int. J. Adv. Manuf. Technol., vol. 66, no. 9–12, pp. 1247–1254, 2013.
[26] “Voxelizer Software.” [Online]. Available: http://voxelizer.com/.
[27] P. Alexander, S. Allen, and D. Dutta, “Part orientation and build cost determination in layered manufacturing,” Comput. Des., vol. 30, no. 97, pp. 343–356, 1998.
[28] Campbell, I., Combrinck, J., De Beer, D., & Barnard, L., "Stereolithography Build Time Estimation Based On Volumetric Calculations," Rapid Prototyping Journal, 14(5), 271-279. Doi: 10.1108/13552540810907938, 2008.
[29] Hollis, R. L., Geometry-Based Estimation for Additive Fabrication. (Doctor of Philosophy), Alabama in Huntsville, Huntsville, Alabama, 2001.
[30] Di Angelo, L., & Di Stefano, P., "A neural network-based build time estimator for layer manufactured objects," International Journal of Advanced Manufacturing Technology, 57(1-4), 215-224. doi: 10.1007/s00170-011-3284-8, 2011
[31] J. D. Hiller and H. Lipson, “Fully Recyclable Multi-Material Printing,” Solid Free. Fabr. Symp., pp. 98–106, 2009.
[32] J. Hiller and H. Lipson, “Design and analysis of digital materials for physical 3D voxel printing,” Rapid Prototyp. J., vol. 15, no. 2, pp. 137–149, 2009.
[33] E. L. Doubrovski, E. Y. Tsai, D. Dikovsky, J. M. P. Geraedts, H. Herr, and N. Oxman, “Voxel-based fabrication through material property mapping: A design method for bitmap printing,” CAD Comput. Aided Des., vol. 60, pp. 3–13, 2015.
[34] A. Brunton, C. A. Arikan, and P. Urban, “Pushing the Limits of 3D Color Printing: Error Diffusion with Translucent Materials,” Siggraph, vol. 1, no. 212, pp. 1–12, 2014.
[35] V. Chandru, S. Manohar, and C. E. Prakash, “Voxel-based modeling for layered manufacturing,” IEEE Comput. Graph. Appl., vol. 15, no. 6, pp. 42–47, 1995.
[36] Lin, F., Seah, H.S., Wu, Z. and Ma, D., "Voxelization and fabrication of freeform models", Virtual and Physical Prototyping, 2(2), pp.65-73, 2007.
[37] D. Ma, F. Lin, and C. K. Chua, “Rapid prototyping applications in medicine. Part 1: NURBS-based volume modelling,” Int. J. Adv. Manuf. Technol., vol. 18, no. 2, pp. 103–117, 2001.
[38] D. Ma, F. Lin, and C. K. Chua, “Rapid prototyping applications in medicine. Part 2: STL file generation and case studies,” Int. J. Adv. Manuf. Technol., vol. 18, no. 2, pp. 118–127, 2001.
[39] Forstmann, S. and Jun, O.H.Y.A., "Efficient, high-quality, GPU-based visualization of voxelized surface data with fine and complicated structures," IEICE TRANSACTIONS on Information and Systems, 93(11), pp.3088-3099, 2010.
[40] S. Patil and B. Ravi, “Voxel-based representation, display and thickness analysis of intricate shapes,” Proc. - Ninth Int. Conf. Comput. Aided Des. Comput. Graph. CAD/CG 2005, vol. 2005, pp. 415–420, 2005.
[41] L. D. Sturm, C. B. Williams, J. A. Camelio, J. White, and R. Parker, “Cyber-Physical Vunerabilities In Additive Manufacturing Systems,” Int. Solid Free. Fabr. Symp. Proc., pp. 951–963, 2014.
[42] M. Cloots, A. B. Spierings, and K. Wegener, “Assessing new support minimizing strategies for the additive manufacturing technology SLM”,” Proc. Solid Free. Fabr. Symp., pp. 131–139, 2013.
[43] Apriori Software. https://www.apriori.com
[44] Plethora: CNC Machining On Demand. https://www.plethora.com
[45] Turley, S.P., Diederich, D.M., Jayanthi, B.K., Datar, A., Ligetti, C.B., Finke, D.A., Saldana, C. and Joshi, S., 2014, January. Automated process planning and CNC-Code generation. In IIE Annual Conference. Proceedings (p. 2138). Institute of Industrial and Systems Engineers (IISE).

[46] Lee, Y.-S., 1998, "Mathematical Modeling Using Different Endmills and Tool Placement Problems for 4- and 5-Axis NC Complex Surface Machining," Int. J. Prod. Res., 36 (3), pp. 785–814.
[47] Reddy, N.S.K. and Rao, P.V., 2005. Selection of optimum tool geometry and cutting conditions using a surface roughness prediction model for end milling. The International Journal of Advanced Manufacturing Technology, 26(11-12), pp.1202-1210.
[48] Slic3r Software. http://slic3r.org/.
[49] Repetier Software. http://www.repetier.com/.
[50] KISSlicer Software. http://www.kisslicer.com/.
[51] ReplicatiorG Software. http://replicat.org/.
[52] 3D Slicer: A multi-platform, free and open source software package for visualization and medical image computing. Available from: http://www.slicer.org/.
[53] S. Tedia and C. B. Williams (2016). "Manufacturability analysis tool for Additive manufacturing using voxel-based geometric modelling", 27th Annual International Solid Freeform Fabrication (SFF) Symposium, 2016
[54] R. Lynn, "Enhancing Awareness of Additive and Subtractive Manufacturability with Voxel-Based Simlations," Georgia Institute of Technology, 2017.
[55] R. H. Todd, W. E. Red, S. P. Magleby, and S. Coe, "Manufacturing: a strategic opportunity for engineering education," Journal of Engineering Education, vol. 90, no. July, pp. 397–405, 2001.
[56] Min Jou, "Development of an e-learning system for teaching machining technology," in Proceedings of the 2005 International Conference on Active Media Technology, 2005. (AMT 2005)., pp. 347–352.
[57] Yeo, R.D., 1972. Computer assisted learning. Improving College and University Teaching, 20(3), pp.167-169.
[58] Greenhalgh, T., 2001. Computer assisted learning in undergraduate medical education. BMJ: British Medical Journal, 322(7277), p.40.
[59] Plasschaert AJ, Wilson NH, Cailleteau JG, Verdonschot EH. Opinions and experiences of dental students and faculty concerning computer-assisted learning. J Dent Educ 1995: 5:1034–1040.9.
[60] Preston JD. Computers in dental education. J Calif Dent As-soc 1997: 25: 729–733.
[61] Plasschaert AJ, Cailleteau JG, Verdonschot EH. The effect of a multimedia interactive tutorial on learning endodontic problem solving. Eur J Dent Educ 1997: 1: 66–69.
[62] Lyon HC, Healy JC, Bell JR, O'Donnel JF, Moore-West M, Wigton RS, Hirai F, Beck JR. PlanAlyzer, an interactive computer-assisted program to teach clinical problem solving in diagnosing anemia and coronary artery disease. Academic Medicine 1992: 67: 821–828.
[63] Agius RM, Bagnall G. Development and evaluation of the use of the Internet as an educational tool in occupational and environmental health and medicine. Occup Med 1998: 48: 337–343.
[64] G. Bengu and W. Swart, "A computer-aided, total quality approach to manufacturing education in engineering," IEEE Transactions on Education, vol. 39, no. 3, pp. 415–422, 1996.
[65] C. Koh, H. S. Tan, K. C. Tan, L. Fang, F. M. Fong, D. Kan, S. L. Lye, and M. L. Wee, "Investigating the Effect of 3D Simulation-Based Learning on the Motivation and Performance of Engineering Students," Journal of Engineering Education, vol. 99, no. 3, pp. 237–251, 2010.
[66] M. Ebner and A. Holzinger, "Successful implementation of user-centered game based learning in higher education: An example from civil engineering," Computers & Education, vol. 49, no. 3, pp. 873–890, 2007.
[67] D. Gillet, A. V. N. NguyenNgoc, and Y. Rekik, "Collaborative Web-Based Experimentation in Flexible Engineering Education," IEEE Transactions on Education, vol. 48, no. 4, pp. 696–704, Nov. 2005. [32] S. Şeker, "Computer - Aided Learning in Engineering Education," Procedia - Social and Behavioural Sciences, vol. 83, pp. 739–742, 2013.
[68] J. A. Tarbutton, T. R. Kurfess, and T. M. Tucker, "Graphics Based Path Planning for Multi-Axis Machine Tools," Computer-Aided Design and Applications, vol. 7, no. 6, 2010.
[69] S.Dinda, S.Tedia, Expediting Build Time, Material, And Cost Estimation For Material Extrusion Processes To Enable Mobile Applications, IDETC 2017, In Press
[70] Cheetham, Graham; Chivers, Geoff (2005). Professions, Competence and Informal Learning. Cheltenham: Edward Elgar Publishing. p. 337

[71] McGee, M G. 1979. “Human spatial Abilities: Psychometric Studies and Environmental, Genetic, Hormonal, and Neurological Influences.” Psychological Bulletin 86 (5): 889–918. doi:10.1017/CBO9781107415324.004
[72] “Medical Imaging - FDA.” [Online]. Available: https://www.fda.gov/Radiation-EmittingProducts /RadiationEmittingProductsandProcedures/MedicalImaging/default.htm
[73] Rengier, F., Mehndiratta, A., von Tengg-Kobligk, H., Zechmann, C.M., Unterhinninghofen, R., Kauczor, H.U. and Giesel, F.L., 2010. 3D printing based on imaging data: review of medical applications. *International journal of computer assisted radiology and surgery*, *5*(4), pp.335-341.
[74] McGurk M, Amis A, Potamianos P, Goodger N (1997) Rapid prototyping techniques for anatomical modelling in medicine. Ann R Coll Surg Engl 79:169–174
[75] “DICOM Homepage.” [Online]. Available: http://www. http://dicom.nema.org/.
[76] Kalet I, Wu J, Lease M, Austin-Seymour M, Brinkley J, Rosse C (1999) Anatomical information in radiation treatment planning. Proc AMIA Symp 291–295
[77] Subburaj K, Nair C, Rajesh S, Meshram S, Ravi B (2007) Rapid development of auricular prosthesis using CAD and rapid prototyping technologies. Int J Oral Maxillofac Surg 36:938–943
[78] Maragiannis, D., Jackson, M.S., Igo, S.R., Schutt, R.C., Connell, P., Grande-Allen, J., Barker, C.M., Chang, S.M., Reardon, M.J., Zoghbi, W.A. and Little, S.H., 2015. Replicating patient-specific severe aortic valve stenosis with functional 3D modeling. Circ Cardiovasc Imaging, 8(10), p.e003626.
[79] Bruyere F, Leroux C, Brunereau L, Lermusiaux P (2008) Rapid prototyping model for percutaneous nephrolithotomy training. J Endourol 22:91–96
[80] “3D Medical Image Processing Software | Materialise Mimics.” [Online]. Available: http://www.materialise.com/en/medical/software/mimics
[81] Lorensen, W.E. and Cline, H.E., 1987, August. “Marching cubes: A high resolution 3D surface construction algorithm”. In *ACM siggraph computer graphics* (Vol. 21, No. 4, pp. 163-169). ACM.
[82] Huotilainen, E., Jaanimets, R., Valášek, J., Marcián, P., Salmi, M., Tuomi, J., Mäkitie, A. and Wolff, J., 2014. “Inaccuracies in additive manufactured medical skull models caused by the DICOM to STL conversion process”. Journal of Cranio-Maxillofacial Surgery, 42(5), pp.e259-e265.
[83] Guarino J, Tennyson S, McCain G, Bond L, Shea K, King H (2007) Rapid prototyping technology for surgeries of the pediatric spine and pelvis: benefits analysis. J Pediatr Orthop 27:955–960
[84] Hurson C, Tansey A, O’Donnchadha B, Nicholson P, Rice J, McElwain J (2007) Rapid prototyping in the assessment, classification and preoperative planning of acetabular fractures. Injury 38:1158–1162
[85] Wurm G, Tomancok B, Pogady P, Holl K, Trenkler J (2004) Cerebrovascular stereolithographic biomodeling for aneurysm surgery. Technical note. J Neurosurg 100:139–145
[86] Giesel FL, Hart AR, Hahn HK, Wignall E, Rengier F, Talanow R, Wilkinson ID, Zechmann CM, Weber M, Kauczor HU, Essig M, Griffiths PD (2009) 3D reconstructions of the cerebral ventricles and volume quantification in children with brain malformations. Acad Radiol 16:610–617
[87] Paiva W, Amorim R, Bezerra D, Masini M (2007) Application of the stereolithography technique in complex spine surgery. Arq Neuropsiquiatr 65:443–445
[88] Armillotta A, Bonhoeffer P, Dubini G, Ferragina S, Migliavacca F, Sala G, Schievano S (2007) Use of rapid prototyping models in the planning of percutaneous pulmonary valved stent implantation. Proc Inst Mech Eng H 221:407–416
[89] Kim MS, Hansgen AR, Wink O, Quaife RA, Carroll JD (2008) Rapid prototyping: a new tool in understanding and treating structural heart disease. Circulation 117:2388–2394
[90] Muller A, Krishnan K, Uhl E, Mast G (2003) The application of rapid prototyping techniques in cranial reconstruction and preoperative planning in neurosurgery. J Craniofac Surg 14:899–914
[91] Wagner J, Baack B, Brown G, Kelly J (2004) Rapid 3-dimensional prototyping for surgical repair of maxillofacial fractures: a technical note. J Oral Maxillofac Surg 62:898–901

[92] D'Urso P, Earwaker W, Barker T, Redmond M, Thompson R, Effeney D, Tomlinson F (2000) Custom cranioplasty using stereolithography and acrylic. Br J Plast Surg 53:200–204
[93] Singare S, Liu Y, Li D, Lu B, Wang J, He S (2008) Individually prefabricated prosthesis for maxilla reconstruction. J Prosthodont 17:135–140
[94] Lee M, Chang C, Ku Y (2008) New layer-based imaging and rapid prototyping techniques for computer-aided design and manufacture of custom dental restoration. J Med Eng Technol 32:83–90
[95] Dai K,Yan M, Zhu Z, SunY (2007) Computer-aided custom-made hemi pelvic prosthesis used in extensive pelvic lesions. J Arthroplasty 22:981–986
[96] Harrysson O, Hosni Y, Nayfeh J (2007) Custom-designed orthopedic implants evaluated using finite element analysis of patient specific computed tomography data: femoral-component case study. BMC Musculoskelet Disord 8:91
[97] He J, Li D, Lu B,Wang Z,TaoZ (2006) Custom fabrication of composite tibial hemi-knee joint combining CAD/CAE/CAM techniques. Proc Inst Mech Eng [H] 220:823–830
[98] Wang Z, Teng Y, LiD (2004) Fabrication of custom-made artificial semi-knee joint based on rapid prototyping technique: computer assisted design and manufacturing. Zhongguo Xiu Fu Chong Jian Wai Ke Za Zhi 18:347–351
[99] Vukicevic, M., Mosadegh, B., Min, J.K., and Little, S.H. (2017) Cardiac 3D Printing and its Future Directions. *JACC Cardiovasc. Imaging*, **10** (2), 171–184.
[100] Vukicevic M, Maragiannis D, Jackson M, Little SH. Functional evaluation of a patient specific 3D printed model of aortic regurgitation [abstr]. Circulation 2015;132:A18647.
[101] Javan R, Herrin D, Tangestanipoor A. Understanding spatially complex segmental and branch anatomy using 3D printing: liver, lung, prostate, coronary arteries, and circle of Willis. Acad Radiol 2016;23:1183–9.
[102] http://3mf.io/wp-content/uploads/2015/04/3MFcoreSpec_1.0.1.pdf
[103] G. Sisias, R. Phillips, C.A. Dobson, M.F. Fagan, C.M. Langton, "Algorithms for accurate rapid prototyping replication of cancellous bone voxel maps". Rapid Prototyping Journal, 8 (1) (2002), pp. 6-24
[104] Lopes, A. and Brodlie, K., 2003. "Improving the robustness and accuracy of the marching cubes algorithm for isosurfacing". *IEEE Transactions on Visualization and Computer Graphics*, *9*(1), pp.16-29.
[105] Raman, S. and Wenger, R., 2008, May. Quality isosurface mesh generation using an extended marching cubes lookup table. In *Computer Graphics Forum* (Vol. 27, No. 3, pp. 791-798). Blackwell Publishing Ltd.
[106] Yoo, Dong-Jin. "Three-dimensional surface reconstruction of human bone using a B-spline based interpolation approach." *Computer-Aided Design* 43.8 (2011): 934-947.
[107] G.A. Anthony, D. Palathinkal, A.B. Liggins, V.J. Raso, J. Carey, R.G. Lambert, A. Amirfazli, "A NURBS-based technique for subject-specific construction of knee bone geometry". Comput Methods Programs Biomed, 92 (2008), pp. 20-34
[108] K.F. Leong, C.K. Chua, Y.M. Ng, "A study of Stereolithography file errors and repair. Part 1". Generic solutions International Journal of Advanced Manufacturing Technology, 12 (6) (1996), pp. 407-414
[109] K.F. Leong, C.K. Chua, Y.M. Ng, "A study of Stereolithography file errors and repair. Part 2". Special cases International Journal of Advanced Manufacturing Technology, 12 (6) (1996), pp. 415-422
[110] R. Maksimovic, S. Stankovic, D. Milovanovic, "Computed tomography image analyzer: 3D reconstruction and segmentation applying active contour models—'Snakes'", International journal of Medical Informatics 58–59 (2000) 29–37.
[111] B.K. Choi, H.Y. Shin, Y.I. Yoon, J.W. Lee, "Triangulation of scattered data in 3D space", Computer-Aided Design 20 (1988) 239–248.
[112] L.L. Schumaker, "Triangulations in CAGD" IEEE Transactions on Computer Graphics and Applications 13 (1) (1993) 47–52.
[113] S. Liu, W. Ma, "Seed-growing segmentation of 3D surfaces from CT—contour data", Computer-Aided Design 31 (1999) 517–563.
[114] D. Ma, F. Lin, C.K. Chua, "Rapid prototyping applications in medicine. Part 2. STL file

generation and case studies", International Journal of Advanced Manufacturing Technology 18 (2001) 118–127.
[115] J.G.K. Gan, C.K. Chua, M. Tong, "Development of a new rapid prototyping interface", Computer in Industry 39 (1999) 61–70.
[116] D.J. Yo,"Three-dimensional human body model reconstruction and manufacturing from CT medical Image Data using a heterogeneous implicit solid based approach", Int J Precis Eng Manuf, 12 (2011), pp. 293-301
[117] C.S. Wang, W.H.A. Wang, M.C. Lin' "STL rapid prototyping bio-CAD model for CT medical image segmentation", Comput Ind, 61 (2010), pp. 187-197
[118] Manmadhachary, A., Kumar, R. and Krishnanand, L., 2016. "Improve the accuracy, surface smoothing and material adaption in STL file for RP medical models". *Journal of Manufacturing Processes*, *21*, pp.46-55.
[119] Hiller, J. and Lipson, H., 2010. Tunable digital material properties for 3D voxel printers. *Rapid Prototyping Journal*, *16*(4), pp.241-247.
[120] Lou Q, Stucki P. Fundamentals of 3D halftoning. In: Electron. publ. artist.imaging, digit. typogr. Berlin, Heidelberg: Springer; 1998. p. 224–39.
[121] Cho W, Sachs EM, Patrikalakis NM, Troxel DE. A dithering algorithm for local composition control with three-dimensional printing. CAD Comput Aided Des 2003;35:851–67.
[122] Aremu, A.O., Brennan-Craddock, J.P.J., Panesar, A., Ashcroft, I.A., Hague, R.J., Wildman, R.D. and Tuck, C., 2017. A voxel-based method of constructing and skinning conformal and functionally graded lattice structures suitable for additive manufacturing. *Additive Manufacturing*, *13*, pp.1-13.
[123] Enderle, J.D. and Bronzino, J.D., 2012. *Introduction to biomedical engineering*. Academic press.
[124] Molteni, R., 2013. "Prospects and challenges of rendering tissue density in Hounsfield units for cone beam computed tomography" Oral surgery, oral medicine, oral pathology and oral radiology, 116(1), pp.105-119.
[125] Hounsfield GN. "Computed medical imaging- nobel lecture", 8 December 1979. J Radiol. 1980;61:459-468.
[126] Haralick, R.M. and Shapiro, L.G., 1991. Glossary of computer vision terms. *Pattern recognition*, *24*(1), pp.69-93.
[127] Rajeshwar Dass, Priyanka, Swapna Devi. (2012, January-March). "Image Segmentation Techniques". IJECT. Volume 3 (issue 1), ISSN: 2230-7109 (Online) | ISSN: 2230-9543 (Print).
[128] Jifeng Ning, Lei Zhang, David Zhang, Chengke Wu. (2010). "Interactive image segmentation by maximal similarity based region merging". journal homepage: www.elsevier.com/locate/pr, Pattern Recognition 43 (2010) 445 -- 456
[129] Salem Saleh Al-amri, N.V. Kalyankar and Khamitkar S.D. (2010, May). "Image Segmentation by Using Threshold Techniques". Journal of Computing. Volume 2, ISSUE 5. [Online].
[130] Hai Gao, Wan-Chi Siu and Chao-Huan Hou. (2001, December). "Improved Techniques for Automatic Image Segmentation". IEEE Transactions on Circuits and Systems for Video Technology. Volume 11 (issue 12).
[131] Otsu, N., "A Threshold Selection Method from Gray-Level Histograms," *IEEE Transactions on Systems, Man, and Cybernetics*, Vol. 9, No. 1, 1979, pp. 62-66.
[132] S. E. Umbaugh, "Computer Vision and Image Processing": A Practical Approach. Englewood Cliffs, NJ: Prentice-Hall, 1998, pp. 151–193.
[133] Zhu, Y., Zhao, M., Zhao, Y., Li, H. and Zhang, P., 2012. Noise reduction with low dose CT data based on a modified ROF model. *Optics express*, *20*(16), pp.17987-18004.
[134] Gallagher, N. and Wise, G., 1981. "A theoretical analysis of the properties of median filters". IEEE Transactions on Acoustics, Speech, and Signal Processing, 29(6), pp.1136-1141.
[135] Alajlan, N., Kamel, M. and Jernigan, E.,. "Detail preserving impulsive noise removal". Signal Processing: Image Communication (2004), 19(10), pp.993-1003.
[136] D. Brownrigg "The weighted median filter" Commun. ACM, 27 (1984), pp. 807-818
[137] A. Restrepo, A.C. Bovik "Adaptive trimmed mean filters for image restoration" IEEE Trans. Acoust. Speech, Signal Proc., 36 (1988), pp. 1326-1337

[138] S.J. Ko, Y.H. Lee “Center weighted median filters and their applications to image enhancement” IEEE Trans. Circuits Syst., 38 (1991), pp. 984-993
[139] T. Sun, Y. Neuvo “Detail preserving median based filters in image processing” Pattern Recogn. Lett., 15 (1994), pp. 341-347
[140] L. Cabrera, P. Escanmilla “Two pixel preselection methods for median type filtering”. Vision, Image Signal Proc. IEE Proc., 145 (1998), pp. 30-40
[141] M. Imme “A noise peak elimination filter” CVGIP: Graph. Models Image Proc., 53 (1991), pp. 204-211
[142] Lee, J.S., “Digital image smoothing and the sigma filter”. Computer vision, graphics, and image processing (1983), 24(2), pp.255-269.
[143] Floyd, R. W., and L. Steinberg, "An Adaptive Algorithm for Spatial Gray Scale," International Symposium Digest of Technical Papers, Society for Information Displays, 1975, p. 36.
[144] Meisel, N.A., Williams, C., Bøhn, J.H., et al. (2015) Design for Additive Manufacturing Considerations for Self-Actuating Compliant Mechanisms Created via Multi-Material PolyJet 3D Printing.
[145] “Digital Materials - Stratasys.” [Online]. Available: http://www.stratasys.com/materials/polyjet/digital-materials
[146] http://www.mouseimaging.ca/
[147] “Additive Manufacturing and Design Software, Netfabb, Autodesk.” [Online]: Available: https://www.autodesk.com/products/netfabb/overview
[148] Pinsky, H.M., Dyda, S., Pinsky, R.W., Misch, K.A. and Sarment, D.P., 2006. Accuracy of three-dimensional measurements using cone-beam CT. *Dentomaxillofacial Radiology*, *35*(6), pp.410-416.
[149] Moerenhout, B.A., Gelaude, F., Swennen, G.R., Casselman, J.W., Van Der Sloten, J. and Mommaerts, M.Y., 2009. Accuracy and repeatability of cone-beam computed tomography (CBCT) measurements used in the determination of facial indices in the laboratory setup. *Journal of Cranio-Maxillofacial Surgery*, *37*(1), pp.18-23.
[150] Sarment, D.P., Sukovic, P. and Clinthorne, N., 2003. Accuracy of implant placement with a stereolithographic surgical guide. *International Journal of Oral & Maxillofacial Implants*, *18*(4).
[151] Magne, P. and Oganesyan, T., 2009. CT Scan--Based Finite Element Analysis of Premolar Cuspal Deflection Following Operative Procedures. International Journal of Periodontics & Restorative Dentistry, 29(4).
[152] Magne, P., 2007. Efficient 3D finite element analysis of dental restorative procedures using micro-CT data. Dental Materials, 23(5), pp.539-548.
[153] Tuan, H.S. and Hutmacher, D.W., 2005. Application of micro CT and computation modeling in bone tissue engineering. *Computer-Aided Design*, *37*(11), pp.1151-1161

APPENDIX A: ME2024 - Spring 2017 DfM - Pre

Q55 This brief survey is meant to gauge your current knowledge of manufacturing technologies and how they influence product design. Please complete this survey PRIOR to watching the "Design for Manufacturing" video and PRIOR to coming to class. This survey will not be graded for correctness. (It will be graded for completion.) If you do not know the answer to a question, please select that option. The purpose of this pre-class survey is to help us learn more about ME 2024 students' prior understanding and experiences, and to help us evaluate the effectiveness of the class in effort to continually improve how we teach. Thank you!

Q56 Please select your ME2024 CRN.
- ❍ 15565 (11:15a) (3)
- ❍ 19697 (11:15a) (4)
- ❍ 15562 (12:20p) (1)
- ❍ 15564 (12:20p) (2)

Q47 Please enter your PID.

Q48 Have you taken ISE 2214: Manufacturing Processes Lab?
- ❍ Yes, I am taking it this semester. (1)
- ❍ Yes, I took it in a previous semester. (2)
- ❍ No, I have not taken this course. (3)

Q49 Have you taken ISE 2204: Manufacturing Processes (lecture)?
- ❍ Yes, I am taking it this semester. (1)
- ❍ Yes, I took it in a previous semester. (2)
- ❍ No, I have not taken this course. (3)

Q50 Do you have any prior experience with 3D Printing?
- ❍ Yes (1)
- ❍ No (2)

If No Is Selected, Then Skip To Do you have any prior experience with...

Q51 How would you rate your level of expertise with 3D Printing?
- ❍ Novice (little experience; lacks confidence in ability to complete task) (1)
- ❍ Advanced beginner (you have some skills, but require frequent assistance) (2)
- ❍ Competent (you are confident in your ability to complete tasks in this area) (3)
- ❍ Proficient (You are confident in your ability to complete tasks in this area and in your ability to learn new abilities) (4)
- ❍ Expert (Deep understanding from extensive experience and are able to quickly learn new abilities to complete new tasks in this area.) (5)

Q52 Do you have any prior experience with machining? (e.g., lathe, mill, cnc, laser cutter)
- ❍ Yes (1)
- ❍ No (2)

If No Is Selected, Then Skip To Have you watched the "Design for Manu...

Q67 Select those machining processes you have had experience with:
- ❑ Lathe (1)
- ❑ Mill (manual) (2)
- ❑ 3-axis CNC mill (3)
- ❑ 4- or 5- axis CNC mill (4)
- ❑ None of the above (5)

Q54 I would rate my level of expertise with machining as,
- ❍ Novice (little experience; lacks confidence in ability to complete task) (1)
- ❍ Advanced beginner (you have some skills, but require frequent assistance) (2)
- ❍ Competent (you are confident in your ability to complete tasks in this area) (3)
- ❍ Proficient (You are confident in your ability to complete tasks in this area and in your ability to learn new abilities) (4)
- ❍ Expert (Deep understanding from extensive experience and are able to quickly learn new abilities to complete

new tasks in this area.) (5)

Q69 Have you watched the "Design for Manufacturing" video lecture?
- Yes (1)
- No (4)

Q70 Have you attended the W12D1 class on "Design for Manufacturing"?
- Yes (1)
- No (2)

Q71 (We hope your answer is "No" to the above questions - please complete this survey before watching the lecture video and before coming to class.)

Q57 For the next 5 questions, please select the preferred manufacturing process that would be able to manufacture all of the parts' features. Please refrain from guessing, and select "Don't know" if you don't know which manufacturing process would be most appropriate.

Q60

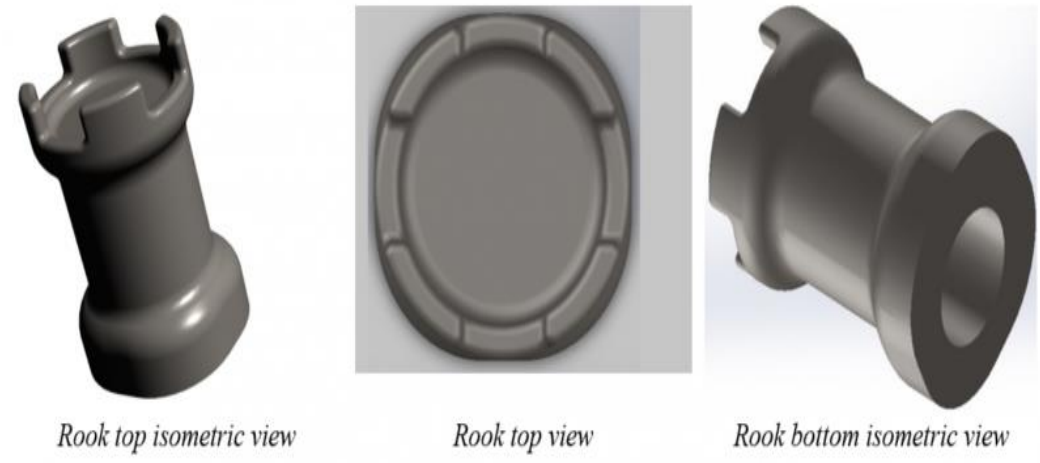

Rook top isometric view *Rook top view* *Rook bottom isometric view*

Q63 Which manufacturing process is most preferred for making the part above?
- 2-axis lathe (1)
- 3-axis mill (2)
- 4-axis mill (3)
- 3D Printer (4)
- Don't know (5)

Q61

Tea pot top view *Tea pot side view*

Q64 Which manufacturing process is most preferred for making the part above?
- 2-axis lathe (1)

- 3-axis mill (2)
- 4-axis mill (3)
- 3D Printer (4)
- Don't know (5)

Q68

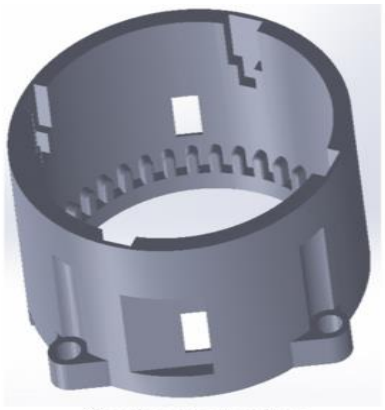

Gearhousing top view

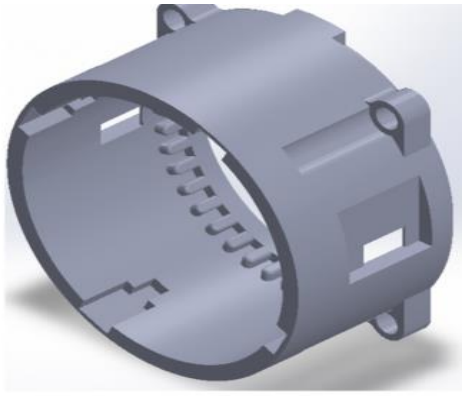

Gearhousing side isometric view

Q65 Which manufacturing process is most preferred for making the part above?

- 2-axis lathe (1)
- 3-axis mill (2)
- 4-axis mill (3)
- 3D Printer (4)
- Don't know (5)

Q69

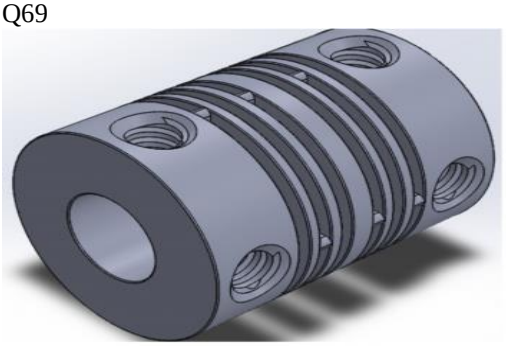

Coupler side isometric view

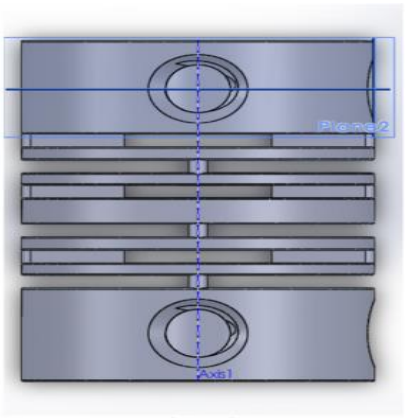

Coupler side view

Q66 Which manufacturing process is most preferred for making the part above?

- 2-axis lathe (1)
- 3-axis mill (8)
- 4-axis mill (9)
- 3D Printer (10)
- 2-axis lathe + 3-axis mill (11)
- 2-axis lathe + 4-axis mill (12)
- × Don't know (13)

Q73

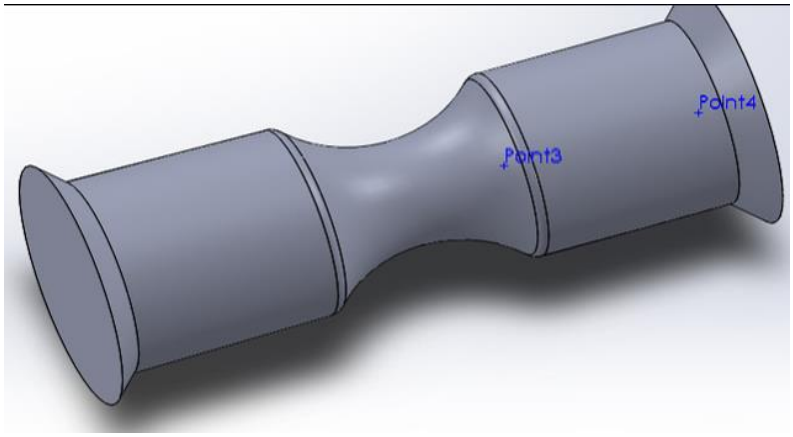

Q Which manufacturing process is most preferred for making the Hourglass part above?

- ❍ 2-axis lathe
- ❍ 3-axis mill
- ❍ 4-axis mill
- ❍ 3D Printer
- ❍ Don't know

APPENDIX B: ME2024 - Spring 2017 DfM - Post

Start of Block: Demographics

Q55 This brief survey is meant to gauge your knowledge of manufacturing technologies and how they influence product design. **Please complete this survey *AFTER* participating in the "Design for Manufacturing" class exercises.**

This survey will not be graded for correctness. (It will be graded for completion. If you do not know the answer to a question, please select that option.

The purpose of this post-class survey is to help us learn more about students' understanding and experiences, and to help us evaluate the effectiveness of the class in effort to continually improve how we teach.

Thank you!

Q56 Please select your ME2024 CRN.
- ❍ 15565 (11:15a) (14)
- ❍ 19697 (11:15a) (15)
- ❍ 15562 (12:20p) (6)
- ❍ 15564 (12:20p) (16)

Q47 Please enter your PID.
_____

Q57 For the next 8 questions, please select the ***preferred manufacturing process*** that would be able to manufacture all of the parts' features.

For the purposes of this assignment, assume that one would prefer to use Subtractive manufacturing over Additive Manufacturing due to cost and time (i.e., select a Subtractive Manufacturing technique if one is capable of making all of a part features).

Please refrain from guessing, and select "Don't know" if you don't know which manufacturing process would be most appropriate.

Q61

Tea pot top view

Tea pot side view

Q64 Which manufacturing process is most preferred for making the Tea Pot part above?
- ❍ 2-axis lathe (1)
- ❍ 3-axis mill (2)

- 4-axis mill (3)
- 3D Printer (4)
- Don't know (5)

Q68

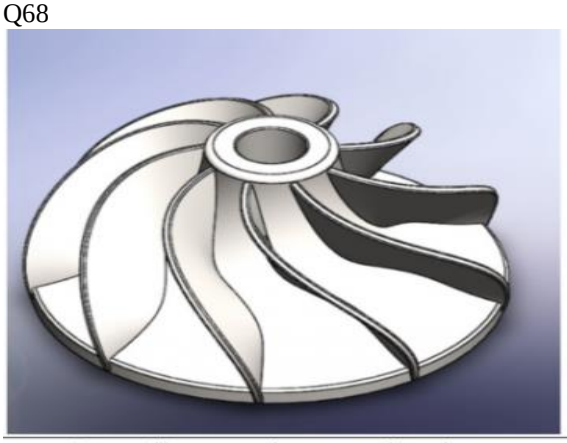

Impeller top isometric view

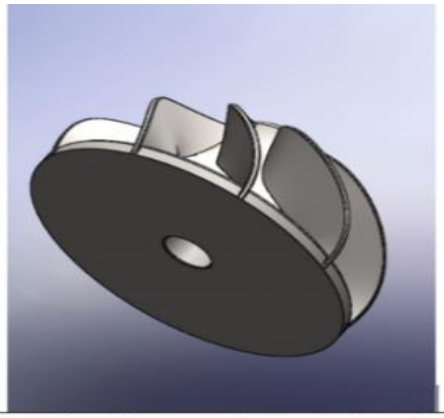

Impeller bottom isometric view

Q65 Which manufacturing process is most preferred for making the Impeller part above?

- 2-axis lathe (1)
- 3-axis mill (2)
- 4-axis mill (3)
- 3D Printer (4)
- Don't know (5)

Q39

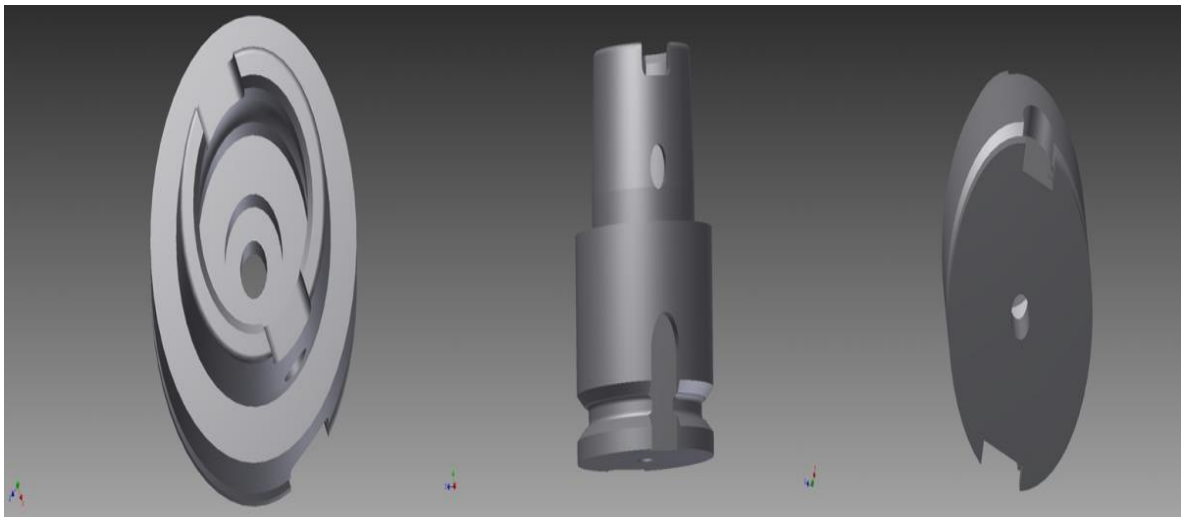

Q33 Which manufacturing process is most preferred for making the part above?

- 2-axis lathe (1)
- 3-axis mill (2)
- 4-axis mill (3)
- 3D Printer (4)
- Don't know (5)

Q21

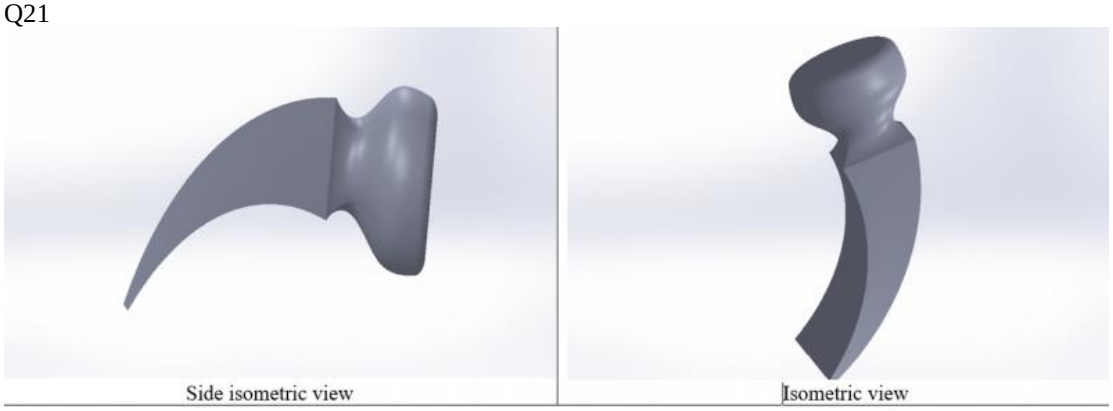

Q20 Which manufacturing process(es) is most preferred for making the Hammer head part above?

- 2-axis lathe (1)
- 3-axis mill (2)
- 4-axis mill (3)
- 3D Printer (4)
- 2-axis lathe + 3-axis mill (6)
- 2-axis lathe + 4-axis mill (7)
- Don't know (5)

Q28 Provide a brief justification of your selection.

_____
_____
_____
_____
_____

Q38

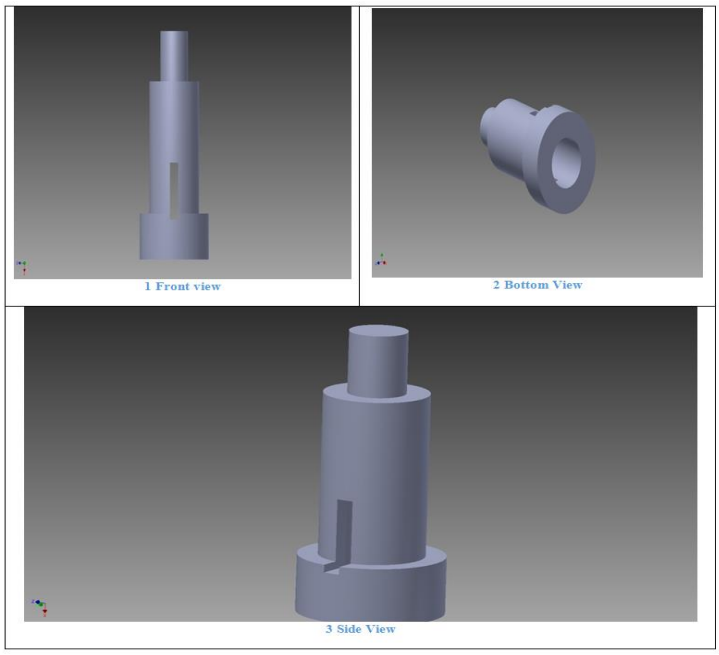

Q38 Which manufacturing process is most preferred for making the above joint?

- 2-axis lathe (1)
- 3-axis mill (2)
- 4-axis mill (3)
- 3D Printer (4)
- 2-axis lathe + 3-axis mill (5)
- 2-axis lathe + 4-axis mill (6)
- Don't know (7)

Q69

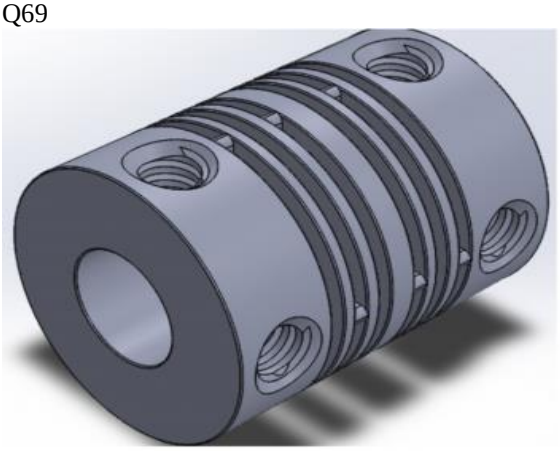

Coupler side isometric view

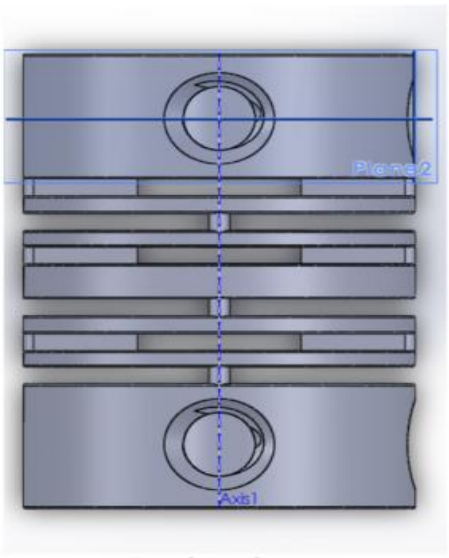

Coupler side view

Q66 Which manufacturing process is most preferred for making the Coupler part above?

- 2-axis lathe (1)
- 3-axis mill (2)
- 4-axis mill (3)
- 3D Printer (4)
- 2-axis lathe + 3-axis mill (6)
- 2-axis lathe + 4-axis mill (7)
- Don't know (5)

Q23 Provide a brief justification of your selection.

_____
_____
_____

Q19

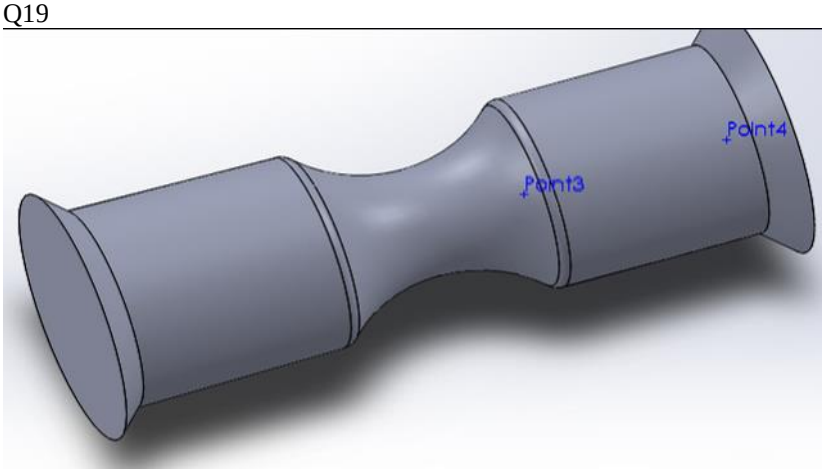

Q18 Which manufacturing process is most preferred for making the Hourglass part above?

- 2-axis lathe (1)
- 3-axis mill (2)
- 4-axis mill (3)
- 3D Printer (4)
- Don't know (5)

Q39

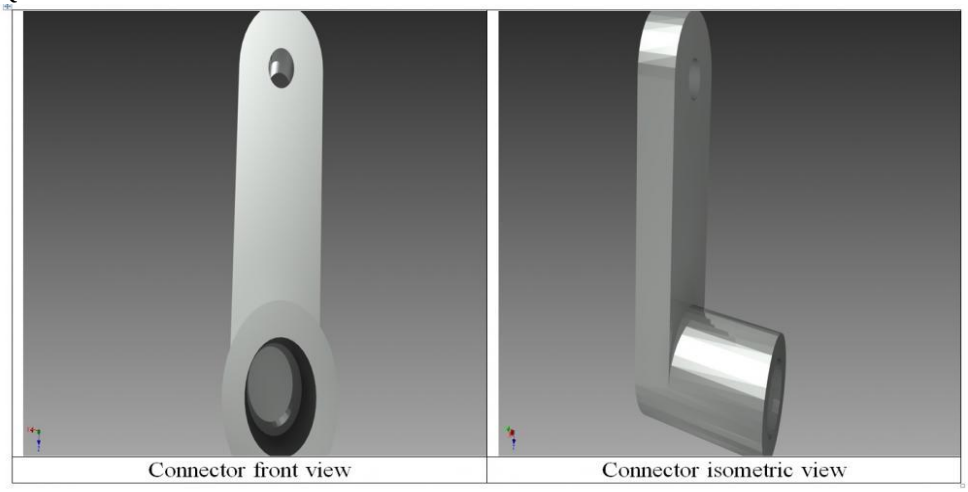

Connector front view | Connector isometric view

Q29 Which manufacturing process is most preferred for making the Connector part above?

- 2-axis lathe (1)
- 3-axis mill (2)
- 4-axis mill (3)
- 3D Printer (4)
- Don't know (5)

Q26 Did you watch the video lecture on DfM: Subtractive Manufacturing?

- Yes, before attending class. (1)
- Yes, after attending class. (2)
- No. (3)

Q25 Did you watch the video lecture on DfM: Additive Manufacturing?

- Yes, before attending class. (1)
- Yes, after attending class. (2)
- No. (3)

Q37 What is the most *useful* thing you learned in the two "Design for Manufacturing" exercises?

_____
_____
_____
_____
_____

Q38 How will the lessons you learned from these exercises change the way you *make decisions* about designing parts and products?

_____
_____
_____
_____
_____

Q39 Please share any feedback on the DfM exercises.

_____
_____
_____
_____
_____